

Loma Linda University

TheScholarsRepository@LLU: Digital Archive of Research, Scholarship & Creative Works

Loma Linda University Electronic Theses, Dissertations & Projects

9-2008

Maturational Changes in Myosin Light Chain Kinase Activity in Ovine Carotids

Elisha Raju Injeti

Follow this and additional works at: <https://scholarsrepository.llu.edu/etd>



Part of the [Pharmacology Commons](#), and the [Physiology Commons](#)

Recommended Citation

Injeti, Elisha Raju, "Maturational Changes in Myosin Light Chain Kinase Activity in Ovine Carotids" (2008).
Loma Linda University Electronic Theses, Dissertations & Projects. 1390.
<https://scholarsrepository.llu.edu/etd/1390>

This Dissertation is brought to you for free and open access by TheScholarsRepository@LLU: Digital Archive of Research, Scholarship & Creative Works. It has been accepted for inclusion in Loma Linda University Electronic Theses, Dissertations & Projects by an authorized administrator of TheScholarsRepository@LLU: Digital Archive of Research, Scholarship & Creative Works. For more information, please contact scholarsrepository@llu.edu.

UNIVERSITY LIBRARIES
LOMA LINDA, CALIFORNIA

LOMA LINDA UNIVERSITY
School of Medicine
in conjunction with the
Faculty of Graduate Studies

Maturational Changes in Myosin Light Chain Kinase Activity in Ovine Carotids

by

Elisha Raju Injeti

A Dissertation submitted in partial satisfaction of
the requirements for the degree of
Doctor of Philosophy in Pharmacology

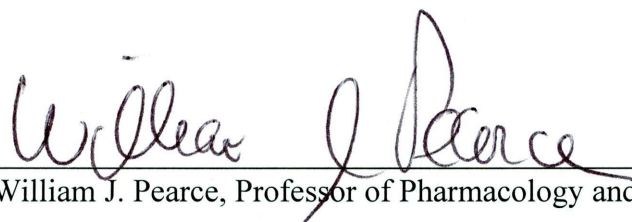
September 2008

NEUTECH
25% COTTON

© 2008

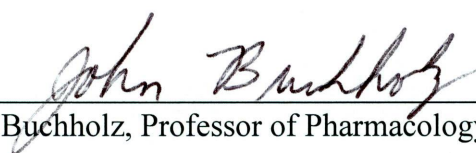
Elisha Raju Injeti
All Rights Reserved

Each person whose signature appears below certifies that this dissertation in his/her opinion is adequate, in scope and quality as a dissertation for the degree of Doctor of Philosophy

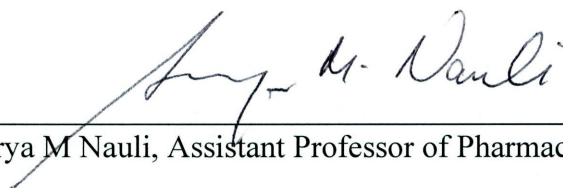


, Chairperson

William J. Pearce, Professor of Pharmacology and Physiology



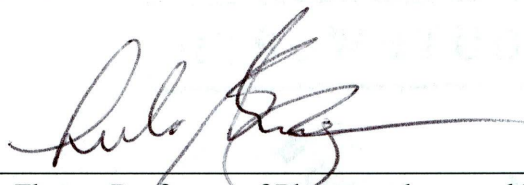
John N. Buchholz, Professor of Pharmacology and Physiology



Surya M Nauli, Assistant Professor of Pharmacology, The University of Toledo, Ohio



Kangling Zhang, Associate Research Professor



Lubo Zhang, Professor of Pharmacology and Physiology

ACKNOWLEDGEMENTS

I express my heartfelt gratitude to all who stood by me in completing this research project:

To Dr. William J. Pearce for his mentorship.

To Dr. John Buchholz, Dr. Lubo Zhang, Dr. Surya Nauli, Dr. Kangling Zhang and Dr. Lincoln Ford for their guidance.

To James Williams, Renan Sandoval, Ryan Tone and Gerhart Grauper for their assistance.

To Loma Linda University School of Medicine and Center for Perinatal Biology for providing the facilities.

CONTENTS

Approval Page	iii
Acknowledgements.....	iv
Table of Contents.....	v
List of Figures.....	viii
List of Abbreviations	ix
Abstract	x
Chapter	
1. Introduction.....	1
Background.....	3
Myosin Light Chain Kinase	5
Myofilament Calcium Sensitivity.....	8
Significance.....	11
2. Maximal Stimulation-Induced In Situ Myosin Light Chain Kinase Activity Is Upregulated In Fetal Compared to Adult Ovine Carotid Arteries	13
Abstract.....	14
Introduction.....	15
Materials and Methods	17
General Preparation	17
Determination of MLCK Abundance	18
Determination of MLC ₂₀ Abundance	18
Determination of Optimal Length for Contractile Response in Intact Carotid Arteries	20
Determination of Optimal Concentration of Myosin Light Chain Phosphatase Inhibitors	20
Determination of Concentration and Time Dependent Effects of ML-7 on MLCK Activity.....	21
Comparison of Chemical and Electrical Methods of MLCK Activation	22

Determination of Current - Contractile Responses in Intact Carotid Arteries.....	23
Determination of MLCK Activity in Intact Carotid Arteries.....	23
Calculations and Statistics.....	23
Results.....	24
Effect of Postnatal Maturation on MLCK and MLC ₂₀ Abundances	24
Length-Tension Relations in Ovine Carotid Arteries	25
Optimum Concentration of Myosin Light Chain Phosphatase Inhibitors	25
Concentration and Time Dependent Effects of ML-7 on MLCK Activity... 26	
Comparison of Chemical and Electrical Methods of MLCK Activation	26
Current-Tension Relations in Ovine Carotid Arteries	27
Measurement of MLCK Activity in Intact Ovine Carotids	27
Discussion	28
Acknowledgements	35
References.....	36
3. Myosin Light Chain Kinase Phosphorylates Regulatory Light Chain More Efficiently In Fetal Than In Adult Ovine Carotid Arteries	51
Abstract	52
Introduction	53
Materials and Methods.....	54
General Preparation.....	54
Preparation of Carotid Artery Homogenates.....	55
Determination of MLCK Abundance in Artery Homogenates	55
Determination of Optimum Calcium and Calmodulin Concentrations for Activating MLCK.....	56
Determination of Optimum Concentration of Phosphatase Inhibitor Cocktail	57
Effects of Protein Kinase Inhibitors on MLCK Velocity.....	57
Determination of V _{max} & K _m of MLCK	58
Calculations and Statistics.....	59
Results.....	59
MLCK Abundance in Artery Homogenates.....	60
Optimum Concentrations of Calcium and Calmodulin for MLCK Activation	60
Optimum Inhibitor of Phosphatase Inhibitor Cocktail.....	60
Effect of Protein Kinase Inhibitors on MLCK Velocity	61
Age-Related Differences in V _{max} and K _m Values for MLCK.....	61

Age-Related Differences in Homogenate Specific Activity and Fractional Activation of MLCK	62
Dicussion.....	62
Acknowledgements.....	67
References	68
4. Amino Acid Sequences Of Regulatory Myosin Light Chain (MLC ₂₀) Isoforms In Vascular Smooth Muscle During Development	79
Abstract	80
Introduction	81
Materials & Methods	81
General Preparation.....	81
Extraction of MLC ₂₀ from Arterial Tissue	82
Ion-Exchange Chromatography	82
Gel Filtration Column Chromatography	83
Electrospray Injection Mass Spectrometry.....	83
Results.....	83
Identification of Fractions Containing MLC ₂₀ from Ion-Exchange Chromatography.....	84
Purification of MLC ₂₀ by Gel Filtration.....	84
Identification of Two Distinct Isoforms of MLC ₂₀ by Electrospray- Injection Mass Spectrometry (ESI-MS).....	84
Discussion	84
5. Conclusion & Future Directions	92
References	98

FIGURES

Figure	Page
1. Structure of MLCK	7
2. Abundance of MLCK in ovine carotid arteries.....	45
3. Length –Tension relations in ovine carotid arteries.....	46
4. Optimum concentrations of Calyculin-A and Phosphatase Inhibitor Cocktail for MLCP inhibition.....	47
5. Concentration and time dependent effects of ML-7 on MLCK activity	48
6. Validation of activation via electrical field stimulation.....	49
7. MLCK velocity in intact ovine carotid arteries	50
8. Optimum calcium and calmodulin required to activate MLCK	74
9. Optimul concentration of Phosphatase Inhibitor cocktail for MLCP inhibition... 75	
10. Effects of protein kinase inhibitors on MLCK velocity	76
11. Age-related differences in Vmax & Km values for MLCK	77
12. Age related differences in the apparent specific activity and fractional activation of MLCK	78
13. Ion Exchange Chromatography of MLC ₂₀	88
14. Gel Filtration Chromatography of MLC ₂₀	89
15. Preparative Gel Analysis of Purified MLC ₂₀	90
16. Amino Acid Sequence of MLC ₂₀	91
17. Summary of MLCK structure, function and regulation	97

LIST OF ABBREVIATIONS

MLC	myosin light chain
MLCK	myosin light chain kinase
MLCP	myosin light chain phosphatase
K ⁺	potassium
PIC	phosphatase inhibitor cocktail
EFS	electrical field stimulation
DTT	dithiothreitol
V _{max}	maximal velocity
K _m	michaelis constant
CaM	calmodulin
Na ⁺	sodium

ABSTRACT OF THE DISSERTATION

Maturational Changes In Myosin Light Chain Kinase Activity In Ovine Carotids

by

Elisha Raju Injeti

Doctor of Philosophy, Graduate Program in Pharmacology
Loma Linda University, September 2008
Dr. William J. Pearce, Chairperson

Vascular reactivity changes dramatically during postnatal maturation due in large part to developmental changes in myofilament calcium sensitivity. Recent findings suggest that reactivity of the thick filament component of calcium sensitivity is upregulated in fetal compared to adult arteries. In light of these findings, the present study tests the hypothesis that upregulation of fetal thick filament reactivity is due to upregulation of myosin light chain kinase (MLCK) activity. To test this hypothesis, MLCK abundance and its activity is measured in intact arteries. The results indicate that MLCK abundance is 6.03 ± 0.96 fold greater in adult than in fetal arteries. Total MLCK activity (%MLC phosphorylated/sec) estimated as the rate of phosphorylation of myosin light chain in intact arteries was greater in fetal (7.39 ± 0.53) than in adult (6.56 ± 0.29) arteries. When total MLCK activity was normalized relative to MLCK & MLC abundance to estimate the apparent specific activity of MLCK (ng MLC phosphorylation/sec/ng MLCK), these estimates were dramatically greater in fetal (1.52 ± 1.11) than in adult (0.26 ± 0.01) arteries.

Further, to test if these differences are due to differences in fractional activation of the enzyme, maximum velocity (V_{max}) of MLCK was estimated in artery homogenates.

The results indicate that V_{\max} (ng MLC phosphorylated/sec) is significantly greater in fetal (163 ± 11) compared to adult (130 ± 9) arteries. When fractional activation was calculated the results showed about 4.9 ± 0.3 fold greater activation of MLCK in fetal compared to adult arteries.

Together, these results support the hypothesis that upregulation of fetal thick filament reactivity is due to upregulation of MLCK activity. These studies were the first to offer a quantitative assessment of age related differences in MLCK activity in intact arteries and indicate the relative extents to which changes in MLCK abundance, activity and fractional activation contribute to these differences. From a clinical science perspective, these studies help in understanding the mechanisms involved in adaptation of fetal vascular system for postnatal life so that, new strategies of pharmacological management of NICU neonates with cerebrovascular and cardiovascular instabilities can be developed.

CHAPTER 1

Introduction

A common feature of many infants in Neonatal Intensive Care facilities is cardiovascular instability. Systematic investigation of this feature has revealed that regulation of vascular contractility is markedly different in immature than in mature arteries. These differences involve numerous mechanisms related to regulation of cytosolic calcium concentrations, but recent studies have also suggested that contractile proteins are regulated very differently in mature and immature arteries. The exact mechanisms responsible for these age-related differences, however, remain unknown, despite their obvious clinical relevance and importance.

From the simplest perspective, the mechanisms regulating contractile protein function can be categorized into two main families. The first includes those that determine the dynamics and extent of myosin phosphorylation in response to changes in cytosolic calcium, and thereby regulate thick-filament contractile function. The second includes those mechanisms that control the ability of actin filaments to bind to phosphorylated myosin, and thereby regulate thin-filament function. For both thick and thin-filament regulation, many of the signal transduction mechanisms involved remain unclear or controversial. However, most studies of thick filament regulation have thus far focused on regulation of MLCP and relatively little has been elucidated regarding the

importance of regulation of MLCK in overall regulation of myofilament calcium sensitivity. Almost nothing is known of thick filament regulation in immature arteries.

In light of recent observations that the regulation of myofilament calcium sensitivity is markedly different in mature and immature arteries, and also that the significance of thick filament regulation changes with maturation, this study proposes to test the general hypothesis that ***age-related differences in myofilament calcium sensitivity involve upregulation of MLCK activity in fetal compared to adult arteries.***

This main hypothesis, in turn, gives rise to at least three main corollaries:

Corollary Hypothesis #1: Age-related differences in myofilament calcium sensitivity involve up-regulation of MLCK abundance in immature arteries;

Corollary Hypothesis #2: Age-related differences in myofilament calcium sensitivity involve increased MLCK intrinsic activity in immature arteries;

Corollary Hypothesis #3: Age-related differences in myofilament calcium sensitivity involve increases in fractional activation of MLCK in immature arteries.

In order to test our main hypothesis and its corollaries, we will conduct experiments designed to address the following specific aims:

Specific Aim # 1: Measure MLCK and MLC abundance in fetal and adult common carotid arteries via quantitative Western blots.

Specific Aim #2: Measure the velocity of myosin light chain phosphorylation in intact tissue and normalize to abundance of MLCK and MLC to estimate the *in-situ* MLCK velocity.

Specific Aim # 3: Measure the maximum velocity of myosin light chain phosphorylation in tissue homogenates using purified chicken gizzard MLC as a substrate to estimate the V_{\max} and K_m of MLCK.

Specific Aim # 4: Measure the fractional activation of MLCK in intact tissue by dividing the *in-situ* MLCK velocity with V_{\max} values of MLCK from artery homogenates.

Given the relatively large amount of tissue required for multiple reliable measurements of MLC phosphorylation from a single artery sample from a single animal, we will perform these experiments using common carotid artery segments from term fetal and non-pregnant adult sheep.

Background

The contractile proteins like actin and myosin are most commonly present in almost all types of eucaryotic cells. These proteins are involved in regulation of important cellular processes like endothelial cell retraction, platelet aggregation and contraction, fibroblast contraction, secretion, receptor capping, nerve growth cone motility and muscle contraction (20, 40, 73, 76). Of all these functions, their role in contractile activity of muscle cells like cardiac, skeletal and smooth muscles is well established and documented in the literature (78). The contractile response of all these muscle types is mainly due to the interaction of myosin heads with the thin filaments formed by actin polymers. More than 100 years ago, Sydney Ringer has shown that this interaction depends on influx of extracellular calcium into muscle cells (62, 63). Numerous studies that followed established not only the central role of calcium in regulating contractile function of cardiac, skeletal and smooth muscles but also elucidated the differences in protein machinery involved in each muscle type.

Especially in smooth muscles, three theories have been proposed to explain the mechanisms regulating contractile proteins. They are (i) phosphorylation theory (ii) leiotonin theory (iii) troponin theory (51). Among these, phosphorylation theory is the most dominant one, which proposes that regulation of contractile activity operates via the phosphorylation and dephosphorylation of the MLC_{20} present on myosin molecule (5, 10, 23, 27, 35, 52, 69, 71). The major opposition to this theory is from Ebashi and co-workers who proposed that regulation of smooth muscle contraction takes place through interaction with proteins called leiotonin A & C and does not require reversible phosphorylation of myosin (14, 47-49). Both these theories were preceded by troponin theory, which claimed that a troponin C-like molecule exists in smooth muscles that regulate contractile function (9, 15, 16, 29). However, two important findings lead to the rejection of troponin theory. Firstly, it was shown that troponin C is actually calmodulin, which is present in a wide variety of cells apart from smooth muscle cells (24, 25, 29). Secondly, the contradictory functions of troponin as an inhibitor in skeletal muscle contraction and activator in smooth muscle contraction lead to its failure. On the other hand, further studies by Ebashi and co-workers, led to the conclusion that leiotonin is infact myosin light chain kinase and that it also exhibits a non-kinase related activity along with kinase activity (17). Given these findings, phosphorylation theory became a widely accepted viable theory to explain the regulation of smooth muscle contractility. These developments led to the emergence of myosin light chain kinase as a crucial enzyme that phosphorylates myosin light chain and is both necessary and sufficient for smooth muscle contraction. This pivotal role of myosin light chain kinase is further

confirmed by a direct demonstration at the level of single smooth muscle cells as well as whole animal studies involving MLCK knock out mice (39, 74).

Myosin Light Chain Kinase

Myosin light chain kinase (MLCK) is a calcium/calmodulin dependent protein kinase that phosphorylates serine-19 residue on the N-terminal of the MLC₂₀. Due to its high specificity for MLC₂₀, it is known as a dedicated protein kinase. It is ubiquitously distributed in smooth muscle, skeletal muscle, and non-muscle cells. Smooth muscle MLCK is product of a single gene that is different from skeletal muscle MLCK and has two splice variant products ranging from 130-150 kDa (short MLCK) and 208-214 kDa (long MLCK) (72). Studies have shown that long MLCK is expressed in non muscle cells like endothelium while the short MLCK is expressed in smooth muscle cells (59, 83). Colocalization studies also suggest that these MLCK isoforms have different distribution profiles implicating different physiological functions in both non-muscle cells and smooth muscle cells (8, 61). This was confirmed by studies conducted on knockout mice that these isoforms have some non-redundant functions (59, 83).

MLCK isoform expression has also been studied from the perspective of developmental biology. Expression of long MLCK isoform during chicken embryogenesis is shown by RT-PCR methods. Direct sequencing of the RT-PCR product from embryonic tissue RNA revealed long MLCK isoform. In addition, cultured embryonic gizzard and vascular smooth muscle cells expressed the short MLCK isoform, albeit at lower levels than in vivo tissues (18). In other studies Gallagher and co-workers have found that long MLCK isoform is most abundant during early development and gradually declines at birth. In contrast, expression of short MLCK isoform is relatively low early

during development and increases to become the predominant MLCK detected in all adult smooth and non-muscle tissues (19, 60). Although these MLCK isoforms have distinct expression and localization patterns, they have identical catalytic domains (30).

Structural analysis of MLCK molecule reveals that it contains three regulatory domains: (i) actin binding domain; (ii) catalytic domain along with regulatory domain (iii) myosin binding domain (Figure 1)(33). The actin binding domain is present on the N-terminal side of the molecule and shows high affinity binding towards actin filaments most likely due to its DFRXXL motifs (68). Short MLCK has three repeats of DFRXXL motif and long MLCK has 5 such repeats along with 6 Ig-like modules. DFRXXL motifs are necessary for short MLCK isoform to bind to actin-containing filaments while in long MLCK isoform they confer high affinity binding to stress fibers in cells (67). The kinase activity for phosphorylation is localized at the catalytic domain of MLCK. This domain is repressed by substrate inhibitory domain during non-stimulatory conditions. In the presence of calcium, calmodulin undergoes a conformational change that exposes two hydrophobic pockets, one in each globular lobe that is important for binding to MLCK. Upon binding calmodulin, MLCK undergoes a conformational change that derepresses the catalytic site, allows substrate access and light chain phosphorylation (45, 46). The C-terminal domain of MLCK has been shown to bind to unphosphorylated smooth muscle myosin. This domain is also independently expressed as a protein called telokin. When the functional significance of the C-terminal domain (telokin) and the molecular morphology of MLCK was studied, it was found that telokin inhibited phosphorylation of myosin by MLCK (70). These results indicate that MLCK binds to the head-tail junction of unphosphorylated myosin through its C-terminal domain, where MLC₂₀ can be

promptly phosphorylated through its catalytic domain following the calcium/calmodulin-dependent activation (58).

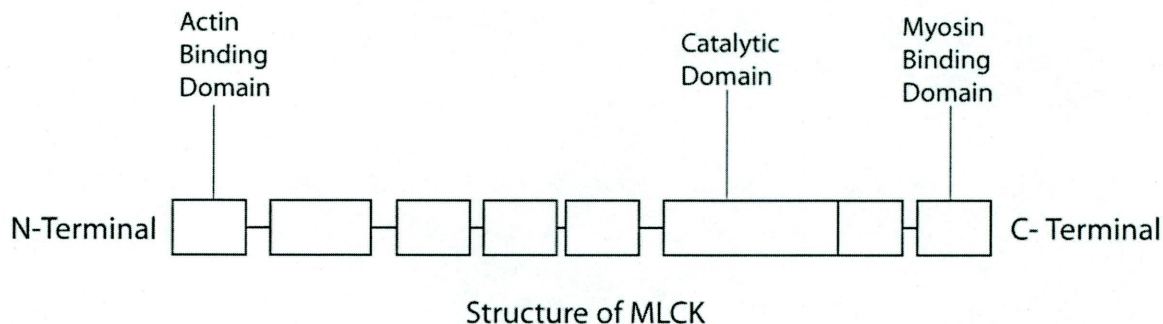


Figure 1. Structure of MLCK

MLCK plays a prominent role in regulation of actomyosin-dependent contraction in both smooth and non-muscle cells where myosin II is activated by myosin light chain phosphorylation. This phosphorylation results in a variety of cellular responses including cytoskeletal remodeling by stress fibers, fibroblast contraction, angiogenesis, changes in endothelial permeability, normal and cancer cell migration, asthma, hypertension, and atherosclerosis (72). Especially in smooth muscle, calcium-dependent MLCK activation results in MLC_{20} phosphorylation and force development. The ability of MLC_{20} phosphorylation to initiate contraction has been demonstrated by treatment of both intact cells and skinned fibers with proteolytically activated MLCK in absence of elevated calcium (38, 39). MLCK activity undergoes dramatic changes depending on the physiological conditions like pregnancy. For example, hormones like progesterone, estrogen, gonadotrophin increases MLCK activity by at least 2 fold (57). In contrast, relaxin inhibits uterine contractility by decreasing MLCK activity (84)

The activity of MLCK is regulated by phosphorylation mediated by a number of different kinases. MLCK phosphorylation at the C-terminus of the calmodulin binding sequence increases K_{CaM} and decreases MLCK activity. Multiple kinases including PKA (1, 12), PKG (56), PKC (36), and CaM kinase-II (28, 77) can phosphorylate MLCK. However, only CaM kinase-II mediated phosphorylation was found to be physiologically significant (75). Another important mechanism for regulating MLCK activity is through telokin, a 17 kD acidic protein that is expressed exclusively in smooth muscle tissues and cells (31, 37). It is expressed at high levels in smooth muscles such as intestinal and urinary smooth muscle but only at very low levels in vascular smooth muscle (11, 31). Other studies suggest that telokin inhibits MLCK activity in broken cell preparations (58, 66). Among these studies very few have looked at age related changes in MLCK activity and virtually none of them have studied the role of MLCK activity in age related changes in myofilament calcium sensitivity.

Myofilament Calcium Sensitivity

Myofilament calcium sensitivity is the increment in force generated for a given increment in intracellular calcium concentration. This increment in force for a given increment in intracellular calcium concentration is more pronounced when the arteries are stimulated by pharmacomechanical methods (32, 33). Clinically, myofilament calcium sensitivity plays a key role in contractile function of vascular smooth muscle during hypertension, myometrium during parturition and in airway smooth muscle during asthma (65). When myofilament calcium sensitivity following G-protein coupled receptor stimulation was observed from a developmental perspective, it was found to be significantly greater in immature than mature arteries (2, 3). Studies on regulation of

myofilament calcium sensitivity have revealed that a number of factors such as rho-kinase (26, 41), PKC (4, 33), caldesmon and calponin (50, 54, 79) play a key role in its regulation. To organize all these different mechanisms that regulate myofilament calcium sensitivity, they can be classified into two main families. The first includes those that determine the relationship between intracellular calcium concentration and extent of myosin light chain phosphorylation and thereby regulate thick filament contractile function (53). These mechanisms can be collectively considered as mediators of thick filament regulation. The second family includes those mechanisms that influence the relations between the extent of myosin light chain phosphorylation and force generated by the contractile proteins. These latter mechanisms can be collectively considered to be the mediators of thin filament regulation. More recent studies have demonstrated that both thick filament and thin filament regulation change with age, and that thick filament regulation is upregulated in immature compared to mature arteries (64).

Thick filament regulation plays a key role in the initiation of smooth muscle contraction. The extent of myosin light chain phosphorylation at any given moment is the net effect of the activities of myosin light chain kinase and myosin light chain phosphatase. Studies investigating thick filament regulation have focused much of their attention on myosin light chain phosphatase (MLCP) activity and its regulation. MLCP is a heterotrimeric protein with a regulatory subunit (MYPT1) and catalytic subunit (PP1c). There are three general mechanisms that regulate MLCP activity by: (i) phosphorylating MYPT1; (ii) dissociating MLCP structure; and (iii) inhibition of activity by CPI-17. All these mechanisms involve specific kinases that increase MLC phosphorylation by depressing MLCP activity. PKC ϵ is a specific kinase that can phosphorylate MYPT1 and

inhibit dephosphorylation of myosin light chain (80). Regarding dissociation of MLCP structure, arachidonic acid has been reported to separate MYPT1 from PP1c and thereby inhibit dephosphorylation of myosin light chain (22). Other studies have shown that phosphorylation of MYPT1 subunit at Thr696 inhibits its activity (34, 41). Other kinases, such as Zip-like kinase (44) and Zip kinase (55), are also likely to be involved in phosphorylation at Thr696 even though their physiological relevance is unknown. Regarding CPI-17 mediated inhibition of MLCP activity; the binding affinity of CPI-17 for PP1c is regulated by phosphorylation of CPI-17 at Thr38 by PKC. Phosphorylated CPI-17 can bind to PP1c and inhibit its activity. Other kinases, such as Rho-kinase (42) and Zip like kinase (44), can also phosphorylate CPI-17 at the same site. All these studies indicate the complex pathways involved in regulation of MLCP.

In contrast to MLCP, relatively very few studies have focused on the role of MLCK in regulating myofilament calcium sensitivity (21, 81). When the physiological significance of MLCK phosphorylation during cycles of contraction and relaxation in smooth muscles was investigated, it was found that MLCK phosphorylation and dephosphorylation occurred at rates sufficient to modulate the Ca²⁺ sensitivity of myosin light chain phosphorylation (85). These results indicate that MLCK is sensitive to small increases in intracellular Ca²⁺ during the initiation of contraction and has an important role in regulation of thick filament reactivity. Recent publications from our lab have shown that myofilament calcium sensitivity of fetal arteries is upregulated compared to adult arteries (64). Additional studies have further shown that thick filament regulation is also upregulated in fetal compared to adult arteries (64). Because thick filament regulation is a function of both MLCK and MLCP activities, these results suggest that

either MLCK and/or MLCP activities are different in fetal and adult arteries. Even when MLCP is completely inhibited by phosphatase inhibitors, age related differences in thick filament regulation are still evident, however. This observation suggests the possibility that MLCK activity may be involved in age-related differences in myofilament calcium sensitivity. Other studies of MLCK activity have shown that it plays an important role in maintaining contractility in saphenous vein (43), pulmonary arteries (6, 7), and myometrium (84). Given this background, the core hypothesis of this project is that age-related differences in myofilament calcium sensitivity involve up-regulation of MLCK activity in fetal compared to adult arteries. A systematic investigation of this hypothesis will illuminate the contribution of MLCK activity to postnatal maturation of vascular contractile function.

Significance

The proposed studies are important from both basic science and clinical science perspectives. From the basic science point of view, the proposed experiments will be the first to offer a quantitative and comprehensive assessment of age-related differences in MLCK abundance and intrinsic activity. Another highly unique aspect of these studies is that these measurements will utilize a custom-designed rapid-freeze apparatus that can electrically stimulate the tissue and simultaneously freeze it at very short intervals of time. These studies will be the first to compare age-related differences in MLCK activities under both in-situ and in-vitro conditions. These novel assessments will give the most physiologically relevant estimates of MLCK activity available to date. Because it is clear that maturation alters thick filament regulation, the proposed studies, regardless of outcome, should clearly indicate the relative extents to which changes in MLCK

abundance, intrinsic activity, and fractional activation contribute to the age-dependent differences in myofilament calcium sensitivity.

From a clinical science perspective, the proposed experiments will help in understanding the mechanisms involved in adaptation of the fetal cardiovascular system for postnatal life. At birth, arterial blood pressure, heart rate, cardiac output increases and vascular resistance must rapidly adjust to these changes. Failure to make these adjustments contributes to central and peripheral vascular disorders including neonatal stroke (86), intracranial hemorrhage (82) and respiratory failure (13). Although the reasons for these disorders are attributed to functional immaturity of cardiovascular system, the proposed studies will explore the role of MLCK and should identify a possible target for new strategies of pharmacological management of NICU neonates with cerebrovascular and cardiovascular instabilities.

CHAPTER 2

MAXIMAL STIMULATION-INDUCED IN SITU MYOSIN LIGHT CHAIN KINASE ACTIVITY IS UPREGULATED IN FETAL COMPARED TO ADULT OVINE CAROTID ARTERIES

Elisha R. Injeti¹, Renan J. Sandoval¹, James M. Williams¹, Alexander V. Smolensky²,
Lincoln E. Ford² and William J. Pearce¹

¹Divisions of Physiology and Pharmacology, Center for Perinatal Biology,
Loma Linda University School of Medicine, Loma Linda, California, 92354

²Department of Medicine, Indiana University School of Medicine, 1800 N. Capitol
Avenue, Indianapolis, IN 46202, USA

Running Head

In Situ MLCK Activity and Postnatal Maturation

Correspondence

William J. Pearce, Ph.D.

Departments of Physiology and Pharmacology
Loma Linda University School of Medicine, Loma Linda, CA, 92354
e-mail: wpearce@llu.edu, phone: 909-558-4800 ext 45210

Abstract

Postnatal decreases in vascular reactivity involve decreases in the thick filament component of myofilament calcium sensitivity, which is measured as the relation between cytosolic calcium concentration and the extent of myosin light chain (MLC₂₀) phosphorylation. The present study tests the hypothesis that downregulation of thick filament reactivity is due to downregulation of myosin light chain kinase (MLCK) activity, in adult compared to fetal arteries. Total MLCK activity, estimated as % MLC₂₀ phosphorylated/sec in intact arteries during optimal inhibition of myosin light chain phosphatase activity, was significantly less in adult ($6.56 \pm 0.29\%$) than in fetal ($7.39 \pm 0.53\%$) preparations. The abundances of MLC₂₀ did not differ significantly in adult and fetal arteries and averaged 1.42 ± 0.21 and 1.21 ± 0.37 $\mu\text{g}/\text{mg}$ wet weight, respectively. Correction of MLCK activities for differences in MLC₂₀ abundance yielded values of 93.2 ± 4.1 and 89.4 ± 6.4 ng MLC₂₀ phosphorylated/sec/mg wet weight, respectively; again, these values were not significantly different. MLCK abundance, however, varied significantly with age and averaged 354.7 ± 25.6 and 58.7 ± 4.24 ng MLCK/mg wet weight in adult and fetal arteries, respectively. Normalization of MLCK activities for MLCK abundance yielded values (in ng MLC₂₀ phosphorylated/sec/ng MLCK) that were significantly less in adult (0.26 ± 0.01) than in fetal (1.52 ± 0.11) arteries. Together, these results emphasize the importance of normalization of MLCK activities relative to MLC₂₀ and MLCK abundances, and indicate that downregulation of apparent specific activity of MLCK contributes significantly to downregulation of thick-filament reactivity in adult compared to fetal ovine carotid arteries.

Key words

Myofilament calcium sensitivity, postnatal maturation, regulatory myosin light chain, thick filament reactivity.

Introduction

Cardiovascular instability is a common feature of many infants in neonatal intensive care facilities. Systematic investigation of this symptomology has revealed that regulation of vascular contractility varies markedly between immature and mature arteries (5, 42). Previous studies from our lab have shown that these age-related differences in contractility involve major differences in intracellular calcium regulation. For equivalent contractile tensions, immature carotid arteries require greater calcium uptake than mature arteries, indicating a greater contractile dependence of immature arteries on extracellular calcium (54). Other studies have further demonstrated that the relative size of intracellular calcium stores change significantly during postnatal maturation (39). Despite these important differences in calcium regulation, however, intracellular calcium dynamics alone cannot completely explain the age-related differences in regulation of vascular contractility. As shown in multiple recent studies, differences in regulation of myofilament calcium sensitivity also contribute heavily to age-related changes in vascular contractility (1, 2).

By definition, myofilament calcium sensitivity is the increment in force generated for a given increment in intracellular calcium concentration (48). Changes in myofilament calcium sensitivity influence contractile function of vascular smooth muscle during hypertension, in myometrium during parturition, and in airway smooth muscle during asthma (47). Regulation of calcium sensitivity, in turn, is mediated through both

thick filament regulatory pathways that establish the relation between intracellular calcium concentration and myosin light chain phosphorylation, and thin filament regulatory pathways that determine the relations between myosin light chain phosphorylation and contractile force (38, 46). When examined from a developmental perspective, G-protein coupled receptor stimulation has enhanced myofilament calcium sensitivity to a much greater extent in immature than in mature cerebral arteries (2, 3). Additional detailed studies have further revealed that the extent of myosin light chain phosphorylation was greater for a given increment of cytosolic calcium in fetal than in adult arteries, suggesting that thick filament regulation was upregulated in the immature arteries (46). In contrast, myosin light chain kinase (MLCK) and myosin light chain phosphatase (MLCP), which are the two main enzymes that dominate thick filament reactivity, were less abundant in fetal than in adult arteries (46). Together, these findings indicate that thick filament reactivity, and the enzymes that govern it, change dramatically during postnatal maturation

To date, most studies of stimulation-induced changes in myosin light-chain phosphorylation have focused on regulation of MLCP (48). Whereas this enzyme is clearly regulated by numerous pathways, MLCK also plays a critically important role in regulation of contraction in both smooth muscle and non-muscle cells. Through a sequence of reactions that are particularly prominent in smooth muscle, calcium-dependent MLCK activation results in MLC_{20} phosphorylation, activation of myosin II actomyosin ATPase activity, initiation of cross-bridge cycling and force development. As the main high-speed kinase responsible for phosphorylating regulatory myosin light chain, MLCK is both necessary and sufficient to initiate smooth muscle contraction (20).

Correspondingly, MLCK-dependent regulation of contractile function has been carefully detailed under both physiological and pathophysiological conditions in many preparations including saphenous vein (31), pulmonary arteries (6) and myometrium (53). In light of this rich background, we designed the present studies to explore the hypothesis that age-related differences in myofilament calcium sensitivity involve up-regulation of MLCK activity in fetal compared to adult arteries. To maximize relevance to contractile function, the experimental approach relied on rapid measurements of MLC₂₀ phosphorylation in whole arteries. Owing to the extensive literature documenting changes in ovine carotid contractility during postnatal maturation, all experiments employed this model.

Materials and Methods

General Preparation

Common carotid arteries were harvested from young adult sheep (18-24 months old) following i.v. injection of 100 mg/kg pentobarbital. Fetal carotid arteries were collected after delivery of each fetus (~140 days gestation) from its pregnant ewe by a midline vertical laparotomy, after which the fetus was rapidly killed by cardiac excision. The arteries were cleaned of extraneous connective and adipose tissue and the endothelium was removed by passing a roughened needle through the lumen, as described in multiple previous studies (40). All procedures used in these studies were approved by the Animal Research Committee of Loma Linda University and adhered to all policies and practices outlined in the National Institutes of Health *Guide for the Care and Use of Laboratory Animals*

Determination of MLCK Abundance

Common carotid arteries from fetal and adult sheep were pulverized in liquid nitrogen using a custom made stainless steel mortar and pestle and then homogenized with glass-on-glass in 4 volumes of buffer containing 0.5 M NaCl, 50 mM Tris HCl at pH 7.5, 10 mM MgCl₂, 1 mM EDTA, 1 mM EGTA, 0.1 mM phenylmethylsulfonyl fluoride, 0.5% Protease Inhibitor Cocktail (Sigma, P8340), and 0.1% betamercaptoethanol. Following centrifugation at 15,000 rpm for 15 minutes at 4⁰ C, the supernatant was assayed for total protein content (Biorad, #500-0006). For each determination, 20 µg of total protein were loaded on a 15-lane, 8% SDS-PAGE gel, and run at 15 mA for 90 minutes and then transferred onto nitrocellulose membrane. The membrane was blocked overnight at 4⁰ C with 5% non-fat dry milk in 20 mM Tris HCl at pH 7.5, 500 mM NaCl and 0.1% Tween-20 and then probed with mouse anti-MLCK primary antibody (Sigma, M7905) at 1:7,000 dilution for 2 hours. Primary antibody-antigen complexes were detected with a goat anti-mouse secondary antibody (Pierce, #1858413), and visualized using direct photon capture with a CCD camera (AlphaInnotech, Chemi-Imager). Adjacent lanes of each gel were loaded with 6 different quantities of a reference MLCK standard prepared from ovine carotids to enable relative quantification. The reference MLCK standard was further calibrated for absolute quantification with purified MLCK from chicken gizzard, which was a gift from Dr. Christine R. Cremo.

Determination of MLC₂₀ Abundance

Common carotid arteries from fetal and adult sheep were pulverized in liquid nitrogen using a custom made stainless steel mortar and pestle. The pulverized tissue was extracted for 2 hours using a buffer containing 8 M Urea, 20 mM Tris, 23 mM Glycine,

10 mM EGTA, 10 mM DTT, 5 mM NaF, 10% Glycerol at pH 8.6 with a tissue to buffer ratio of 1:300. After two hours of extraction on an orbital shaker, the homogenates were centrifuged at 12,000G for 20 minutes after which the supernates were removed and the pellets were extracted a second time. The supernates were combined and their absolute content of MLC₂₀ was assayed by separating 10 µl sample aliquots on 15% SDS gels at a constant voltage (100V) for 2 hours. Varying known quantities of purified MLC₂₀ from chicken gizzard was run on multiple adjacent lanes to enable construction of a standard curve. The purified MLC₂₀ used as an absolute reference was prepared from chicken gizzard and was a gift from Dr. Christine R. Cremo. The gels were transferred onto nitrocellulose membranes at constant current (50 mA) for 3 hours after which immunoblotting was performed as previously described (46). Briefly, membranes were blocked with 5% milk in TBS (20 mM Tris HCl, 500 mM NaCl, pH 7.5) for 90 minutes. The blocked membranes were incubated in primary anti-MLC antibody (Sigma, M4401) at 1:300 dilution with 5% milk in Tween-TBS for 3 hours, followed by incubation for 90 minutes at a 1:1000 dilution of a goat anti-mouse secondary antibody (Pierce, #1858413) conjugated with horse radish peroxidase. All washes were carried out with Tween-TBS containing 5% milk. Antibody-antigen complexes were detected by chemiluminescence using a mixture of equal volumes of enhanced luminol reagent and oxidizing reagent (Pierce, #34096). Membranes were then scanned to determine the integrated optical density values of MLC₂₀ bands using direct photon capture (Chemi-Imager, Alpha-Innotech), and these values were converted into MLC₂₀ masses using the standard curve on each membrane. To enable comparisons between age groups, the values of MLC₂₀ mass were expressed as µg MLC₂₀ per mg wet weight of tissue.

Determination of Optimal Length for Contractile Response in Intact Carotid Arteries

Given that maximum MLCK activity occurs during maximal rates of contraction, which in turn develop only at optimal artery stretch, the optimal stretch ratios for carotid arteries from each age group were determined. Common carotid arteries obtained from adult sheep and near term fetuses were cleaned of adhering tissues, cut into 2-mm lengths, and placed in Krebs solution containing 122 mM NaCl, 25.6 mM NaHCO₃, 5.56 mM dextrose, 5.17 mM KCl, 2.49 mM MgSO₄, 1.60 mM CaCl₂, 0.114 mM ascorbic acid and 0.027 mM EGTA that was continuously bubbled with 95% O₂ and 5% CO₂. Each segment was mounted within a warmed tissue bath on wires and suspended between a force transducer and a post attached to a micrometer. After equilibration in Krebs solution at 38.5 °C (normal ovine core temperature) for at least 30 minutes, micrometer readings were obtained at 0.05 g tension, which enabled measurements of unstressed diameter (D₀) for each segment. The artery segments were then stretched in regular multiples of unstressed baseline diameter to yield stretch ratios (D/D₀) ranging from 1.0 to 3.0 times unstressed diameter. At each stretch ratio, the arteries were briefly contracted with 122 mM K⁺ until a peak response was obtained, after which the segments were returned to normal Krebs and equilibrated for 30 minutes before the next increment in stretch was applied. When contractile responses to K⁺ had been recorded at all stretch ratios, active tensions were calculated and plotted against their corresponding stretch ratios for both fetal and adult arteries, as previously described (42).

Determination of Optimal Concentration of Myosin light Chain Phosphatase Inhibitors

Both adult and fetal carotid artery segments were cleaned, wire-mounted and then stretched to their optimal length. Following equilibration and initial contraction with 122

mM K⁺ Krebs, the arteries were washed three times with Na⁺ Krebs buffer and incubated with four different concentrations (0, 10, 30, and 100 nM) of calyculin-A for an hour. Next, the segments were instantly frozen after exactly 9 seconds of contraction with 122 mM K⁺ using an acetone/TCA freezing solution held on dry ice at -70 °C. Arteries were similarly frozen following incubation in four different concentrations (0, 3, 10, and 30 μL/mL) of Phosphatase Inhibitor Cocktail (Sigma, P2850). Frozen segments were extracted and analyzed on 10% urea glycerol gels to quantify the extent of myosin light chain phosphorylation as previously described (46). Briefly, the gels were loaded with equal amounts of total protein and run for two and half hours at constant voltage (200V) and then transferred onto nitrocellulose membrane at constant current (50 mA) for 3 hours. Membranes were then blocked as described in the section titled "Determination of MLC₂₀ abundance" and analyzed for MLC₂₀ phosphorylation.

Determination of Concentration and Time Dependent Effects of ML-7 on MLCK Activity

Artery segments from both fetal and adult animals were prepared as described in the previous section. Following equilibration and contraction with 122 mM K⁺ Krebs, the arteries were washed three times with Na⁺ Krebs and incubated with five different concentrations (0, 10, 30, 100, and 300 nM) of ML-7 for 30 minutes followed by incubation with Phosphatase Inhibitor Cocktail (10 μL/mL) for an hour. Next, the segments were instantly frozen after exactly 9 seconds of contraction with 122 mM K⁺ using an acetone/TCA buffer on dry ice at -70 °C. Frozen segments were extracted and analyzed on urea gels to quantify the extent of myosin light chain phosphorylation as previously described (46). In a companion set of experiments, the time course of MLC₂₀

phosphorylation in response to potassium contraction was determined in the presence and absence of the optimal concentration of ML-7 to verify the efficacy of inhibition by ML-7. Arteries were frozen at exactly 0, 3, 6, and 9 seconds after contraction and analyzed for MLC₂₀ phosphorylation via urea gels.

Comparison of Chemical and Electrical Methods of MLCK Activation

To enable measurement of MLCK activity in intact tissues, we fabricated a rapid freeze apparatus following a design described by Maass-Moreno et al. (32). Our apparatus included a specialized low volume tissue cuvette (1.5 ml) equipped with large surface area platinum foil electrodes arranged to deliver high current density via electrical field stimulation (EFS). Current magnitude was measured directly via oscilloscope as a voltage-drop across a known resistance. Artery segments were mounted in the cuvette between a stationary hook and a force transducer that continuously monitored contractile force. The force transducer was mounted on a digital micrometer that enabled precise positioning ($\pm 1 \mu\text{m}$) and stretch of the artery segments. The time of freezing was precisely controlled using a computer-based timing circuit that operated high-speed solenoid valves and enabled very rapid (≤ 200 msec) exchange of Krebs buffer for -70°C acetone/TCA buffer. Arteries were stimulated with 100 mA of current at 60 Hz and 4 ms duration and simultaneously frozen at exactly 0, 2, 4 & 8 seconds and analyzed for MLC₂₀ phosphorylation. Comparison measurements were made, by stimulating with 122 mM K⁺ or 25 μM 5HT with freeze times of 0, 4, 8, & 12 seconds and subsequent analysis for MLC₂₀ phosphorylation.

Determination of current –contractile responses in intact carotid arteries:

Both fetal and adult arteries were mounted in the rapid freeze apparatus, equilibrated after which contractile responses to 122 K+ Krebs were determined. The segments were then rinsed, equilibrated in normal sodium Krebs buffer for one hour, then stimulated with graded EFS currents of 40, 50, 55, 60, 70, 75, 80, 90 & 100 mA. Contractile responses to EFS were normalized relative to the responses to K+-Krebs.

Determination of MLCK Activity in Intact Carotid Arteries

To measure MLCK activity, *in-situ*, common carotid arteries were prepared as described in section titled “*Determination optimal length for contractile response in intact carotid arteries*” and then mounted in the rapid freeze apparatus. Following equilibration and contraction with 122 mM K+ Krebs, the arteries were washed and incubated in 10 μ L/mL of PIC for an hour. Next, EFS (90 mA @ 60 Hz) was applied and segments were frozen at 0, 1, 2, and 3 seconds of stimulation. Frozen segments were extracted and analyzed on urea gels to quantify the extent of myosin light chain phosphorylation as described in section titled “*Determination of MLC₂₀ abundances*”. The slope of this relation, which was an estimate of the rate of phosphorylation of myosin light chain, was calculated as a measure of MLCK activity. The apparent specific activity of MLCK was estimated by dividing the rate of MLC₂₀ phosphorylation by absolute MLCK abundance.

Calculations and Statistics

Standard curves relating protein mass to optical density in Western blots, or stimulation current to contractile response, were fit to the logistic equation using least –

squares error minimization routines, and sample protein masses were calculated directly using the inverse function of the best fit standard curve. The abundances of MLCK and MLC₂₀ were calibrated relative to MLCK and MLC₂₀ purified from chicken gizzard and were expressed in units of ng MLCK. Values of %MLC₂₀ phosphorylation values were calculated as the unphosphorylated mass divided by the sum of phosphorylated and unphosphorylated masses as previously described (46). Relations between %MLC₂₀ phosphorylation and inhibitor concentrations or time were fit to rectangular hyperbolae, also using least-squares error minimization routines. Throughout the text, all values indicate the mean ± the standard error for the number of animals indicated; values of N refer to the numbers of animals and not the numbers of segments or experiments unless indicated otherwise. Unpaired comparisons between two variables were performed using Behren's-Fisher comparisons with pooled variance. All data sets were verified to be normally distributed using SPSS v16 software. In all cases, statistical significance implies P<0.05.

Results

A total of 207 and 245 carotid segments were taken for study from 29 ovine fetuses and 35 adult sheep respectively.

Effect of Postnatal Maturation on MLCK and MLC₂₀ Abundances

Estimates of MLCK abundance in fetal tissue averaged 58.7 ± 4.2 ng MLCK/mg tissue wet weight. These values were significantly less than average MLCK in adult tissue (354.7 ± 25.6 ng MLCK/mg tissue wet weight). MLCK abundance was 6.03 ± 0.96 fold greater in adult than in fetal arteries (**Figure 1**). None of the gels examined exhibited

more than a single immunoreactive band for MLCK, and no evidence of a low molecular weight immunopositive product of MLCK (telokin) was observed in either age group.

MLC₂₀ abundance in fetal arteries averaged (1.21 ± 0.37 $\mu\text{g}/\text{mg}$ wet weight) whereas abundance in adult arteries averaged (1.42 ± 0.21 $\mu\text{g}/\text{mg}$ wet weight). These results indicate that MLC₂₀ abundances, unlike MLCK abundances, did not vary significantly with age.

Length–Tension Relations in Ovine Carotid Arteries

As shown in **Figure 2**, the stretch ratio (D/D_0) associated with the maximum contractile response was significantly greater in adult (2.58 ± 0.07) than in fetal (1.70 ± 0.06) arteries. These results agree with our previous findings that fetal and adult arteries have different optimum lengths, which are probably attributable to age-related differences in artery wall thickness and compliance (42)

Optimum Concentration of Myosin Light Chain Phosphatase Inhibitors

In both fetal and adult arteries, 30 nM calyculin-A maximally increased the %MLC₂₀ phosphorylation associated with contraction (**Figure 3, upper panel**). The maximum %MLC₂₀ phosphorylation averaged $47.9 \pm 3.40\%$ in fetal, and $27.6 \pm 1.46\%$ in adult, arteries. Maximal increases in %MLC₂₀ phosphorylation produced by Phosphatase Inhibitor Cocktail were observed at 10 $\mu\text{L}/\text{mL}$ in both age groups (**Figure 3, lower panel**), and maximum %MLC₂₀ phosphorylation averaged $50.9 \pm 2.57\%$ in fetal, and $55.6 \pm 3.10\%$ in adult arteries. Because PIC at 10 $\mu\text{L}/\text{mL}$ yielded greater maximal %MLC₂₀ phosphorylation than calyculin-A, all further studies used 10 $\mu\text{L}/\text{mL}$ PIC to inhibit MLCP. Because PIC was designed to inhibit more types of phosphatase than

calyculin-A (28), and the difference between the maximum %MLC₂₀ produced by PIC and calyculin A was much greater for adult than fetal arteries, the results also suggest that adult arteries may express a different combination of phosphatases than expressed in fetal arteries.

Concentration and Time Dependent Effects of ML-7 on MLCK Activity

ML-7 at a concentration of 100 μ M maximally inhibited both fetal and adult MLCK activity (**Figure 4, upper panel**). ML-7 also exhibited a dose-dependent decrease in contractile response of the artery segments in response to 122 mM K⁺ (data not shown). Using this optimal concentration of ML-7, its effects on the time courses of MLC₂₀ phosphorylation were then examined. As shown in **Figure 4 (lower panel)**, 100 μ M of ML-7 completely inhibited any time dependent increase in MLC₂₀ phosphorylation or contraction (data not shown) following 122 mM K⁺ stimulation. These results indicate that MLCK is most probably the only kinase involved in MLC₂₀ phosphorylation during the first 9 seconds of contraction. The results do not exclude MLC₂₀ phosphorylation by other kinases at later time points, but largely rule out the participation of non-MLCK phosphorylation during the initial contraction.

Comparison of Chemical and Electrical Methods of MLCK Activation

Electrical field stimulation yielded peak phosphorylation values at 2 seconds followed by a rapid decline. In contrast, contraction with 122 mM K⁺ and 25 μ M 5-HT exhibited peak values of MLC₂₀ phosphorylation after 8 seconds of stimulation (**Figure 5, upper panel**). The 5-HT and K⁺ results agreed with our previous measurements, and suggested that MLC₂₀ phosphorylation was very fast and was probably limited by the rate

of diffusion of the agonist through the artery wall in large arteries. Correspondingly, the data suggest that electrical field stimulation was the optimal approach for activating MLCK, *in situ*

Current–Tension Relations in Ovine Carotid Arteries

To assure maximal activation of MLCK, the contractile responses produced by graded currents of electrical field stimulation in both fetal and adult arteries were examined. As shown in **Figure 5 (lower panel)**, 90 mA of current at 60 Hz and 4 ms duration yielded 109% and 106% of the response to 122 mM K⁺-Krebs in fetal and adult arteries, respectively. Because these stimulation parameters yielded maximal contractile responses, they were used in all subsequent experiments.

Measurement of MLCK Activity in Intact Ovine Carotids

As shown in **Figure 6 (upper panel)**, both fetal and adult arteries reached peak MLC₂₀ phosphorylation in ≈ 2 seconds. The slopes of these curves, which were taken as a measure of total MLCK activity, averaged 7.39 ± 0.53 and 6.56 ± 0.29 %MLC₂₀ phosphorylation/sec in fetal and adult arteries, respectively. To correct for age-related differences in MLC₂₀ abundances, the %MLC₂₀ phosphorylation values were multiplied by MLC₂₀ abundance to calculate maximal tissue rates of MLC₂₀ phosphorylation, which averaged 93.2 ± 4.1 and 89.4 ± 6.4 ng MLC₂₀ phosphorylated per second per mg wet weight in adult and fetal arteries, respectively; these values were not significantly different. To correct for age-related differences in MLCK abundances, these activity values were normalized relative to MLCK abundance yielding average activity values of

0.26 ± 0.01 and 1.52 ± 0.11 ng MLC₂₀ phosphorylated/sec/ng MLCK in adult and fetal arteries, respectively (**Figure 6 lower panel**); these values were significantly different.

Discussion

Among the many significant contributions made by the late Andrew Somlyo, perhaps one of the most important was his identification of the critical importance of myofilament calcium sensitivity as a determinant of smooth muscle contractility (27). This discovery fueled a rapid sequence of investigations into the mechanisms translating changes in cytosolic calcium concentration into increased MLC₂₀ phosphorylation and subsequent force development (48). In light of abundant evidence that myosin phosphatase was subject to multiple pathways of regulation (16), numerous studies have identified arachidonic acid (13), protein kinase C (34), rho kinase (25), CPI-17 (30), protein kinase G (50), and zip kinase (33) as regulators of myosin phosphatase activity, and thus of myofilament calcium sensitivity. In contrast, very little attention has been paid to the role of MLCK as a determinant of myofilament calcium sensitivity, due in large part to evidence suggesting that endogenous MLCK activity is subject predominantly to inhibition and not activation (49), which diminishes its potential to explain physiological enhancement of myofilament calcium sensitivity. Aside from this perspective, however, multiple lines of evidence have demonstrated that myofilament calcium sensitivity is upregulated in immature compared to mature arteries (2), as is the relation between cytosolic calcium concentration and MLC₂₀ phosphorylation (46). Because this upregulation persists even in the presence of inhibition of myosin phosphatase activity (**Figure 3**), developmental differences in myofilament calcium sensitivity appear to involve significant differences in MLCK activity.

For MLCK, multiple studies have demonstrated that changes in its activity involve significant changes in its abundance in multiple tissue types including airway smooth muscle (22), venous smooth muscle (31), and arterial smooth muscle (15). Consistent with this view, Western blots revealed a 6.0-fold greater abundance of MLCK in adult compared to fetal arteries (**Figure 1**). This result agreed with previous studies of the effects of postnatal maturation on MLCK abundance in rat pulmonary arteries (6). Regarding the MLCK isoform detected, other studies have shown that MLCK is a product of a single gene, but has two splice variants ranging from 130-150 kDa (short MLCK) and 208-214 kDa (long MLCK) (48). During chicken embryogenesis, and presumably vertebrate embryogenesis as well, the expression of mRNA and protein of the long isoform MLCK was more prominent (11). In our Western blots, we did not find multiple isoforms of MLCK, or the c-terminal truncation product telokin (41), in either age group. These studies strongly suggest that MLCK abundance increases dramatically during postnatal maturation and this alone cannot explain the greater thick filament reactivity observed in fetal compared to adult arteries (46).

The tissue activity for any enzyme is a product of both its abundance and its specific activity. To examine the potential involvement of postnatal changes in the specific activity of MLCK, the present approach focused on activity measurements made in whole arteries instead of in broken cell preparations. Although this approach differed from the majority of previous studies of MLCK activity, it offered multiple advantages, including preservation of the spatial organization and interaction of MLCK with other smooth muscle contractile proteins. Previous studies have demonstrated convincingly not only that MLCK binds both actin and myosin with high affinity (12), but also that protein-

protein interactions could potentially influence MLCK function (26). Another advantage of whole artery measurements was that the endogenous concentrations of MLCK along with its substrate and cofactors, as well as possible endogenous activators and inhibitors were fully preserved. Previous studies have suggested strongly that the levels of many of these proteins are labile and can change in response to numerous physiological perturbations including development, pregnancy and hormonal treatment (8, 35, 53). In light of the greater physiological relevance of *in situ* studies, a few previous studies of MLCK function have also employed *in situ* measurements of MLCK activity (9, 21).

In intact arteries, the force and velocity of contraction are highly dependent on the extent of stretch (44). Because maximal force generation in intact arteries occurs only at optimal stretch, it follows that maximal MLCK activity should also be observable only at optimal stretch (14). Given this consideration, the first priority of these studies was to determine optimum length for both fetal and adult carotids using a classical functional “length-tension” approach. Consistent with previous findings (42), adult arteries required a significantly greater extent of stretch to attain optimum length than did fetal arteries (**Figure 2**). This large magnitude of age-related difference in optimum length suggests that measurements of *in situ* MLCK activity not made at optimal length could lead to significant errors. Because previous studies of *in situ* MLCK activity have not always acknowledged the importance of optimal length as a prerequisite for reliable estimation of maximal *in situ* MLCK activity, some inconsistencies among such studies may arise directly from this issue (8, 21).

Given that the extent of MLC_{20} phosphorylation reflects the integrated difference between the activities of MLCK and myosin phosphatase, any estimate of MLCK activity

in situ requires complete inhibition of myosin phosphatase. As shown by Ishihara and colleagues (18) smooth muscle phosphatase can be potently inhibited by calyculin-A in the sub-micromolar concentration range. Addition of an optimal concentration of calyculin-A (30 nM) to whole arteries significantly increased the rate of MLC₂₀ phosphorylation indicating that calyculin-A was effective in our preparations (**Figure 3 upper panel**). However, further validation experiments indicated that 10 µl/ml of the Phosphatase Inhibitor Cocktail (PIC, Sigma, P2850), which contains multiple phosphatase inhibitors (cantharidin, bromo-tetramisole and microcystin LR), was even more effective than calyculin alone and produced an optimally effective inhibition of phosphatase activity as indicated by greater overall values of %MLC₂₀ phosphorylation (**Figure 3 lower panel**). In light of these results, all measurements of *in situ* MLCK activity included 10 µl/ml of the Phosphatase Inhibitor Cocktail. Here again, not all previous studies of *in situ* MLCK activity have included optimal concentrations of phosphatase inhibitors; the variable extent of phosphatase inhibition probably contributes significantly to the heterogeneity among the results of such studies (8, 9, 21).

Aside from abundant evidence suggesting that MLC₂₀ is the only known substrate for MLCK (24), a variety of other kinases also appear capable of phosphorylating MLC₂₀. These include Protein Kinase A (51), Protein Kinase C (17), Rho-Kinase (4), Integrin-Linked Kinase (52), and P21 –Activated Kinase (7). A key feature of these other kinases, however, is that their rates of phosphorylation of MLC₂₀ are generally much slower than that of MLCK (36, 37), which suggests that measurements of MLC₂₀ phosphorylation over short time courses should reflect MLCK activity almost exclusively. To verify this concept, some measurements of MLCK activity included

varying concentrations of ML-7 (**Figure 4, upper panel**), a specific inhibitor of MLCK (45). These measurements indicated that 100 μM ML-7 maximally inhibited potassium-induced MLC_{20} phosphorylation in both fetal and adult arteries. More importantly, 100 μM ML-7 completely inhibited all phosphorylation of MLC_{20} during a 9-second exposure to potassium (**Figure 4, lower panel**), indicating that at least in fetal and adult ovine carotid arteries, MLCK is the only kinase phosphorylating MLC_{20} in less than 10 seconds.

Another important concern related to *in situ* measurements of MLCK activity is the rate of activation in an artery with multiple layers of smooth muscle. Upon exposure to a chemical stimulus such as potassium, the outermost cells will be activated first and the innermost cells will be activated only after a delay due to the time required for the agonist to diffuse through the artery wall (23). This problem can be particularly important when arteries of significantly different wall thicknesses are compared, as is the case for fetal and adult ovine carotid arteries (42). To verify the importance of this problem, we fabricated a vessel cuvette designed to enable highly accurate rapid freezing of artery segments based on a modification of the design first published by Maass-Moreno (32). This device made possible the activation of arterial rings with either pharmacological agonists or electrical field stimulation delivered by large surface area platinum plate electrodes. The key advantage of activation with electrical field stimulation was that it produced simultaneous activation of all smooth muscle cells within the mounted segment (23, 32). With this device, activation of smooth muscle with either 25 μM serotonin or 122 mM potassium-Krebs produced a significant increase in MLC_{20} phosphorylation that reached peak magnitude in approximately 8 seconds. In contrast, activation with

electrical field stimulation produced a much more rapid increase in MLC₂₀ phosphorylation that reached peak magnitude in approximately 2 seconds, after which phosphorylation levels decayed rapidly back to baseline values (**Figure 5, upper panel**). Based on these results, all further measurements of MLCK activity relied on activation only with electrical field stimulation. Further validation experiments indicated that maximal activation of both fetal and adult arteries were attained by stimulation current at or above 90 mA (**Figure 5, lower panel**).

Using our rapid-freeze apparatus, maximal activation with electrical field stimulation during optimal inhibition of myosin phosphatase activity produced increases in MLC₂₀ phosphorylation that were faster (as %MLC₂₀ phosphorylated/sec) in fetal (7.4%) than in adult (6.6%) artery segments (**Figure 6, upper panel**). In light of age-related differences in MLC₂₀ abundance, we also calculated the absolute tissue velocities of MLC₂₀ phosphorylation and these values (as ng MLC₂₀ phosphorylated/sec/mg wet weight) did not vary significantly among fetal (89.4 ± 6.4) and adult (93.2 ± 4.1) arteries. This finding agreed well with our previous findings in these artery types that maximum active stresses (in mN/mm²) also do not vary significantly among fetal and adult arteries (42). Together, these results suggest that both fetal and adult arteries are adapted to produce near-equivalent rates of MLC₂₀ phosphorylation and contractile forces, although through much different mechanisms. When *in situ* MLCK activity was estimated by normalizing the absolute tissue velocities of MLC₂₀ phosphorylation by MLCK abundance, the fetal values (in ng MLC₂₀ phosphorylated /ng MLCK /sec) were almost 6-fold greater (1.52 ± 0.11) than observed in adult (0.26 ± 0.01) arteries (**Figure 6, lower panel**). These large differences in MLCK specific activity appear to be counterbalanced by opposite

differences in MLCK abundance such that overall tissue velocities in MLC_{20} phosphorylation, and generation of contractile force, are similar in the two age groups.

As a whole, the present results emphasize the physiological importance of changes in MLCK activity during postnatal maturation of contractile function of ovine carotid arteries. The data suggest that increasing postnatal expression of MLCK is closely coordinated with parallel decreases in MLCK specific activity through unknown mechanisms. Age-related shifts in MLCK isoform do not appear to be involved based on Western blot results, but this conclusion requires further detailed exploration at both the proteomic and genomic levels. Post-translational modifications of MLCK activity are also possible, particularly in light of evidence that MLCK can serve as a substrate for multiple kinases abundant in smooth muscle (49). Another possibility is that MLCK may be differentially regulated by endogenous inhibitors, such as polyamines (43). Perhaps more likely, endogenous levels of calmodulin may vary with age (10), particularly in light of recent observations that calmodulin concentrations may be rate-limiting in some tissues (19). In addition, age-related differences in the extent of MLCK activation may also play a critical role, as suggested by a broad variety of evidence indicating that calcium handling and mobilization are very different in mature and immature arteries (39). Finally, it remains possible that the spatial organization of MLCK and MLC_{20} is very different in fetal and adult arteries; activation of MLCK that is not co-localized near MLC_{20} will produce neither phosphorylation nor contractile force. This possibility might also be a consequence of the growing list of non-kinase functions attributed to MLCK (26, 29). Aside from the mechanisms involved, the present data clearly indicate that postnatal changes in MLCK function make an important contribution to corresponding

changes in thick filament reactivity, myofilament calcium sensitivity, and overall vascular contractility.

Acknowledgements

The work reported in this manuscript was supported by USPHS Grants HL54120, HD31266, HL64867 and the Loma Linda University School of Medicine. The authors also acknowledge the excellent technical assistance and insights of Mr. James M. Williams. The generous gifts of purified MLCK and MLC₂₀ provided by Dr. Christine R. Cremo from the University of Nevada at Reno are also greatly appreciated.

References

1. Akopov SE, Zhang L, and Pearce WJ. Developmental changes in the calcium sensitivity of rabbit cranial arteries. *Biol Neonate* 74: 60-71, 1998.
2. Akopov SE, Zhang L, and Pearce WJ. Physiological variations in ovine cerebrovascular calcium sensitivity. *Am J Physiol* 272: H2271-2281, 1997.
3. Akopov SE, Zhang L, and Pearce WJ. Regulation of Ca²⁺ sensitization by PKC and rho proteins in ovine cerebral arteries: effects of artery size and age. *Am J Physiol* 275: H930-939, 1998 Sep.
4. Amano M, Ito M, Kimura K, Fukata Y, Chihara K, Nakano T, Matsuura Y, and Kaibuchi K. Phosphorylation and activation of myosin by Rho-associated kinase (Rho-kinase). *J Biol Chem* 271: 20246-20249, 1996.
5. Belik J, Halayko AJ, Rao K, and Stephens NL. Pulmonary and systemic vascular smooth muscle mechanical characteristics in newborn sheep. *Am J Physiol* 263: H881-886, 1992.
6. Belik J, Kerc E, and Pato MD. Rat pulmonary arterial smooth muscle myosin light chain kinase and phosphatase activities decrease with age. *Am J Physiol Lung Cell Mol Physiol* 290: L509-516, 2006.
7. Brzeska H, Szczepanowska J, Matsumura F, and Korn ED. Rac-induced increase of phosphorylation of myosin regulatory light chain in HeLa cells. *Cell Motil Cytoskeleton* 58: 186-199, 2004.
8. Chitano P, Voynow JA, Pozzato V, Cantillana V, Burch LH, Wang L, and Murphy TM. Ontogenesis of myosin light chain kinase mRNA and protein content in guinea pig tracheal smooth muscle. *Pediatr Pulmonol* 38: 456-464, 2004.
9. Chitano P, Worthington CL, Jenkin JA, Stephens NL, Gyapong S, Wang L, and Murphy TM. Ontogenesis of myosin light chain phosphorylation in guinea pig tracheal smooth muscle. *Pediatr Pulmonol* 39: 108-116, 2005.

10. Cho YH, Wheeler MA, and Weiss RM. Ontogeny of cyclic AMP and cyclic GMP phosphodiesterase activities and of calmodulin levels in guinea pig ureter. *J Urol* 139: 1095-1098, 1988.
11. Fisher SA and Ikebe M. Developmental and tissue distribution of expression of nonmuscle and smooth muscle isoforms of myosin light chain kinase. *Biochem Biophys Res Commun* 217: 696-703, 1995.
12. Gao Y, Ye LH, Kishi H, Okagaki T, Samizo K, Nakamura A, and Kohama K. Myosin light chain kinase as a multifunctional regulatory protein of smooth muscle contraction. *IUBMB Life* 51: 337-344, 2001 Jun.
13. Gong MC, Fuglsang A, Alessi D, Kobayashi S, Cohen P, Somlyo AV, and Somlyo AP. Arachidonic acid inhibits myosin light chain phosphatase and sensitizes smooth muscle to calcium. *J Biol Chem* 267: 21492-21498, 1992.
14. Hai CM. Length-dependent myosin phosphorylation and contraction of arterial smooth muscle. *Pflugers Arch* 418: 564-571, 1991.
15. Han YJ, Hu WY, Chernaya O, Antic N, Gu L, Gupta M, Piano M, and de Lanerolle P. Increased myosin light chain kinase expression in hypertension: Regulation by serum response factor via an insertion mutation in the promoter. *Mol Biol Cell* 17: 4039-4050, 2006.
16. Hartshorne DJ and Siemankowski RF. Regulation of smooth muscle actomyosin. *Annu Rev Physiol* 43: 519-530, 1981.
17. Ikebe M, Hartshorne DJ, and Elzinga M. Phosphorylation of the 20,000-dalton light chain of smooth muscle myosin by the calcium-activated, phospholipid-dependent protein kinase. Phosphorylation sites and effects of phosphorylation. *J Biol Chem* 262: 9569-9573, 1987.
18. Ishihara H, Martin BL, Brautigan DL, Karaki H, Ozaki H, Kato Y, Fusetani N, Watabe S, Hashimoto K, Uemura D, and et al. Calyculin A and okadaic acid: inhibitors of protein phosphatase activity. *Biochem Biophys Res Commun* 159: 871-877, 1989.
19. Isotani E, Zhi G, Lau KS, Huang J, Mizuno Y, Persechini A, Geguchadze R, Kamm KE, and Stull JT. Real-time evaluation of myosin light chain kinase

- activation in smooth muscle tissues from a transgenic calmodulin-biosensor mouse. *Proc Natl Acad Sci U S A* 101: 6279-6284, 2004.
20. Itoh T, Ikebe M, Kargacin GJ, Hartshorne DJ, Kemp BE, and Fay FS. Effects of modulators of myosin light-chain kinase activity in single smooth muscle cells. *Nature* 338: 164-167, 1989.
 21. Jiang H, Rao K, Halayko AJ, Liu X, and Stephens NL. Ragweed sensitization-induced increase of myosin light chain kinase content in canine airway smooth muscle. *Am J Respir Cell Mol Biol* 7: 567-573, 1992.
 22. Jiang H, Rao K, Liu X, Liu G, and Stephens NL. Increased Ca²⁺ and myosin phosphorylation, but not calmodulin activity in sensitized airway smooth muscles. *Am J Physiol* 268: L739-746, 1995.
 23. Kamm KE and Murphy RA. Velocity and myosin phosphorylation transients in arterial smooth muscle: effects of agonist diffusion. *Experientia* 41: 1010-1017, 1985.
 24. Kamm KE and Stull JT. Dedicated myosin light chain kinases with diverse cellular functions. *J Biol Chem* 276: 4527-4530, 2001.
 25. Kimura K, Ito M, Amano M, Chihara K, Fukata Y, Nakafuku M, Yamamori B, Feng J, Nakano T, Okawa K, Iwamatsu A, and Kaibuchi K. Regulation of myosin phosphatase by Rho and Rho-associated kinase (Rho-kinase). *Science* 273: 245-248, 1996 Jul 12.
 26. Kishi H, Mikawa T, Seto M, Sasaki Y, Kanayasu-Toyoda T, Yamaguchi T, Imamura M, Ito M, Karaki H, Bao J, Nakamura A, Ishikawa R, and Kohama K. Stable transfectants of smooth muscle cell line lacking the expression of myosin light chain kinase and their characterization with respect to the actomyosin system. *J Biol Chem* 275: 1414-1420, 2000.
 27. Kitazawa T, Kobayashi S, Horiuti K, Somlyo AV, and Somlyo AP. Receptor-coupled, permeabilized smooth muscle. Role of the phosphatidylinositol cascade, G-proteins, and modulation of the contractile response to Ca²⁺. *J Biol Chem* 264: 5339-5342, 1989.
 28. Knapp J, Aleth S, Balzer F, Schmitz W, and Neumann J. Calcium-independent activation of the contractile apparatus in smooth muscle of mouse aorta by protein

- phosphatase inhibition. *Naunyn Schmiedebergs Arch Pharmacol* 366: 562-569, 2002.
29. Kohama K, Ye LH, Hayakawa K, and Okagaki T. Myosin light chain kinase: an actin-binding protein that regulates an ATP-dependent interaction with myosin. *Trends Pharmacol Sci* 17: 284-287, 1996 Aug.
 30. Li L, Eto M, Lee MR, Morita F, Yazawa M, and Kitazawa T. Possible involvement of the novel CPI-17 protein in protein kinase C signal transduction of rabbit arterial smooth muscle. *J Physiol* 508 (Pt 3): 871-881, 1998.
 31. Liu G, Liu X, Rao K, Jiang H, and Stephens NL. Increased myosin light chain kinase content in sensitized canine saphenous vein. *J Appl Physiol* 80: 665-669, 1996.
 32. Maass-Moreno R, Burdyga T, Mitchell RW, Seow CY, Ragozzino J, and Ford LE. Simple freezing apparatus for resolving rapid metabolic events associated with smooth muscle activation. *J Appl Physiol* 90: 2453-2459, 2001 Jun.
 33. MacDonald JA, Borman MA, Muranyi A, Somlyo AV, Hartshorne DJ, and Haystead TA. Identification of the endogenous smooth muscle myosin phosphatase-associated kinase. *Proc Natl Acad Sci U S A* 98: 2419-2424, 2001 Feb 27.
 34. Masuo M, Reardon S, Ikebe M, and Kitazawa T. A novel mechanism for the Ca(2+)-sensitizing effect of protein kinase C on vascular smooth muscle: inhibition of myosin light chain phosphatase. *J Gen Physiol* 104: 265-286, 1994.
 35. Matsui K, Higashi K, Fukunaga K, Miyazaki K, Maeyama M, and Miyamoto E. Hormone treatments and pregnancy alter myosin light chain kinase and calmodulin levels in rabbit myometrium. *J Endocrinol* 97: 11-19, 1983.
 36. Miller-Hance WC, Miller JR, Wells JN, Stull JT, and Kamm KE. Biochemical events associated with activation of smooth muscle contraction. *J Biol Chem* 263: 13979-13982, 1988.
 37. Mita M, Yanagihara H, Hishinuma S, Saito M, and Walsh MP. Membrane depolarization-induced contraction of rat caudal arterial smooth muscle involves Rho-associated kinase. *Biochem J* 364: 431-440, 2002.

38. Murphy RA and Walker JS. Inhibitory mechanisms for cross-bridge cycling: the nitric oxide-cGMP signal transduction pathway in smooth muscle relaxation. *Acta Physiol Scand* 164: 373-380, 1998 Dec.
39. Nauli SM, Williams JM, Akopov SE, Zhang L, and Pearce WJ. Developmental changes in ryanodine- and IP(3)-sensitive Ca(2+) pools in ovine basilar artery. *Am J Physiol Cell Physiol* 281: C1785-1796, 2001 Dec.
40. Nauli SM, Zhang L, and Pearce WJ. Maturation depresses cGMP-mediated decreases in. *Am J Physiol Heart Circ Physiol* 280: H1019-1028, 2001 Mar.
41. Numata T, Katoh T, and Yazawa M. Functional role of the C-terminal domain of smooth muscle myosin light chain kinase on the phosphorylation of smooth muscle myosin. *J Biochem (Tokyo)* 129: 437-444, 2001.
42. Pearce WJ, Hull AD, Long DM, and Longo LD. Developmental changes in ovine cerebral artery composition and reactivity. *Am J Physiol* 261(2 Pt 2): R458-R465, 1991.
43. Qi DF, Schatzman RC, Mazzei GJ, Turner RS, Raynor RL, Liao S, and Kuo JF. Polyamines inhibit phospholipid-sensitive and calmodulin-sensitive Ca²⁺-dependent protein kinases. *Biochem J* 213: 281-288, 1983.
44. Rembold CM, Meeks MK, Ripley ML, and Han S. Longer muscle lengths recapitulate force suppression in swine carotid artery. *Am J Physiol Heart Circ Physiol* 292: H1065-1070, 2007.
45. Saitoh M, Ishikawa T, Matsushima S, Naka M, and Hidaka H. Selective inhibition of catalytic activity of smooth muscle myosin light chain kinase. *J Biol Chem* 262: 7796-7801, 1987.
46. Sandoval RJ, Injeti ER, Gerthoffer WT, and Pearce WJ. Postnatal maturation modulates relationships among cytosolic Ca²⁺, myosin light chain phosphorylation, and contractile tone in ovine cerebral arteries. *Am J Physiol Heart Circ Physiol* 293: H2183-2192, 2007.
47. Savineau JP and Marthan R. Modulation of the calcium sensitivity of the smooth muscle contractile apparatus: molecular mechanisms, pharmacological and pathophysiological implications. *Fundam Clin Pharmacol* 11: 289-299, 1997.

48. Somlyo AP and Somlyo AV. Ca²⁺ sensitivity of smooth muscle and nonmuscle myosin II: modulated by G proteins, kinases, and myosin phosphatase. *Physiol Rev* 83: 1325-1358, 2003 Oct.
49. Stull JT, Tansey MG, Word RA, Kubota Y, and Kamm KE. Myosin light chain kinase phosphorylation: regulation of the Ca²⁺ sensitivity of contractile elements. *Adv Exp Med Biol* 304: 129-138, 1991.
50. Surks HK, Mochizuki N, Kasai Y, Georgescu SP, Tang KM, Ito M, Lincoln TM, and Mendelsohn ME. Regulation of myosin phosphatase by a specific interaction with cGMP- dependent protein kinase Ialpha. *Science* 286: 1583-1587, 1999.
51. Walsh MP, Persechini A, Hinkins S, and Hartshorne DJ. Is smooth muscle myosin a substrate for the cAMP-dependent protein kinase? *FEBS Lett* 126: 107-110, 1981.
52. Wilson DP, Sutherland C, Borman MA, Deng JT, Macdonald JA, and Walsh MP. Integrin-linked kinase is responsible for Ca²⁺-independent myosin diphosphorylation and contraction of vascular smooth muscle. *Biochem J*, 2005.
53. Word RA, Stull JT, Casey ML, and Kamm KE. Contractile elements and myosin light chain phosphorylation in myometrial tissue from nonpregnant and pregnant women. *J Clin Invest* 92: 29-37, 1993.
54. Zurcher SD and Pearce WJ. Maturation modulates serotonin- and potassium-induced calcium-45 uptake in ovine carotid and cerebral arteries. *Pediatr Res* 38: 493-500, 1995.

Figure Legends

Figure 1: Abundance of MLCK in Ovine Carotid Arteries:

Supernates from artery homogenates containing 20 μg of total protein were loaded on 8% SDS-PAGE gels along with varying masses of a reference standard for MLCK in adjacent lanes. The integrated density values of MLCK were converted to their respective masses using a standard curve and then normalized to tissue wet weight. The results expressed here indicate abundance relative to the fetal values. Error bars indicate SEM for 7 fetal and 7 adult animals

Figure 2: Length-Tension Relations in Ovine Carotid Arteries:.

Carotid artery segments of fetal and adult sheep were wire mounted and stretched to D/D_0 ratios ranging from 1.0 to 3.0. At each stretch ratio, contractile responses to 122 mM K^+ were recorded and then normalized relative to maximum response. The vertical error bars indicate standard errors for a total of 79 artery segments from 5 fetuses and 96 artery segments from 6 adult sheep.

Figure 3: Optimum Concentrations of Calyculin-A and Phosphatase Inhibitor Cocktail for MLCP Inhibition.

Calyculin-A (upper panel) and Phosphatase Inhibitor Cocktail (PIC, lower panel) were added to inhibit MLCP activity. Artery segments from both age groups were incubated in 0, 10, 30, or 100 (nM) calyculin-A for an hour and then depolarized with 122 mM K^+ for 9 seconds, then immediately frozen and analyzed for MLC_{20} phosphorylation using urea glycerol gels (upper panel). Total of 20 artery segments from each group were used from 5 fetuses and 5 adult sheep. Similar measurements were conducted with PIC at 0, 3, 10, or 30 $\mu\text{l/ml}$ concentrations in 20 artery segments each from 5 fetus and 5 adults, respectively (lower panel). The results shown indicate averages \pm SEM for the number of fetal and adult sheep indicated in parentheses.

Figure 4: Concentration and Time Dependent Effects of ML-7 on MLCK Activity.

Concentration dependent effects of ML-7 on MLCK activity were by treatment with 0, 10, 30, 100 or 300 μM of ML-7 for 30 minutes followed by incubation with 10 $\mu\text{l/ml}$ of PIC for an hour. The segments were then instantly frozen after 9 seconds of contraction with 122 mM K^+ and analyzed for MLC_{20} phosphorylation (upper panel). Time courses of MLC_{20} phosphorylation were then determined in the presence and absence of 100 μM ML-7 (lower panel) by freezing at 0, 3, 6 and 9 seconds after contraction with 122 mM K^+ . A total of 65 segments each from 5 fetuses and 5 adult arteries were used for this study. All the results indicate averages \pm SEM for the number of fetal and adult sheep indicated in parentheses.

Figure 5: Validation of Activation Via Electrical Field Stimulation:

A total of 21 artery segments from three adults were wire mounted in a custom-made rapid freeze apparatus and stimulated with either electrical field stimulation, 122 mM K^+ or 25 μM 5HT and frozen at different time points (upper panel). The segments were then extracted and analyzed for MLC_{20} phosphorylation using urea glycerol gels. Peak MLC_{20} phosphorylation was observed much earlier with electrical stimulation than with either form of chemical stimulation.

To determine the optimal current used for electrical field stimulation, two fetal artery segments and two adult artery segments were mounted in vitro, equilibrated at optimal length, and electrically stimulated at 60 Hz with duration of 4 msec at 40, 50, 55, 60, 70, 75, 80, 90, and 100 mA (lower panel). The corresponding contractile responses were normalized relative to the responses to 122 mM K^+ . The data shown represent the means of 3 fetal and 3 adult artery segments. To confirm that 90 mA produced maximal activation in all segments, each segment used was first contracted with 122 mM K^+ , and the resulting contractile response was used to normalize all subsequent responses to EFS. For all segments used, EFS produced more than 100% of the contractile force produced by 122 mM K^+ .

Figure 6: MLCK Velocity in Intact Ovine Carotid Arteries:

Fetal and adult artery segments were wire-mounted and positioned in the rapid freeze apparatus, activated via electrical field stimulation, and frozen at exactly 0, 1, 2 & 3 seconds. The segments were then analyzed for MLC₂₀ phosphorylation. The initial rate of change of MLC₂₀ phosphorylation was taken as a measure of MLCK velocity (upper panel). To correct for age-related differences in MLC₂₀ and MLCK abundances, the %MLC₂₀ phosphorylation ratios were multiplied by the corresponding mass ratios of MLC₂₀/MLCK abundance (lower panel). The initial slopes (“V=”) are given for each age group. A total of 20 artery segments from 5 fetuses and 20 artery segments from 5 adults were used for this study. The values shown indicate averages ± SEM, and asterisks indicate statistically significant differences between corresponding fetal and adult values.

Figures

FIGURE-1

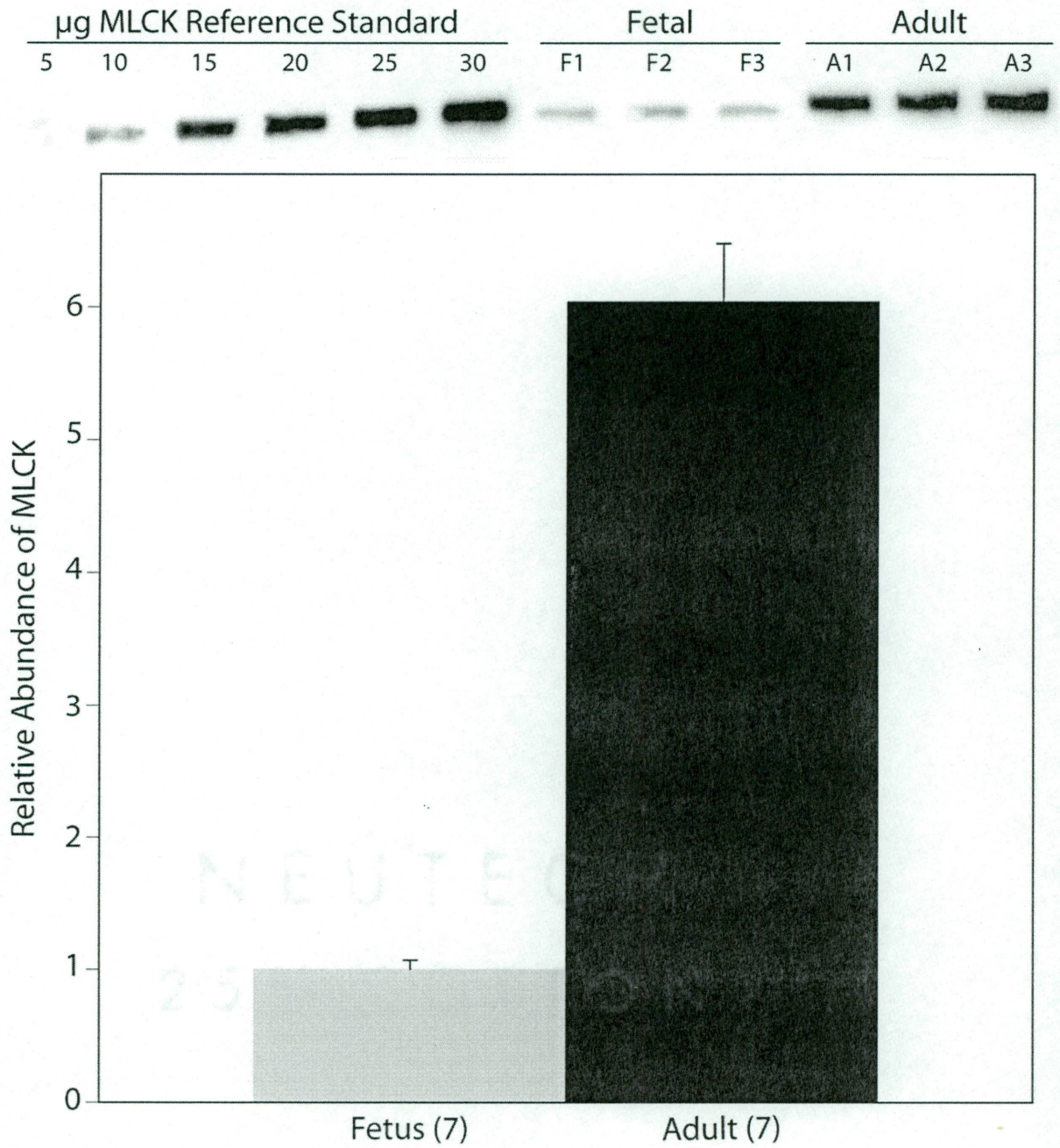
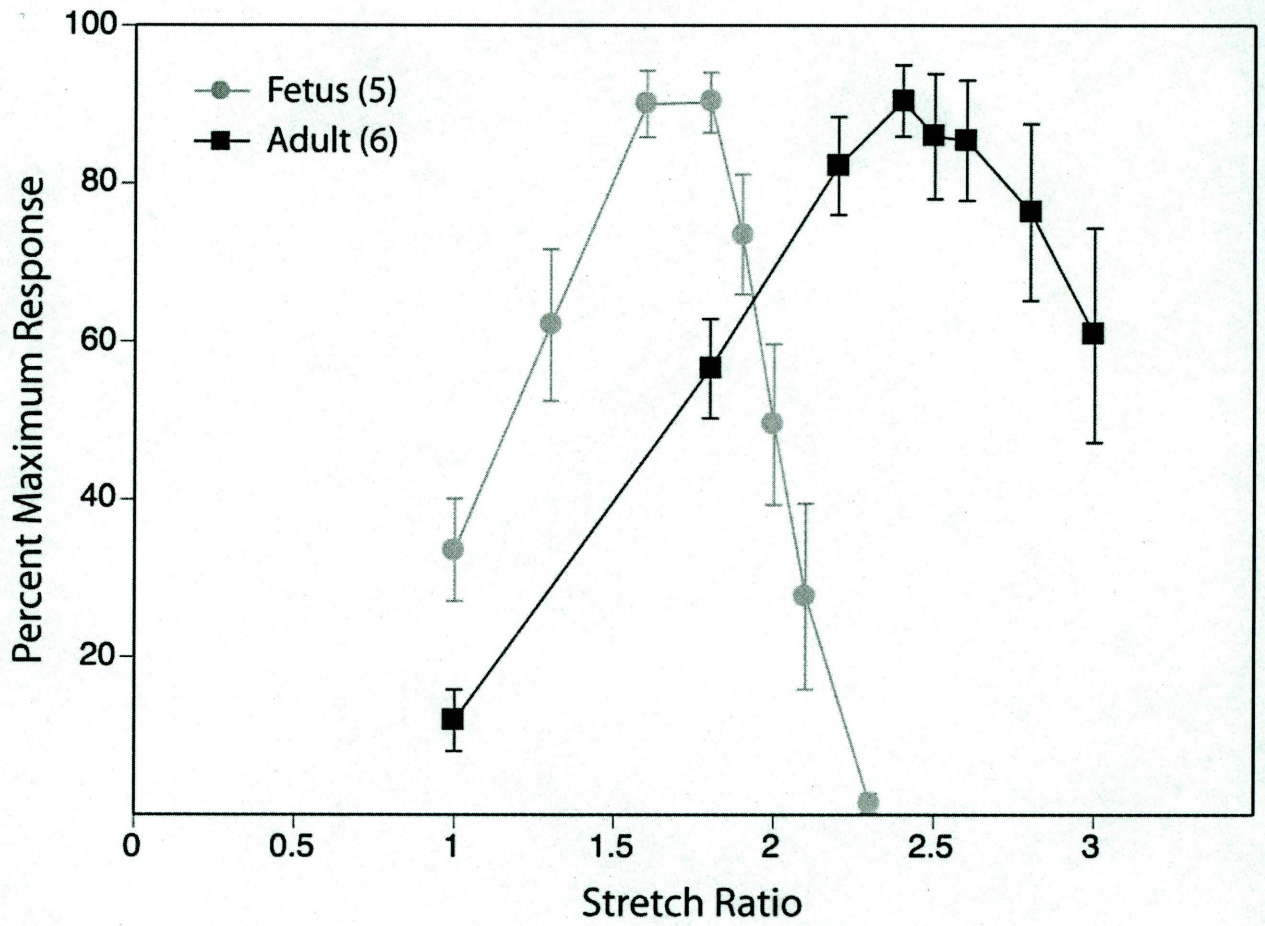


FIGURE-2



NEUTECH
25% COTTON

FIGURE-3

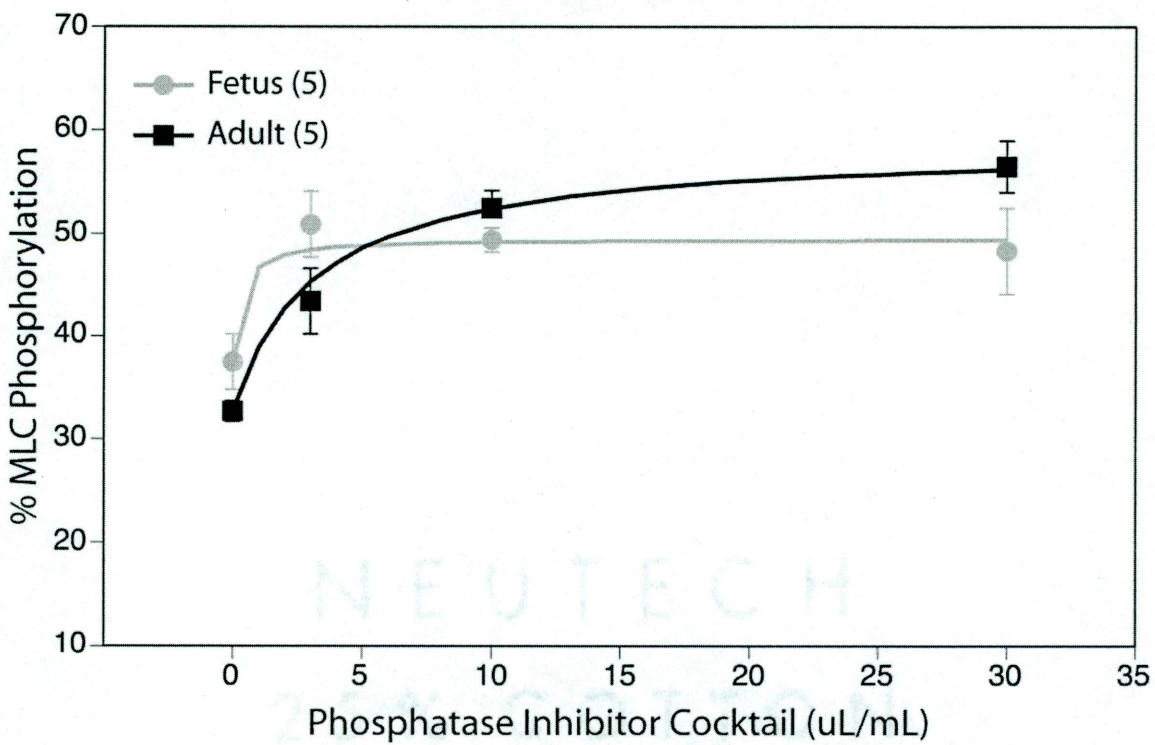
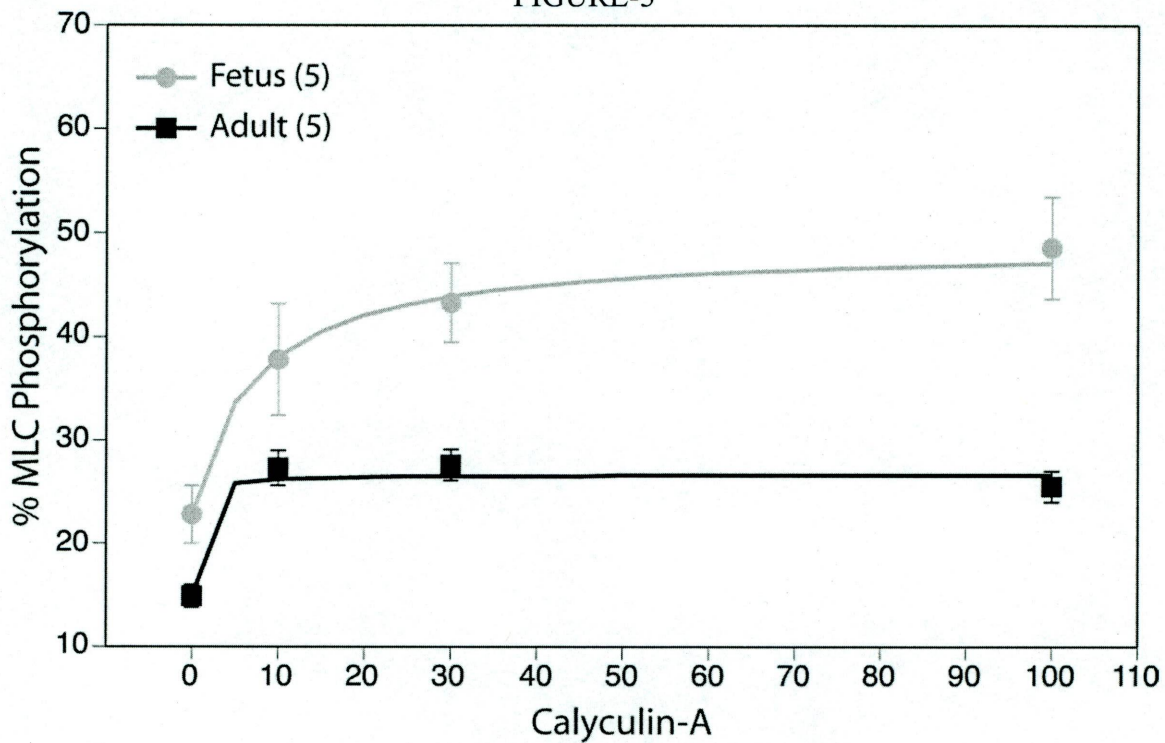


FIGURE-4

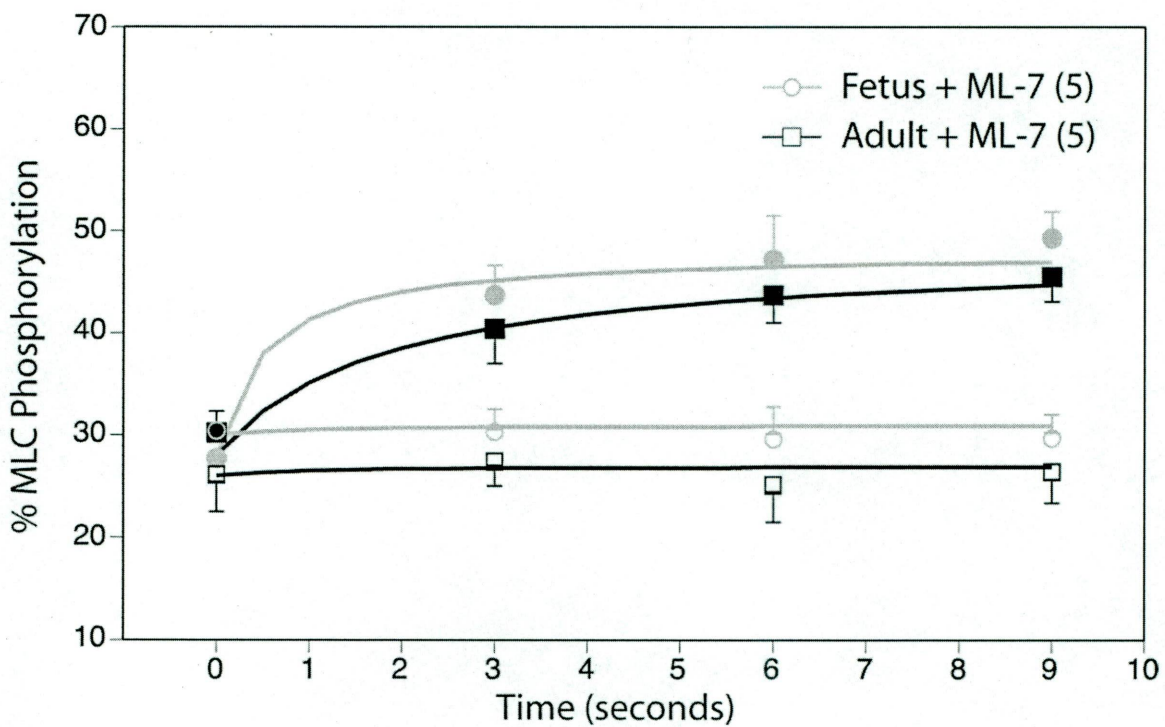
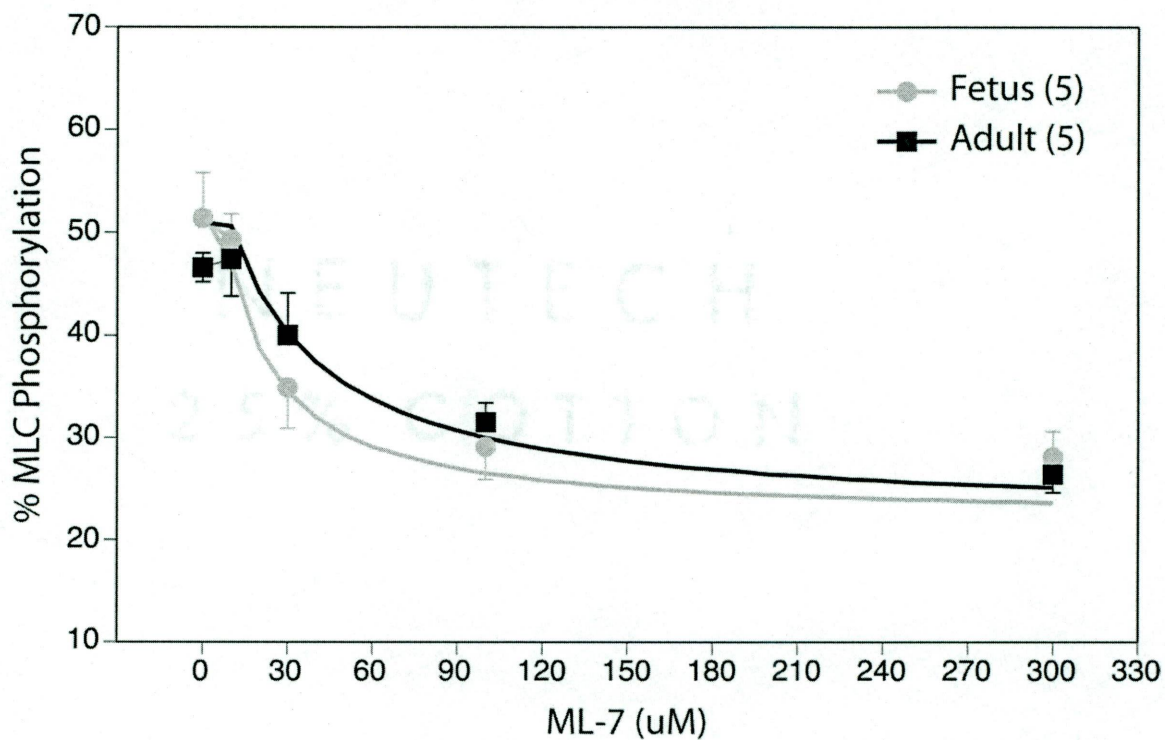


FIGURE-5

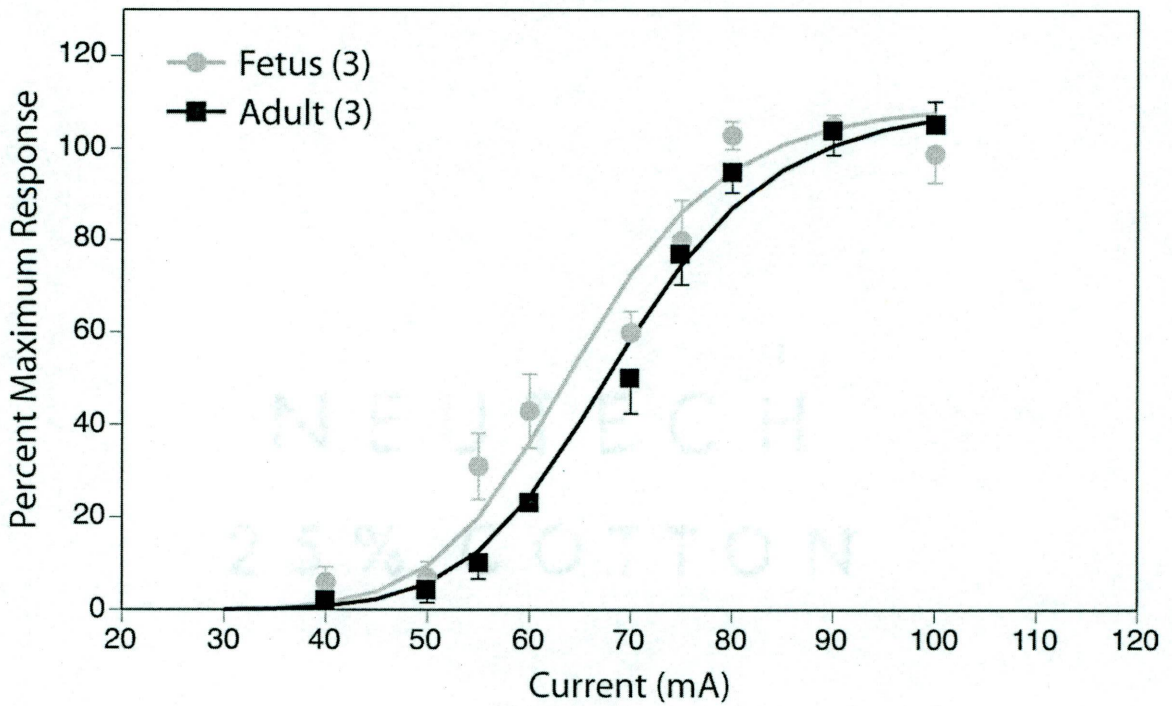
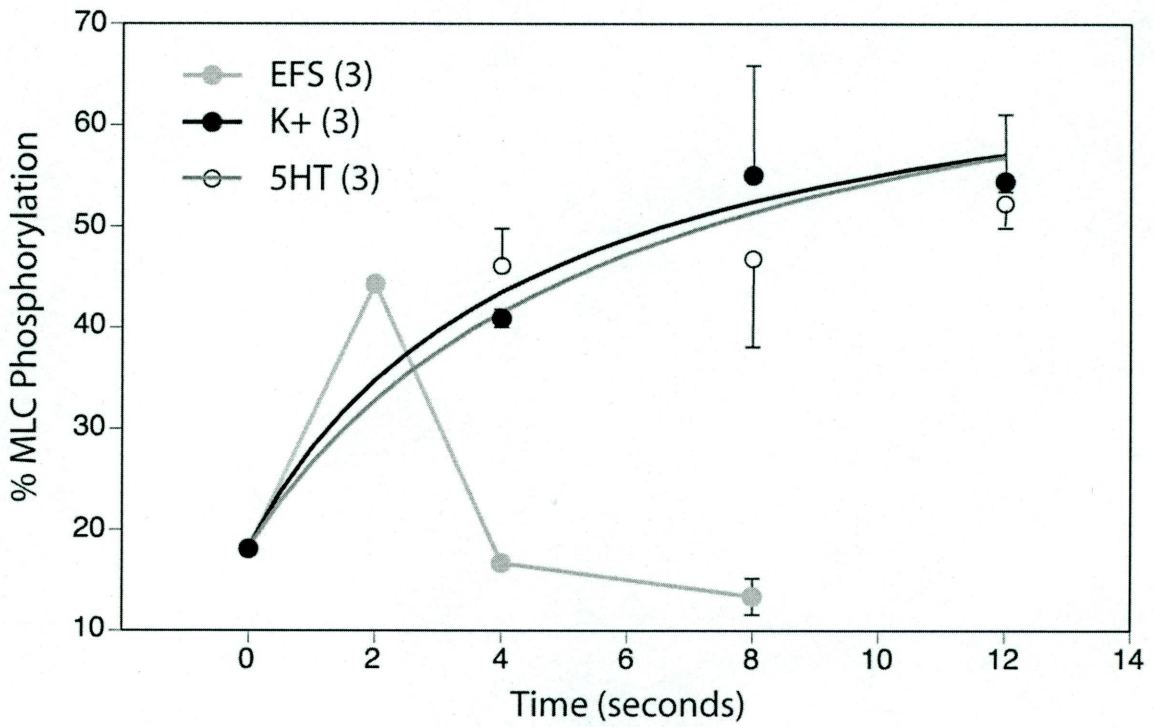
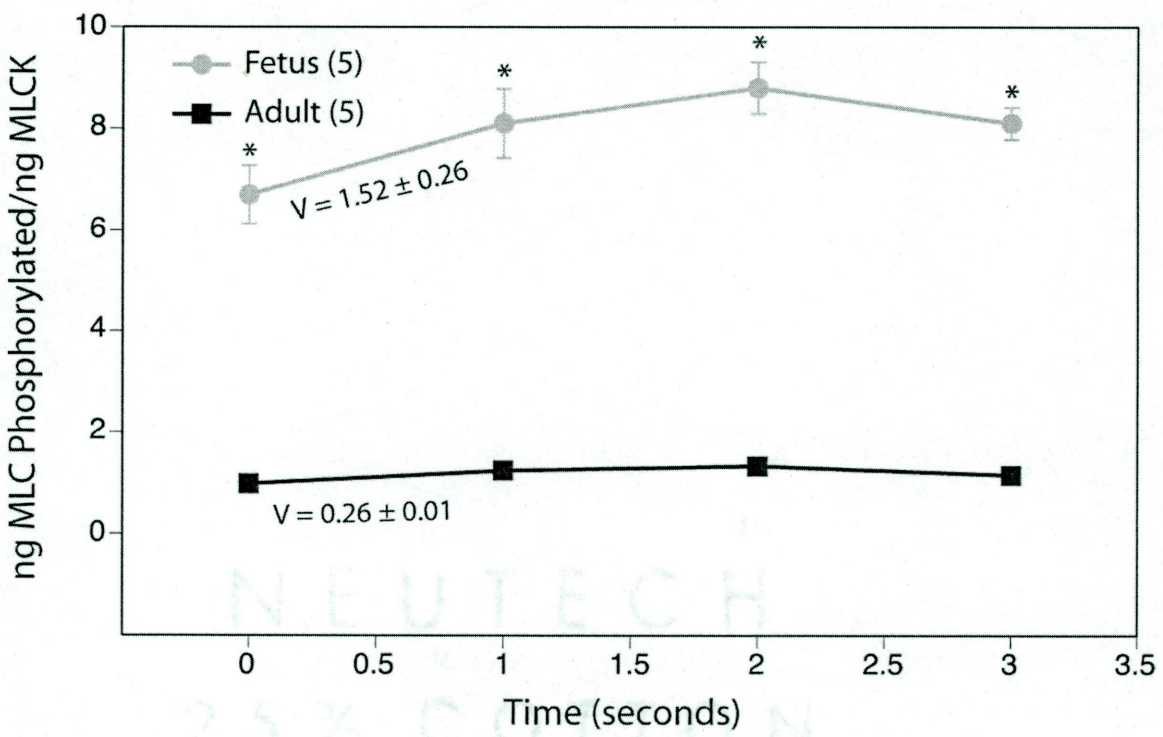
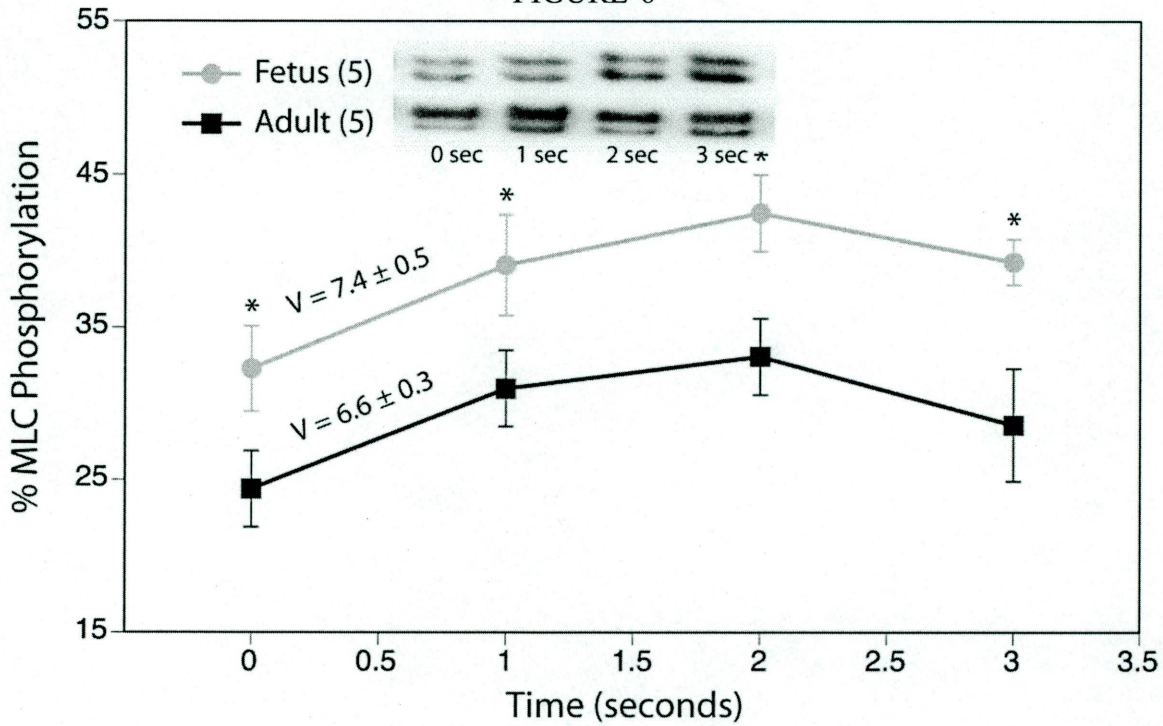


FIGURE-6



CHAPTER 3

MYOSIN LIGHT CHAIN KINASE PHOSPHORYLATES REGULATORY LIGHT CHAIN MORE EFFICIENTLY IN FETAL THAN IN ADULT OVINE CAROTID ARTERIES

Elisha R. Injeti¹, Renan J. Sandoval¹, Gerhart Graupner¹,
Christine R. Cremo², and William J. Pearce¹

¹Department of Physiology and Pharmacology, Center for Perinatal Biology,
Loma Linda University School of Medicine, Loma Linda, California, 92354

²Department of Biochemistry and Molecular Biology,
University of Nevada School of Medicine, Reno, Nevada 89557

Running Head

MLCK Activity and Postnatal Maturation

Correspondence

William J. Pearce, Ph.D.

Departments of Physiology and Pharmacology
Loma Linda University School of Medicine, Loma Linda, CA, 92354
e-mail: wpearce@llu.edu, phone: 909-558-4800 ext 45210

Abstract

We have recently shown that MLCK velocity measured *in-situ* is upregulated in fetal compared to adult arteries and contributes to age related differences in contractility. The present study tests the hypothesis that maturational down-regulation of MLCK velocity *in-situ* is attributable to corresponding decreases in catalytic activity and fractional activation of MLCK. To test this hypothesis, V_{\max} and K_m of MLCK were estimated under verified optimal conditions in tissue homogenates prepared from carotid arteries harvested from term fetal lambs and non-pregnant adult sheep. Purified chicken gizzard MLC₂₀ served as the substrate for MLCK, and all velocity measurements included normalization relative to absolute MLCK concentration. Fetal values of maximal MLCK velocity (ng MLC₂₀ phosphorylated/sec) averaged (163 ± 11) , and were significantly greater than corresponding adult values (130 ± 9) . Substrate affinity values (in μM) did not differ significantly and averaged 4.80 ± 1.20 and 3.30 ± 0.98 in fetal and adult homogenates, respectively. When estimates of maximal MLCK activity measured *in-situ* were divided by homogenate estimates of V_{\max} , the resulting values of fractional activation were significantly greater in fetal, $(7.20 \pm 0.52\%)$ than in adult $(1.46 \pm 0.07\%)$, homogenates. Together, these results support the hypothesis that increased enzyme specific activity and increased fractional activation both contribute to the greater MLCK velocities observed in fetal compared to adult ovine carotid arteries.

Key words

Enzyme kinetics, myofilament calcium sensitivity, postnatal maturation, thick filament reactivity.

Introduction

The transition from fetal to postnatal life involves numerous dramatic changes in vascular structure and reactivity. These changes clearly involve altered patterns of sarcolemmal receptor expression and calcium handling that continuously alter pharmacomechanical coupling throughout fetal and postnatal maturation (24, 35). An important component of these maturational adjustments are a gradual postnatal decrease in the magnitude of agonist-induced myofilament calcium sensitization (2, 3, 5). These decreases in myofilament calcium sensitization involve altered relations between cytosolic calcium concentration and the extent of myosin light chain phosphorylation, which is defined as thick filament reactivity (25, 32). In turn, this altered thick filament reactivity is attributable in large part to enhanced rates of myosin phosphorylation, *in situ*, despite a lower abundance of myosin light chain kinase in fetal relative to adult arteries (32).

Whereas multiple previous studies have documented that MLCK abundance and activity are often tightly correlated (16, 17, 21, 31), studies of fetal and postnatal development have demonstrated the opposite correlation; in immature arteries the MLCK abundance is low but activity is high (8, 9). Our previous studies agree with this latter finding. It remains possible however, that age-related differences in substrate concentration could be involved. Similarly, the expression of essential cofactors such as calmodulin could be reduced in mature arteries, although published evidence argues against this possibility (10). In adult arteries, elevated abundances of endogenous inhibitors of MLCK activity, such as polyamines (30) or telokin (14), might also explain reduced rates of myosin phosphorylation. In addition, age-dependent post-translational

modification of MLCK resulting in altered specific activity also remains possible; studies with Protein Kinase A, Protein Kinase C, and Calcium-Calmodulin Kinase II have demonstrated that each of these kinases can attenuate MLCK specific activity (34). Age-related differences in the extent of activation of MLCK could also play a significant role, particularly in light of abundant evidence demonstrating that agonist-induced increases in cytosolic calcium vary considerably with fetal and postnatal age.

The present studies examine the MLCK-dependent mechanisms potentially responsible for greater rates of MLC₂₀ phosphorylation observed in immature compared to mature arteries. In particular, these studies focus on the two mechanisms most likely to play a role in age-related differences in MLC₂₀ phosphorylation, namely MLCK specific activity and fractional activation. To explore the importance of these mechanisms, a dilute homogenate assay was developed to directly estimate the kinetics of MLCK-mediated MLC₂₀ phosphorylation in homogenates prepared from fetal and adult ovine carotid arteries. The estimates so obtained enabled direct calculation of the maximal extent of fractional activation observed in situ.

Materials and Methods

General Preparation

Carotid arteries were obtained from non-pregnant adult female sheep (18-24 months old) and near term (~140 days gestation) fetuses. To obtain fetal arteries, pregnant ewes were anesthetized with 30 mg/kg pentobarbital, intubated and then placed on 1.5- 2.0 % halothane. Each fetus was then exteriorized through a midline vertical laparotomy and killed by rapid removal of the heart. Adult animals were sacrificed by intravenous

administration of 100 mg/kg pentobarbital. Carotid arteries were dissected and cleaned of extraneous connective and adipose tissue. The endothelium was removed by passing a roughened needle through the lumen, after which arteries were immediately frozen in liquid nitrogen and stored at -80°C until homogenized. All procedures used in these studies were approved by the Animal Research Committee of Loma Linda University and adhered to all policies and practices outlined in the National Institutes of Health *Guide for the Care and Use of Laboratory Animals*

Preparation of Carotid Artery Homogenates

Frozen carotid arteries (~150 mg per animal) were homogenized in ice cold buffer containing 20 mM imidazole, 1 mM cysteine, 60 mM KCl, 1 mM MgCl_2 , 10 mM sodium azide, 0.25 mM PMSF, and 1 mM DTT, at pH 7.5. The homogenization buffer also contained phosphatase inhibitor cocktail (Sigma P-2850) at a concentration of 10 $\mu\text{L}/\text{mL}$ buffer and 0.5% protease inhibitor cocktail (Sigma, P8340). Homogenization was carried out for 15 minutes at 4°C using a motor-driven glass-on-glass mortar and pestle and then centrifuged for 1 minute at 6000 G after which an aliquot of supernatant was taken for protein determination. Final adjustments in protein concentration were made to assure that the amount of MLCK in each homogenate was similar. Fresh homogenates were prepared daily for each enzyme velocity measurement.

Determination of MLCK Abundance in Artery Homogenates

From each artery homogenates, 15 μg of total protein were loaded on a 15-lane, 8% SDS-PAGE gel, and run at 15 mA for 90 minutes and then transferred onto nitrocellulose membrane. The membrane was blocked overnight at 4°C with 5% non-fat dry milk in 20

mM Tris HCl at pH 7.5, 500 mM NaCl and 0.1% Tween-20 and then probed with mouse anti-MLCK primary antibody (Sigma, M7905) at 1:7,000 dilution for 2 hours. Primary antibody-antigen complexes were detected with a goat anti-mouse secondary antibody (Pierce, #1858413), and visualized using direct photon capture with a CCD camera (AlphaInnotech, Chemi-Imager). Purified chicken gizzard MLCK was used as reference standard to quantify absolute amount of MLCK present in homogenates.

Determination of Optimum Calcium and Calmodulin Concentrations for Activating MLCK

Fetal and adult homogenates were adjusted to contain equivalent amounts of MLCK both before and after a 400-fold dilution. Exogenous MLC_{20} was added to the dilute homogenates to raise MLC_{20} concentration to 1.5 μ M. Aliquots of both homogenate concentrations were incubated with 0, 0.3, 0.6, or 1 μ M calmodulin for 20 minutes at 4 $^{\circ}$ C and then for 10 minutes at 37 $^{\circ}$ C. Next, calcium at 0, 0.3, 1, 3 or 10 mM was added with 1 mM ATP to initiate the reaction. The reaction was terminated at exactly 0, 1, 2 and 3 seconds by adding ice cold 10 mM EDTA and then transferring the samples to dry ice. The samples were then analyzed for MLC_{20} phosphorylation using 10% urea glycerol gels. These gels were run for 150 minutes at a constant voltage of 200V and then transferred onto nitrocellulose membrane at a constant current of 50 mA for 180 minutes. Membranes were blocked with 5% milk in TBS (20 mM Tris HCl, 500 mM NaCl, pH 7.5) for 90 minutes. After blocking, the membranes were incubated in primary anti- MLC_{20} antibody (MY-21, Sigma M4401) at 1:300 dilution with 5% milk in Tween-TBS for 3 hours, followed by incubation in goat anti-mouse secondary antibody (Pierce, #1858413 at 1:1000 dilution) conjugated with horse radish peroxidase for 90 minutes. All

washes were carried out with Tween-TBS containing 5% milk. Antibody-antigen complexes were detected by chemiluminescence using a mixture of equal volumes of enhanced luminol reagent and oxidizing reagent. Membranes were then scanned to determine the integrated optical density values of both phosphorylated and unphosphorylated MLC₂₀ bands using a Chemi Imager, (AlphaInnotech). Masses (ng) of MLC₂₀ phosphorylated were determined using a standard curve prepared from multiple masses of purified MLC₂₀ run on each gels. The slope of the relation between ng MLC₂₀ phosphorylated and time was taken as a measure of MLCK activity.

Determination of Optimum Concentration of Phosphatase Inhibitor Cocktail (PIC)

Tissue homogenates containing equivalent amounts of MLCK were collected and incubated with 0, 3, 10, & 30 ($\mu\text{L}/\text{mL}$) of PIC for 20 minutes at 4 °C in a final volume of 40 μL . Next, the homogenates were brought up to 37 °C and maintained at that temperature for 10 minutes after which 3 mM calcium and 1 mM ATP were added to activate MLCK. After exactly 3 seconds, the reaction was rapidly terminated by adding ice cold 10 mM EDTA and the homogenates were transferred to dry ice. The samples were then analyzed for MLC₂₀ phosphorylation using 10% urea glycerol gels as described in preceding section “Determination of optimum calcium and calmodulin concentrations for activating MLCK.”

Effects of Protein Kinase Inhibitors on MLCK Velocity

Suggestions from multiple previous studies that PKA (1), PKC (26), and CaM-Kinase II (13) can inhibit MLCK activity necessitated a series of experiments to verify that the observed age-related variations in MLCK activity were not due to differential

inhibition by these kinases. Artery homogenates were incubated with H-89 (PKA inhibitor) at 0, 0.05, 0.15 or 0.5 μM for 20 minutes at 4 $^{\circ}\text{C}$ and then for 10 minutes at 37 $^{\circ}\text{C}$. MLCK velocity was measured in presence of this inhibitor by adding 3 mM calcium and 1 mM ATP to initiate the reaction. The reaction was terminated at exactly 0, 1, 2 & 3 seconds by adding ice cold 10 mM EDTA and then transferring the samples to dry ice. The MLCK velocity was calculated as the rate of change of MLC_{20} phosphorylation as determined from band densities measured in 10% urea glycerol gels. Similar measurements were made in the presence of calphostin-C (PKC Inhibitor) at 0, 0.05, 0.15, 0.5 μM or with KN-93 (CaM Kinase-II inhibitor) at 0, 1, 3, or 10 μM concentrations, respectively.

Determination of V_{max} & K_{m} of MLCK

To retard the reaction rate enough to enable accurate measurements of product (phosphorylated MLC_{20}) accumulation, and also negate the influence of endogenous substrate concentration, the artery homogenates were diluted approximately 400-fold. MLCK concentrations were standardized across all homogenates using Western blots with purified chicken gizzard MLCK as absolute standards on each gel. The maximal velocity of MLCK was determined by incubating artery homogenates with purified chicken gizzard myosin light chain at 1.5, 3, 5, 7.5, 10, 15 & 20 μM for 10 minutes at 37 $^{\circ}\text{C}$. MLCK activity was then initiated, terminated and quantitated as described in the section "Determination of optimum calcium and calmodulin concentrations for activating MLCK."

Calculations and Statistics

All curve fitting was performed using least-square error minimization routines. Non-linear fits for concentration-response relations were fit as rectangular hyperbolae. Non-linear fits for standard curves (optical density vs. mass) were fit to the logistic equation. Coefficients of fit for the standard curves were used to prepare inverse forms of the logistic equation that enabled direct calculation of sample masses from band optical densities. Linear fits for the Lineweaver-Burke (double-reciprocal) plots were performed via linear regression. The MLC_{20} masses were calculated directly from optical density values using standard curves prepared from known absolute masses of purified MLC_{20} loaded on each gel. Apparent specific activity in homogenates was calculated by dividing estimates of homogenate V_{max} by the corresponding mass of $MLCK$ measured in the same homogenate. Throughout the text, all values indicate the mean \pm the standard error for the number of animals indicated; values of N refer to the numbers of animals and not the numbers of segments or experiments. Unpaired comparisons between two variables were performed using a Behren's-Fisher comparison with pooled variance. All data sets were verified to be normally distributed using SPSS v16. Unless stated otherwise, a statistical power of 0.8 was attained for all comparisons yielding no significant difference. In all cases, statistical significance implies $P < 0.05$.

Results

A total of 3.4 gm and 2.3 gm of carotid arterial tissue were used for these studies. These tissues were harvested from a total of 16 fetuses and 16 adult sheep respectively.

MLCK Abundance in Artery Homogenates

Fetal artery homogenates contained 2.43 ± 0.21 ng MLCK/ μ g protein and adult homogenates contained 8.82 ± 0.80 ng MLCK/ μ g protein. For undiluted samples, 145 ng of MLCK from both fetal and adult homogenates were taken for measuring MLCK velocity.

Optimum Concentrations of Calcium and Calmodulin for MLCK

In undiluted artery homogenates the MLCK velocity (ng MLC₂₀ phosphorylated/sec) observed in the presence of 0.3 μ M calmodulin and 3 mM calcium averaged 41.9 ± 2.0 in fetal arteries and 32.2 ± 10.0 in adult arteries. Changes in either of these calmodulin or calcium concentrations did not significantly increase MLCK velocity in either undiluted or diluted fetal or adult artery homogenates (**Figure 1**). Indeed, the results revealed that concentrations of calmodulin greater than 0.3 μ M tended to decrease MLCK velocity in both fetal and adult homogenates. Given these results, all measurements of maximal MLCK velocity were performed at 0.3 μ M added calmodulin and 3 mM added calcium.

Optimum Concentration of Phosphatase Inhibitor Cocktail

Sigma's Phosphatase Inhibitor Cocktail (PIC) inhibited MLCP in a concentration-dependent manner in both fetal and adult arteries (**Figure 2**). The mass of MLC₂₀ phosphorylated in 3 seconds averaged 60.0 ± 3.3 ng in fetal arteries and 52.9 ± 3.9 ng in adult arteries, in the presence of 10 μ L/mL of PIC. Increases in PIC concentration above 10 μ L/mL did not further increase the mass of MLC₂₀ phosphorylated. Based on this result, all subsequent measurements of MLCK velocity included PIC at a concentration of 10 μ L/mL.

Effect of Protein Kinase Inhibitors on MLCK Velocity

In fetal tissue homogenates, MLCK velocities (ng MLC₂₀ phosphorylated/sec) were not significantly different in control samples (42.2 ± 13.1) and in samples treated with 0.5 μ M H-89 (22.5 ± 9.1). However, in adult artery homogenates MLCK velocities were significantly greater in control samples (38.0 ± 7.4) than in samples treated with 0.5 μ M H-89 (18.2 ± 3.6). Similar studies of MLCK velocities in the presence of 0.5 μ M calphostin-C showed no significant differences compared to control values in either fetal (24.2 ± 5.8) or adult (27.9 ± 3.7) artery homogenates. In addition, MLCK velocities in the presence of 3 μ M KN-93 were significantly lower than control values in both fetal (15.0 ± 6.7) and adult (13.9 ± 3.6) homogenates. As these results did not exhibit any increase in MLCK velocities (**Figure 3**), kinase inhibitors were not added to homogenates used to determine maximal MLCK activities.

Age Related Differences in V_{\max} and K_m Values for MLCK

MLCK velocities (ng MLC₂₀ phosphorylated /sec) exhibited classical hyperbolic substrate dependence in both fetal and adult homogenates (**Figure 4**). As determined by non-linear regression, estimates of V_{\max} for MLCK in fetal homogenates (163 ± 11) were significantly greater than in adult homogenates (130 ± 9). The K_m values were not significantly different in fetal samples ($4.8 \pm 1.2 \mu$ M) and adult ($3.3 \pm 1.0 \mu$ M) samples. The kinetic values obtained by non-linear regression were not significantly different than those obtained by Lineweaver-Burke analysis for either fetal or adult homogenates.

Age Related Differences in Homogenate Specific Activity and Fractional Activation of MLCK

To estimate the specific activities of MLCK, values of ng MLC₂₀ phosphorylated/sec were divided by the absolute MLCK mass in each assay to obtain velocity values in units of ng MLC₂₀ phosphorylated/sec/ng MLCK. The resulting values (**Figure 5**) were significantly greater in fetal samples (20.6 ± 1.3) than adult samples (18.0 ± 1.28). To calculate in situ fractional activation of the enzyme, the MLCK specific activity (in units of ng MLC₂₀ phosphorylated/sec/ng MLCK) measured in our previous studies in situ were divided by apparent specific activity obtained in the homogenates. These ratios indicate that maximal in situ fractional activation in fetal arteries ($7.20 \pm 0.52\%$) is significantly greater than adult arteries ($1.46 \pm 0.07\%$).

Discussion

MLCK is a dedicated serine/threonine kinase that phosphorylates only T18 and S19 of MLC₂₀ to initiate smooth muscle contraction (18). When activated by calcium-calmodulin (33), it is a very fast enzyme that can phosphorylate MLC₂₀ in as little as 2 seconds following nerve stimulation in some preparations (6, 22). To a certain extent, MLCK competes with other kinases, including protein kinase A (36), rho-kinase (7), and integrin-linked kinase (11), for the phosphorylation sites on MLC₂₀. In contrast to MLCK, the rates of phosphorylation of MLC₂₀ by these other kinases is relatively slow (23), which provides a convenient basis for the separation of their effects from those of MLCK. Correspondingly, when MLC₂₀ phosphorylation was measured over a short duration in the absence of added calcium and calmodulin, MLC₂₀ phosphorylation did not change significantly from basal levels suggesting that MLCK was the only kinase

responsible for the MLC_{20} phosphorylation observed in the artery homogenates (**Figure 1**). Correspondingly, MLCK activation yielded maximal rates of MLC_{20} phosphorylation in the presence of 3 mM calcium and 0.3 μ M calmodulin. Calmodulin at concentrations above 0.3 μ M produced no further increases in MLCK velocity. In light of these results, which agreed well with other MLCK homogenate studies (21), all measurements of MLCK velocity included 3 mM calcium and 0.3 μ M calmodulin.

Given that the extent of MLC_{20} phosphorylation reflects the integrated difference between the activities of MLCK and myosin phosphatase, any estimate of homogenate MLCK activity requires complete inhibition of myosin phosphatase. In arterial smooth muscle, the predominant phosphatase that dephosphorylates MLC_{20} is in the PP1c family (12), which is potently inhibited by cantharidin and microcystin (20). MLC_{20} is also potentially subject to non-specific dephosphorylation by alkaline phosphatase, particularly in homogenates (29). To defeat these phosphatase activities, the artery homogenates included a commercially prepared mixture (Sigma P-2850) of cantharidin, microcystin, and bromotetramisole (an alkaline phosphatase inhibitor). As indicated in **Figure 2**, maximal levels of MLC_{20} phosphorylation were attained in both fetal and adult homogenates treated with 10 μ l/ml of the phosphatase inhibitor cocktail. All subsequent homogenate experiments contained this concentration of these inhibitors.

Another complication in measurements of MLCK activity is the possible presence of endogenous inhibitors of the enzyme (14, 30). The approach taken to negate this complication was to develop an artery homogenate preparation in which MLCK concentration was diluted approximately 400-fold. This dilution offered multiple advantages. First, it eliminated any possible effects of unknown endogenous inhibitors or

activators of MLCK. Second, it essentially eliminated any possible effects of differences in endogenous substrate concentration. Third, it retarded the rate of MLC₂₀ phosphorylation, which enabled more accurate measurements of reaction rate. Finally, it eliminated any possible age-related differences in calmodulin concentration (10).

In situ, MLCK activity can potentially be attenuated by phosphorylation of the enzyme by several different kinases (34). Among these, Protein Kinase A was the first discovered to reversibly inhibit MLCK (1). Not long after this discovery, Nishikawa et al. reported that Protein Kinase C could also reversibly inhibit MLCK activity (26). Subsequently, Hashimoto and Soderling (13) further reported that Calcium-Calmodulin Kinase II could effectively inhibit MLCK activity. In light of this evidence, the experimental design included a series of validation experiments to confirm that the inhibitory activities of protein kinase A, protein kinase C, and calcium-calmodulin kinase II on MLCK were negligible in the homogenates used to measure MLCK activity. Whereas selective inhibition of an inhibitory kinase should increase overall MLCK activity, this result was not observed following selective inhibition of PKA by H-89, PKC by calphostin, or CaM Kinase II by KN-93 (**Figure 3**).

Definition of the optimal conditions for our artery homogenates enabled measurements of MLCK activity at varying MLC₂₀ concentrations. The use of purified chicken gizzard MLC₂₀ in these measurements eliminated any possible effects due to age-related differences in MLC₂₀ abundance or isoform (15). This approach revealed that MLCK maximal velocity was slightly but significantly greater in fetal (163 ± 11 ng MLC₂₀ phosphorylated/sec) than adult (130 ± 9 ng MLC₂₀ phosphorylated/sec) homogenates (**Figure 4**). In contrast, estimates of substrate affinity (K_m) were not

significantly different in fetal (4.8 μ M) and adult (3.3 μ M) homogenates. When homogenate velocities were divided by the equivalent mass of MLCK in each assay tube to estimate apparent MLCK specific activity, the calculated values (in ng MLC₂₀ phosphorylated/sec/ng MLCK) were slightly but significantly greater in fetal (20.6 \pm 1.4) than in adult (18.0 \pm 1.3) homogenates (**Figure 5, left panel**). Together, these data are consistent with the findings of Belik obtained in rat pulmonary arteries (8), and suggest that small but important differences exist between fetal and adult MLCK specific activity.

Even though the estimates of apparent MLCK specific activity were greater in fetal than adult artery homogenates, the difference appears too small (\approx 14%) to explain the much larger difference in apparent MLCK specific activity previously observed in situ (\approx 6-fold). This finding strongly suggests that factors other than just MLCK abundance and specific activity contributed to the age-related differences in MLCK velocity observed in situ. One of the most likely factors contributing to the observed age-related differences in MLCK activity in situ, is fractional activation. Activation of MLCK typically follows smooth muscle cytosolic calcium concentration, and this variable is regulated very differently in mature and immature arteries as shown in multiple previous studies (4), (24). In support of this hypothesis, estimates of in situ fractional activation based on the homogenate values of V_{max} indicate it to be several-fold greater in fetal (7.20%) than in adult (1.46%) arteries (**Figure 5, right panel**). This finding suggests that physiological activation of MLCK varies dramatically with postnatal age.

Other factors could also potentially contribute to age-related differences in the kinetics of MLC₂₀ phosphorylation. One possibility is that age-related differences in calmodulin abundance *in situ* might play a role, although the limited evidence available

indicates that *in situ* calmodulin availability is greater in adult than in fetal tissues (10). Another intriguing possibility is that age-dependent differences in MLC₂₀ isoform with different kinetic influences may play some role as suggested by Inoue (15). MLCK activity might also be influenced by age-dependent post-translational modification through a mechanism that is sensitive to homogenization. This effect might help explain the small differences in MLCK kinetics observed in the homogenates. Because the only known post-translational modification of MLCK activity is inhibitory phosphorylation (34), this effect would require a greater extent of inhibitory phosphorylation of adult compared to fetal MLCK, *in situ*. Age-related differences in telokin expression probably were not involved because this endogenous MLCK inhibitor was not detected.

Alternatively, it remains possible that the spatial organization and colocalization of MLC₂₀ and MLCK could also play a major role (34), particularly if the relative distribution of these two molecules changes during postnatal development as suggested by studies of chicken gizzard (27). This possibility is particularly attractive given the growing list of non-contractile functions assigned to MLCK (19).

Aside from the mechanisms potentially responsible for age-related differences in the kinetics of MLC₂₀ phosphorylation, it is important to note that the active stresses produced by fetal and adult arteries under identical conditions of activation are not significantly different (28). From this perspective, it is clear that the physiological function of MLCK is highly specialized in both fetal and adult arteries. A key feature of this specialization is that both the apparent specific activity and maximal fractional activation of MLCK are significantly greater in fetal than adult arteries. Together, these

adaptations appear to counterbalance the markedly reduced expression of MLCK that is characteristic of fetal arteries.

Acknowledgements

The work reported in this manuscript was supported by USPHS Grants HL54120, HD31266, HL64867, AR40917 (to C. R. C.), 1P20RR018751 (COBRE Proteomics Core facility at the University of Nevada School of Medicine) and the Loma Linda University School of Medicine. The authors also acknowledge the excellent technical assistance and insights of Mr. James M. Williams.

References

1. Adelstein RS, Conti MA, and Pato MD. Regulation of myosin light chain kinase by reversible phosphorylation and calcium-calmodulin. *Ann N Y Acad Sci* 356: 142-150, 1980.
2. Akopov SE, Zhang L, and Pearce WJ. Developmental changes in the calcium sensitivity of rabbit cranial arteries. *Biol Neonate* 74: 60-71, 1998.
3. Akopov SE, Zhang L, and Pearce WJ. Intracranial-extracranial differences in the Ca²⁺ sensitivity of rabbit arteries. *Proc Soc Exp Biol Med* 214: 76-82, 1997.
4. Akopov SE, Zhang L, and Pearce WJ. Maturation alters the contractile role of calcium in ovine basilar arteries. *Pediatr Res* 44: 154-160, 1998.
5. Akopov SE, Zhang L, and Pearce WJ. Physiological variations in ovine cerebrovascular calcium sensitivity. *Am J Physiol* 272: H2271-2281, 1997.
6. Aksoy MO, Murphy RA, and Kamm KE. Role of Ca²⁺ and myosin light chain phosphorylation in regulation of smooth muscle. *Am J Physiol* 242: C109-116, 1982.
7. Amano M, Ito M, Kimura K, Fukata Y, Chihara K, Nakano T, Matsuura Y, and Kaibuchi K. Phosphorylation and activation of myosin by Rho-associated kinase (Rho-kinase). *J Biol Chem* 271: 20246-20249, 1996.
8. Belik J, Kerc E, and Pato MD. Rat pulmonary arterial smooth muscle myosin light chain kinase and phosphatase activities decrease with age. *Am J Physiol Lung Cell Mol Physiol* 290: L509-516, 2006.
9. Chitano P, Worthington CL, Jenkin JA, Stephens NL, Gyapong S, Wang L, and Murphy TM. Ontogenesis of myosin light chain phosphorylation in guinea pig tracheal smooth muscle. *Pediatr Pulmonol* 39: 108-116, 2005.
10. Cho YH, Wheeler MA, and Weiss RM. Ontogeny of cyclic AMP and cyclic GMP phosphodiesterase activities and of calmodulin levels in guinea pig ureter. *J Urol* 139: 1095-1098, 1988.

11. Deng JT, Van Lierop JE, Sutherland C, and Walsh MP. Ca²⁺-independent smooth muscle contraction. a novel function for integrin-linked kinase. *J Biol Chem* 276: 16365-16373, 2001.
12. Hartshorne DJ, Ito M, and Erdodi F. Myosin light chain phosphatase: subunit composition, interactions and regulation. *J Muscle Res Cell Motil* 19: 325-341, 1998 May.
13. Hashimoto Y and Soderling TR. Phosphorylation of smooth muscle myosin light chain kinase by Ca²⁺/calmodulin-dependent protein kinase II: comparative study of the phosphorylation sites. *Arch Biochem Biophys* 278: 41-45, 1990.
14. Herring BP, El-Mounayri O, Gallagher PJ, Yin F, and Zhou J. Regulation of myosin light chain kinase and telokin expression in smooth muscle tissues. *Am J Physiol Cell Physiol* 291: C817-827, 2006.
15. Inoue A, Yanagisawa M, Takano-Ohmuro H, and Masaki T. Two isoforms of smooth muscle myosin regulatory light chain in chicken gizzard. *Eur J Biochem* 183: 645-651, 1989.
16. Jiang H, Rao K, Halayko AJ, Liu X, and Stephens NL. Ragweed sensitization-induced increase of myosin light chain kinase content in canine airway smooth muscle. *Am J Respir Cell Mol Biol* 7: 567-573, 1992.
17. Jiang H, Rao K, Liu X, Halayko AJ, Liu G, and Stephens NL. Early changes in airway smooth muscle hyperresponsiveness. *Can J Physiol Pharmacol* 72: 1440-1447, 1994.
18. Kamm KE and Stull JT. Dedicated myosin light chain kinases with diverse cellular functions. *J Biol Chem* 276: 4527-4530, 2001.
19. Kishi H, Mikawa T, Seto M, Sasaki Y, Kanayasu-Toyoda T, Yamaguchi T, Imamura M, Ito M, Karaki H, Bao J, Nakamura A, Ishikawa R, and Kohama K. Stable transfectants of smooth muscle cell line lacking the expression of myosin light chain kinase and their characterization with respect to the actomyosin system. *J Biol Chem* 275: 1414-1420, 2000.
20. Knapp J, Aleth S, Balzer F, Schmitz W, and Neumann J. Calcium-independent activation of the contractile apparatus in smooth muscle of mouse aorta by protein

- phosphatase inhibition. *Naunyn Schmiedebergs Arch Pharmacol* 366: 562-569, 2002.
21. Liu G, Liu X, Rao K, Jiang H, and Stephens NL. Increased myosin light chain kinase content in sensitized canine saphenous vein. *J Appl Physiol* 80: 665-669, 1996.
 22. Miller-Hance WC, Miller JR, Wells JN, Stull JT, and Kamm KE. Biochemical events associated with activation of smooth muscle contraction. *J Biol Chem* 263: 13979-13982, 1988.
 23. Mita M, Yanagihara H, Hishinuma S, Saito M, and Walsh MP. Membrane depolarization-induced contraction of rat caudal arterial smooth muscle involves Rho-associated kinase. *Biochem J* 364: 431-440, 2002.
 24. Nauli SM, Williams JM, Akopov SE, Zhang L, and Pearce WJ. Developmental changes in ryanodine- and IP(3)-sensitive Ca(2+) pools in ovine basilar artery. *Am J Physiol Cell Physiol* 281: C1785-1796, 2001 Dec.
 25. Nauli SM, Williams JM, Gerthoffer WT, and Pearce WJ. Chronic hypoxia modulates relations among calcium, myosin light chain phosphorylation, and force differently in fetal and adult ovine basilar arteries. *J Appl Physiol* 99: 120-127, 2005.
 26. Nishikawa M, Shirakawa S, and Adelstein RS. Phosphorylation of smooth muscle myosin light chain kinase by protein kinase C. Comparative study of the phosphorylated sites. *J Biol Chem* 260: 8978-8983, 1985.
 27. Paul ER, Ngai PK, Walsh MP, and Groschel-Stewart U. Embryonic chicken gizzard: expression of the smooth muscle regulatory proteins caldesmon and myosin light chain kinase. *Cell Tissue Res* 279: 331-337, 1995.
 28. Pearce WJ, Hull AD, Long DM, and Longo LD. Developmental changes in ovine cerebral artery composition and reactivity. *Am J Physiol* 261(2 Pt 2): R458-R465, 1991.
 29. Perrie WT, Smillie LB, and Perry SB. A phosphorylated light-chain component of myosin from skeletal muscle. *Biochem J* 135: 151-164, 1973.

30. Qi DF, Schatzman RC, Mazzei GJ, Turner RS, Raynor RL, Liao S, and Kuo JF. Polyamines inhibit phospholipid-sensitive and calmodulin-sensitive Ca²⁺-dependent protein kinases. *Biochem J* 213: 281-288, 1983.
31. Rao K, He JA, Halayko AJ, Pan N, Kepron W, and Stephens NL. Increased ATPase activity and myosin light chain kinase (MLCK) content in airway smooth muscle from sensitized dogs. *Adv Exp Med Biol* 304: 369-376, 1991.
32. Sandoval RJ, Injeti ER, Gerthoffer WT, and Pearce WJ. Postnatal maturation modulates relationships among cytosolic Ca²⁺, myosin light chain phosphorylation, and contractile tone in ovine cerebral arteries. *Am J Physiol Heart Circ Physiol* 293: H2183-2192, 2007.
33. Sobieszek A. Ca-linked phosphorylation of a light chain of vertebrate smooth-muscle myosin. *Eur J Biochem* 73: 477-483, 1977.
34. Stull JT, Tansey MG, Word RA, Kubota Y, and Kamm KE. Myosin light chain kinase phosphorylation: regulation of the Ca²⁺ sensitivity of contractile elements. *Adv Exp Med Biol* 304: 129-138, 1991.
35. Teng GQ, Williams J, Zhang L, Purdy R, and Pearce WJ. Effects of maturation, artery size, and chronic hypoxia on 5-HT receptor type in ovine cranial arteries. *Am J Physiol* 275: R742-753, 1998 Sep.
36. Walsh MP, Persechini A, Hinkins S, and Hartshorne DJ. Is smooth muscle myosin a substrate for the cAMP-dependent protein kinase? *FEBS Lett* 126: 107-110, 1981.

Figure Legends

Figure 1: Optimum Calcium and Calmodulin Concentrations Required to Activate MLCK.

Undiluted artery homogenates containing equivalent amounts of MLCK were incubated for 30 minutes with 0, 0.3, 0.6 or 1 μ M calmodulin, then activated with 0, 0.3, 1, 3 or 10 mM calcium and 1 mM ATP, and frozen at 0, 1, 2 & 3 seconds. MLCK velocity was estimated as the rate of MLC₂₀ phosphorylation based on measurements made with urea glycerol gels. The upper panel and lower panels indicate average velocities \pm SEM for 3 adult and 3 fetal sheep, respectively. Similar results were also obtained in diluted artery homogenates.

Figure 2: Optimum Concentration of Phosphatase Inhibitor Cocktail for MLCP Inhibition

Concentration dependent inhibition of MLCP by Phosphatase Inhibitor Cocktail (PIC) was evident in both fetal and adult arteries. The artery homogenates were incubated in 0, 3, 10, or 30 μ l/ml PIC for 30 minutes, activated with 3 mM calcium and 1 mM ATP, and then rapidly frozen at exactly 3 seconds. MLC₂₀ phosphorylation was measured using urea glycerol gels. The results indicate averages \pm SEM for 3 animals in each group.

Figure-3: Effects of Protein Kinase Inhibitors on MLCK Velocity

Artery homogenates containing equivalent amounts of MLCK were incubated with one of four different concentrations of protein kinase inhibitors for 30 minutes followed by activation with 3 mM calcium and 1 mM ATP and rapid freezing at 0, 1, 2, or 3 seconds. Top, middle and lower panels indicate MLCK velocities in the presence and absence of H-89 (PKA inhibitor), Calphostin-C (PKC inhibitor) and KN-93 (CaM Kinase-II inhibitor) for 4 animals for each group. Vertical error bars indicate standard errors. None of the inhibitors significantly increased the extent of MLC₂₀ phosphorylation in either age group.

Figure-4: Age Related Differences in V_{max} & K_m Values for MLCK

Artery homogenates containing equivalent amounts of MLCK were incubated for 10 minutes with different concentrations (1.5, 3, 5, 7.5, 10, 15, or 20 μM) of purified chicken gizzard MLC_{20} . MLCK velocities exhibited classical substrate dependence in both age groups. Estimates of kinetic parameters obtained via nonlinear regression agreed well with those obtained by Lineweaver-Burk analysis (inset). The K_m values calculated via nonlinear regression are indicated in the right panel. The results represent averages from 6 animals in each group. Vertical error bars indicate standard errors.

Figure-5: Age Related Differences in the Apparent Specific Activity and Fractional Activation of MLCK

Apparent specific activity was calculated as the estimated maximum velocity divided by MLCK content (left panel). Fractional activation of the in situ enzyme was calculated as the ratio of maximal velocity measured in intact arteries to the maximal velocity measured in the homogenates. Shown are averages for 6 animals from each group for specific activity measurements and 5 animals from each group for fractional activation. Vertical error bars indicate standard errors for the numbers of animals indicated in parentheses.

Figures

FIGURE 1

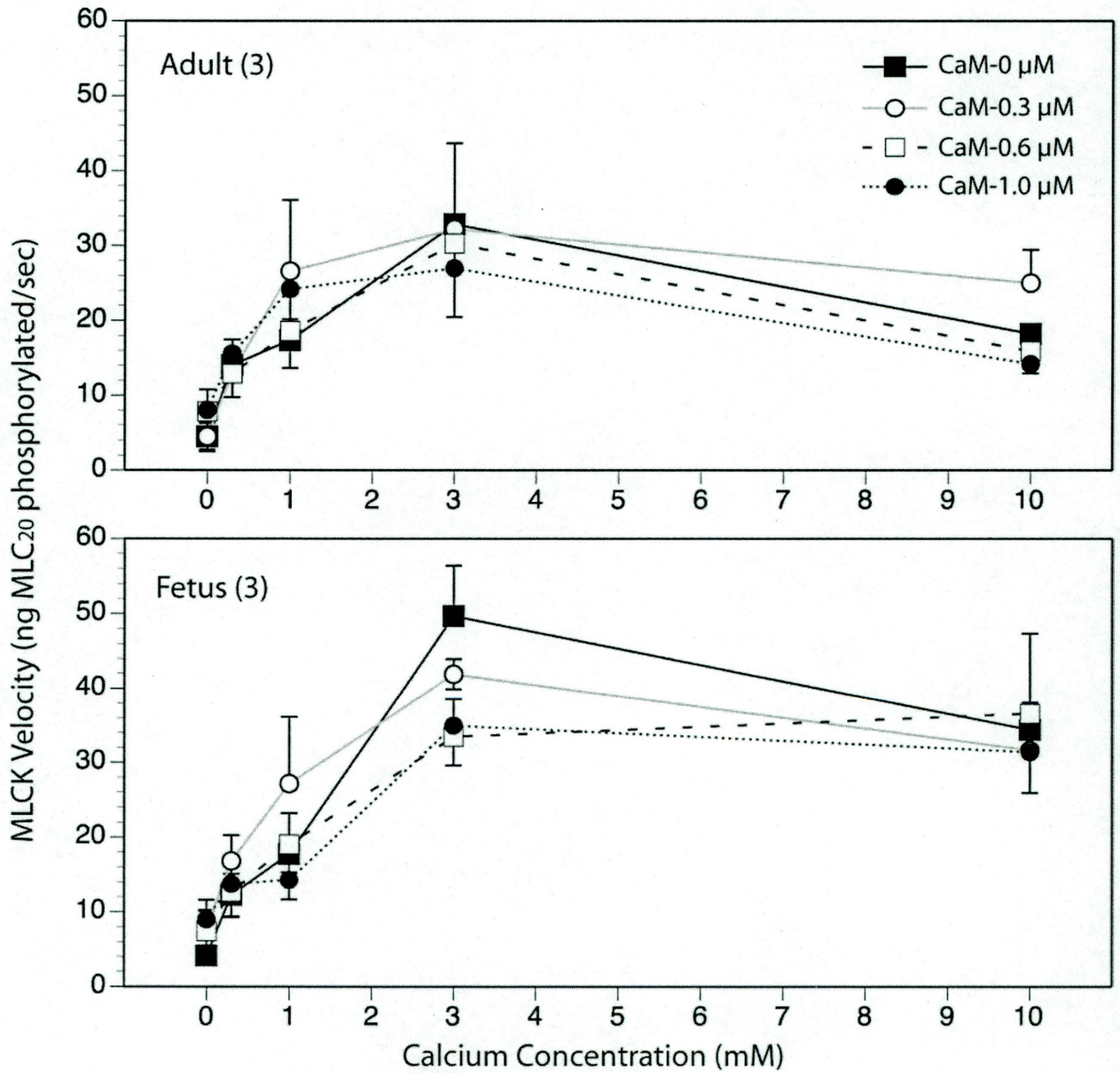


FIGURE-2

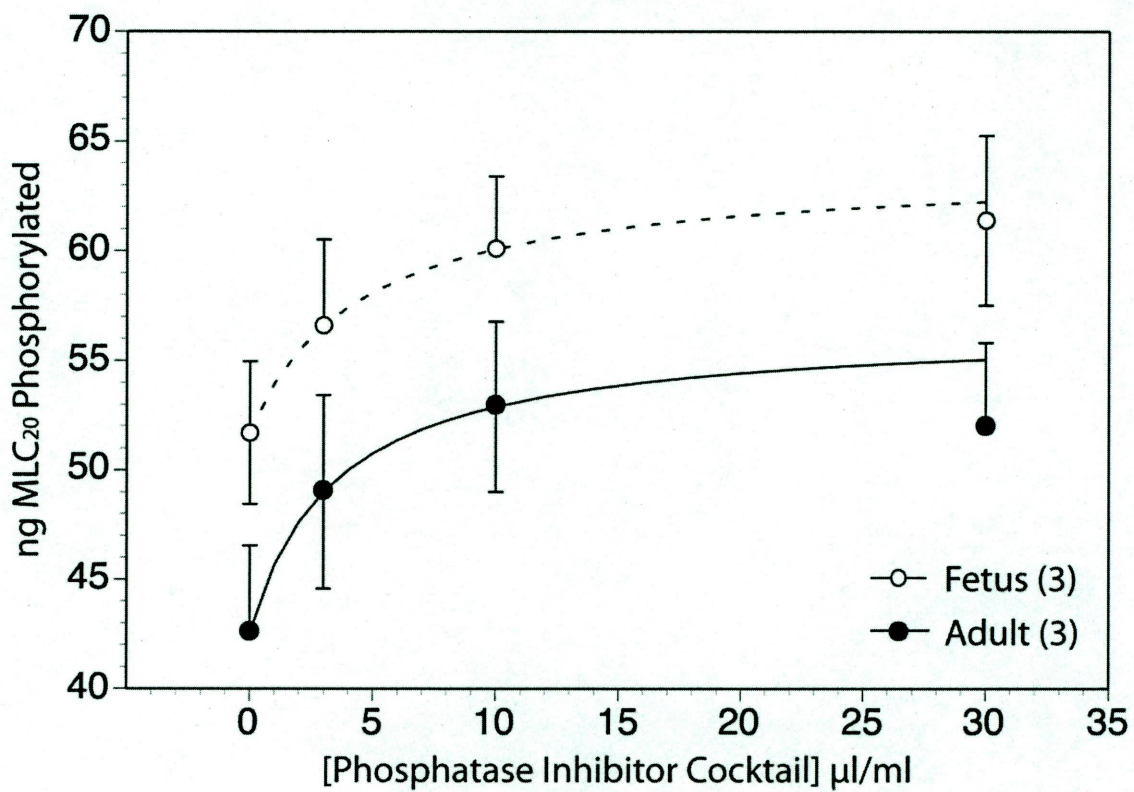


FIGURE 3

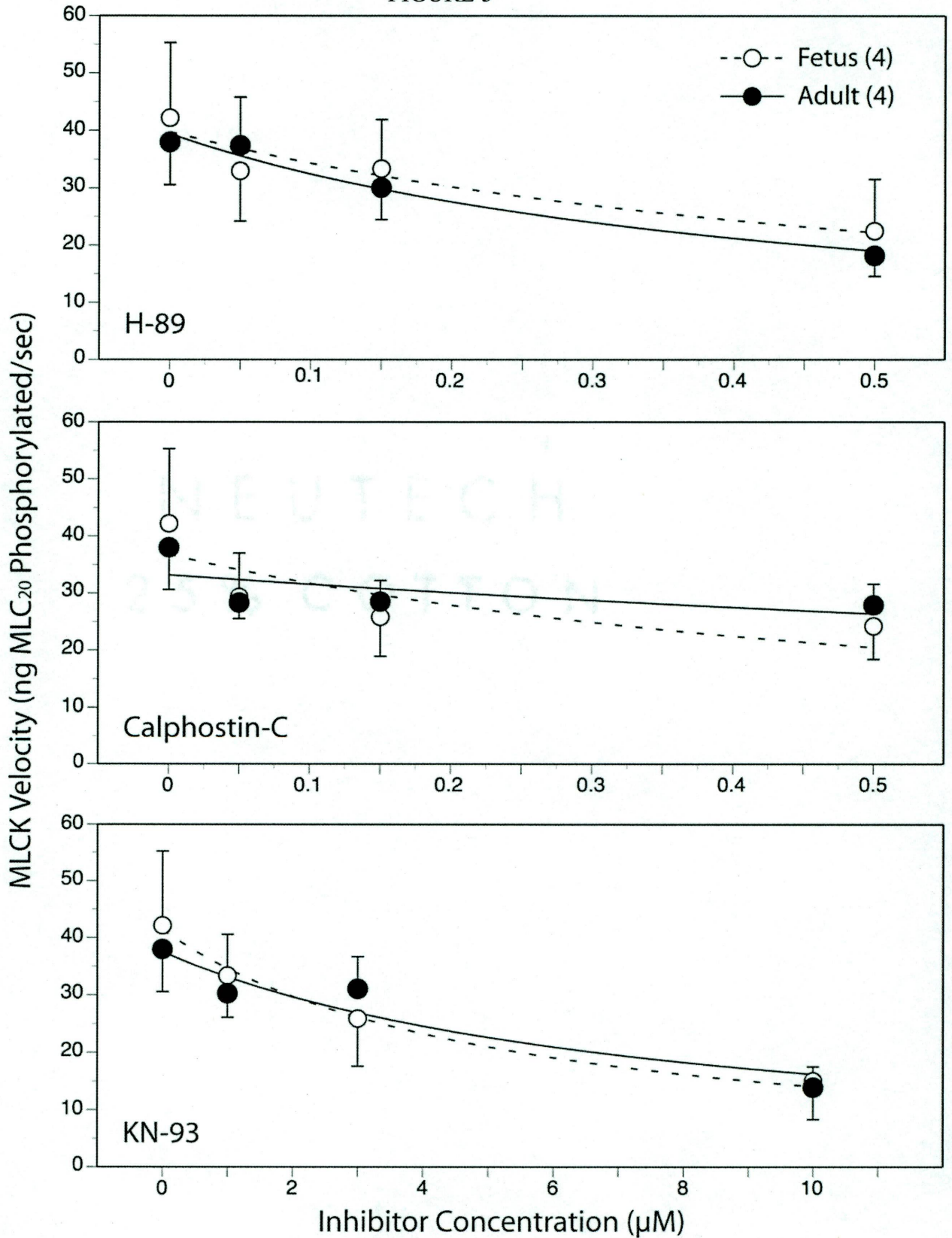
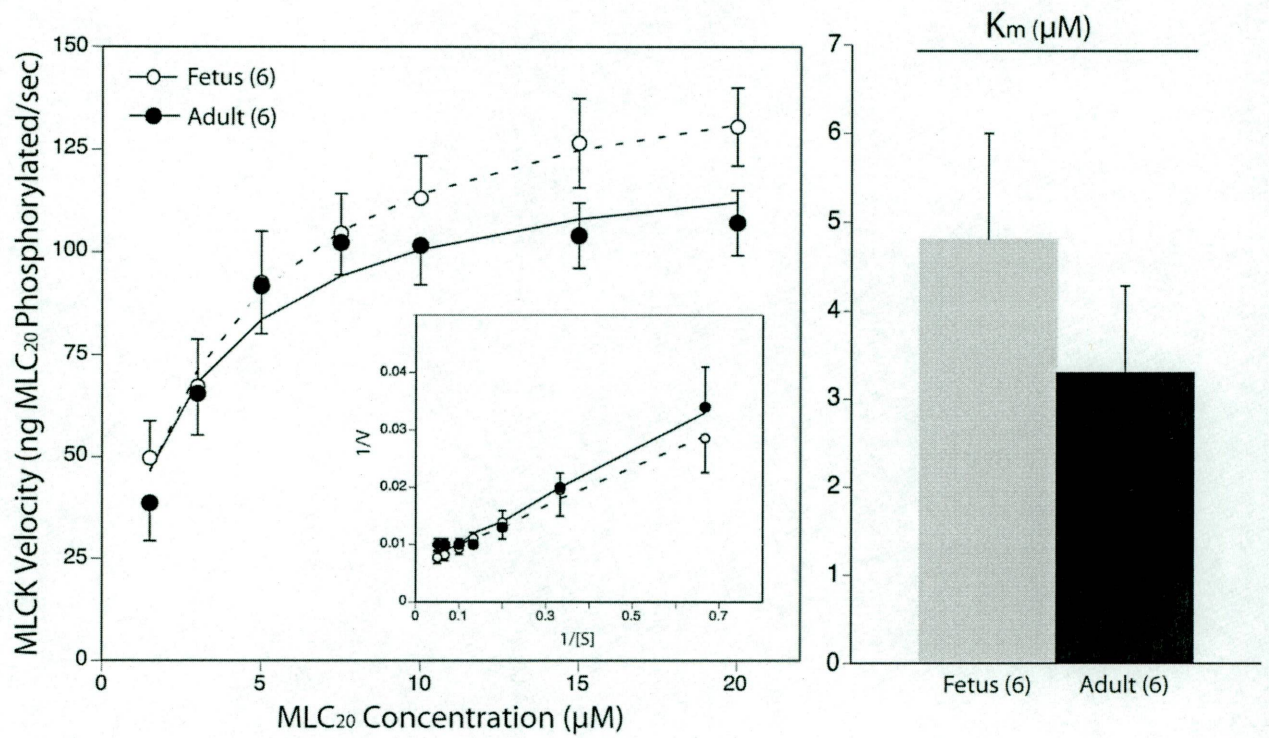
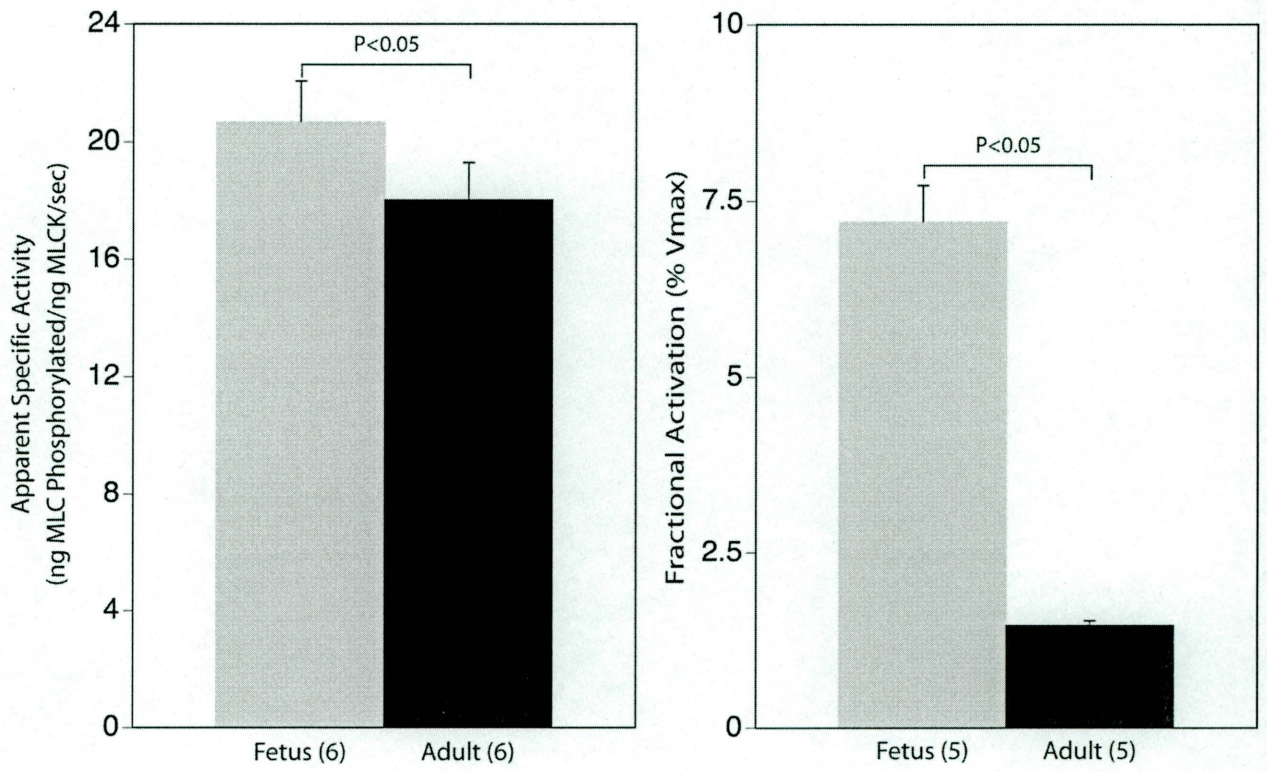


FIGURE 4



NEUTECH
25% COTTON

FIGURE 5



CHAPTER 4

AMINO ACID SEQUENCES OF REGULATORY MYOSIN LIGHT CHAIN (MLC₂₀) ISOFORMS IN VASCULAR SMOOTH MUSCLE DURING DEVELOPMENT

Elisha R. Injeti¹, Gerhart Graupner¹, Kang-Ling Zhang² and William J.Pearce¹

¹Divisions of Physiology and Pharmacology, Center for Perinatal Biology,
Loma Linda University School of Medicine, Loma Linda, California, 92354

²Department of Biochemistry, Loma Linda University School of Medicine, Loma
Linda, California, 92354

Running Head

MLC₂₀ isoforms and Postnatal Maturation

Correspondence

William J.Pearce, Ph.D.

Departments of Physiology and Pharmacology
Loma Linda University School of Medicine, Loma Linda, CA, 92354
e-mail: wpearce@llu.edu, phone: 909-558-4800 ext 45210

Abstract

Myosin light chain kinase (MLCK) is an important enzymatic regulator of vascular contractility that phosphorylates the regulatory protein, myosin light chain 20 (MLC₂₀). We have recently demonstrated that the *in-situ* specific activity of MLCK is strikingly greater in fetal compared to adult sheep carotid arteries. Because cell-specific splicing isoforms of myosin-related genes have been identified in vascular smooth muscle, defining a late stage in the differentiation pathway from the synthetic to contractile phenotype, we tested the hypothesis that developmental alteration in MLCK activity may be at least partially dependent on developmental regulation of MLC₂₀ isoforms. MLC₂₀ was sequenced using a combination of biochemical purification and electron-spray ionization-mass spectrometry (ESI-MS). Our results demonstrate the presence of two isoforms of MLC₂₀ with high level of amino acid sequence conservation in both N-terminal and C-terminal regions of ovine MLC₂₀. Isoform 1 closely resembles chicken MLC₂₀ and is expressed in both fetal and adult ovine arteries. Isoform 2 resembles mouse MLC₂₀ and is expressed in adult tissue only. These findings support our hypothesis that differential expression of these MLC₂₀ isoforms with developmental age may be involved in alteration of MLCK activity.

Key Words

Postnatal maturation, regulatory myosin light chain, protein sequences.

Introduction

We have recently shown that myosin light chain kinase abundance is higher in adult over fetal smooth muscle cells from extracranial sheep arteries, but *in-situ* specific activity is strikingly enhanced in fetal over adult smooth muscle cells. The underlying mechanisms for this developmentally regulated difference are not clear; one possibility is differential substrate (MLC₂₀) reactivity owing to altered structural properties of functional significance, or to altered substrate stability. Altered structural properties of MLC₂₀ may be due to altered post-translational modification of the substrate protein, or due to the expression of substrate isoforms. The phosphorylation of MLC₂₀ at canonical sites is well documented, but the presence of MLC₂₀ isoforms in diverse mammalian tissues has not been addressed with the high resolution and sensitivity afforded by mass spectrometry. The present study examines the age-dependent occurrence of MLC₂₀ isoforms in vascular tissue using electrospray-injection mass spectrometry.

Materials and Methods

General Preparation

Vascular smooth muscle tissue was obtained by collecting arteries from non-pregnant adult female sheep (18-24 months old) and near term (~140 days gestation) fetuses as previously described. Arteries were cleaned of extraneous connective tissue and endothelium was removed by passing a roughened needle through the lumen. Arteries were then immediately frozen in liquid nitrogen and stored at -80 °C until homogenized. All procedures used in these studies were approved by the Animal Research Committee of Loma Linda University and adhered to all policies and practices

outlined in the National Institutes of Health *Guide for the Care and Use of Laboratory Animals*

Extraction of MLC₂₀ from Arterial Tissue

About 25g of arteries were pulverized in liquid nitrogen using stainless steel mortar and pestle as previously described. The pulverized arteries were then homogenized in 6 volumes of buffer containing 50 mM KCl, 20 mM Tris, 15 mM beta-mercaptoethanol at pH 8 followed by centrifugation for 15 minutes at 5010G. The supernatant is discarded and washing is repeated with the same buffer along with 1% triton-X100. Following this washing, the artery homogenate is washed another 4 times with the same buffer with out any triton-X100. The pellet is collected and extracted for MLC₂₀ by continuously stirring with buffer containing 8 M Urea, 20 mM Tris, 15 mM beta-mercaptoethanol for 2 hours at room temperature. After extraction, large proteins were precipitated by adding buffer containing 95% Ethanol and 15 mM beta-mercaptoethanol and stirring for 1 hour at 4 °C followed by centrifugation at 14160G for 20 minutes. The supernatant containing MLC₂₀ is collected.

Ion-Exchange Chromatography of MLC₂₀

About 35g of preswelled DE52 is equilibrated overnight in buffer containing 20 mM Tris and 15 mM beta-mercaptoethanol at 4 °C by continous stirring. The DE52 is allowed to settle and when a distinct line appears between DE52 and the buffer, the supernatant is siphoned off carefully. MLC₂₀ extract is then added to this reconstituted DE52 and stirred overnight at 4 °C. DE52 is then poured into column and proteins are eluted with 150 mM KCl, 10 mM Tris, 15 mM beta-mercatoethanol overnight at 4 °C. The eluant is collected

as 120 fractions each containing 4 mL volume and analyzed for MLC₂₀ using dot-blot method followed by immunoblotting.

Gel filtration Chromatography

The fractions containing MLC₂₀ are identified and pooled together and then precipitated with ammonium sulphate followed by an overnight dialysis using dialyzing solution containing 5M urea, 10 mM EDTA at pH 10.6. The dialysate is then run on S-200 gel filtration column. A total of 120 fractions were collected overnight each containing 2 mL volume and then analyzed for MLC₂₀ using dot-blot method followed by immunoblotting. The purity of the fractions containing MLC₂₀, is further verified by running them on 15% SDS gels and staining with sypro ruby red dye.

Electrospray-Injection Mass Spectrometry (esi-ms)

For mass spectrometric analysis in-gel proteolysis by trypsin and ArgC were performed essentially as described by Shevchenko (Nature Protocols, 2006). Protein acylation before tryptic digest was performed to increase retrieval of hydrophilic N-terminal fragments. Proteolytic fragments were resolved and identified by electrospray-injection mass spectrometry (ESI-MS) on a Waters/Micromass Q-TOF Ultima instrument at the LLU mass spectrometry core.

Results

A total of 40 gm arterial tissue was used for these studies. These tissues were harvested from a total of 40 fetuses and 20 adult sheep respectively

Identification of Fractions Containing MLC₂₀ from Ion-Exchange Chromatography

Extraction supernatant containing MLC₂₀ was bound to DE52 resin and eluted with 150 mM KCl. The fractions were then assayed for total protein content and MLC₂₀. The fractions from #22 to #35 showed high protein content as well as greater MLC₂₀ abundance.

Purification of MLC₂₀ by Gel Filtration

In line with the literature, only few fractions (#62 to #68) of the S-200 eluate containing MLC₂₀ were free of apparent contaminations by protein species of high molecular weight (Fig. 4A). Further purification by 15% SDS-PAA of pooled S-200 eluate was performed (Fig. 4B). A single band migrating at 20kD confirmed the presence of purified MLC₂₀.

Identification of Two Distinct Isoforms of MLC₂₀ by Electrospray-Injection Mass Spectrometry (esi-ms)

Two distinct isoforms of smooth muscle ovine MLC₂₀ were identified in band 2. Isoform 1 closely resembles chicken MLC₂₀ and is expressed in adult and fetal tissue. Isoform 2 closely resembles mouse MLC₂₀ and is expressed in adult tissue only.

Discussion

In contrast to most previous studies of smooth muscle MLC expression, two distinct isoforms of smooth muscle ovine MLC₂₀ with essentially the same molecular weight were identified in adult arteries.

The first ovine isoform is virtually identical to the major isoform of chicken gizzard MLC₂₀, except for a possible deletion of the most N-terminal amino acids, as seen in

bovine smooth muscle MLC₂₀. The first ovine isoform is expressed in both adult and fetal arteries.

The second ovine isoform is virtually identical to rat smooth muscle MLC₂₀ and strongly resembles the porcine MLC3 isoform, except for a possible deletion of the most N-terminal amino acids, as seen in bovine smooth muscle MLC₂₀. The second ovine isoform is expressed in adult tissue only, establishing the paradigm of developmentally expressed MLC₂₀ isoforms.

The absence of the N-terminal four coding amino acids of the MLC₂₀ consensus sequence from sheep MLC₂₀ needs to be confirmed by an alternative proteolytic digestion procedure (V8 protease).

Most amino acid substitutions (which also define the porcine MLC3 isoform) in ovine vascular isoform 2 are seen within a twelve amino acid stretch between residues 112 and 124 (conventional numbering), directly C-terminally contiguous to the first putative helix of the second EF hand. Another unique isoform substitution (DA) is located 12 amino acids before the end of the last putative helix in the first large EF hand.

Isoform-specific amino acid substitutions are seen within the first and second EF-Hand regions in positions consistent with a possible role in exerting influence on the exact positioning of adjacent helical structures

These results constitute the first demonstration of smooth muscle MLC₂₀ isoforms in mammalian tissues, specifically in vascular tissue. Whereas the source tissue includes multiple cell types (endothelia, smooth muscle cells, fibroblasts), only smooth muscle cells are known to contain substantial amounts of smooth muscle-specific MLC₂₀.

Amino acid substitutions of the porcine MLC3 type in ovine MLC isoform 2 may influence the exact positioning of helical elements within the functional domains of MLC₂₀ and thereby affect interactions with MLCK and/or myosin cross-bridges.

Age-related variations in MLC isoform expression may help explain developmental differences in regulation of myofilament calcium sensitivity and overall vascular contractility.

Figure Legends

Figure 1: Extraction and Ion-Exchange Chromatography of MLC₂₀

MLC₂₀ was prepared from snap-frozen sheep arteries. Ethanolic extraction supernatant containing MLC₂₀ was bound to DE52 resin and eluted at 150 mM KCl. MLC₂₀-containing fractions were identified by immunoblot, pooled and further purified by gel filtration over a S-200 column.

Figure 2: Purification of MLC₂₀ by Gel Filtration

Crude MLC₂₀ eluted from the DE52 column was concentrated by ammonium sulfate precipitation, dialyzed against 5M urea, 10 mM EDTA at pH 10.6, and eluted from an S-200 column. Eluate fractions containing MLC₂₀ were identified by immunoblot.

Figure 3: Analytical and Preparative Gels of Ovine Smooth Muscle MLC₂₀

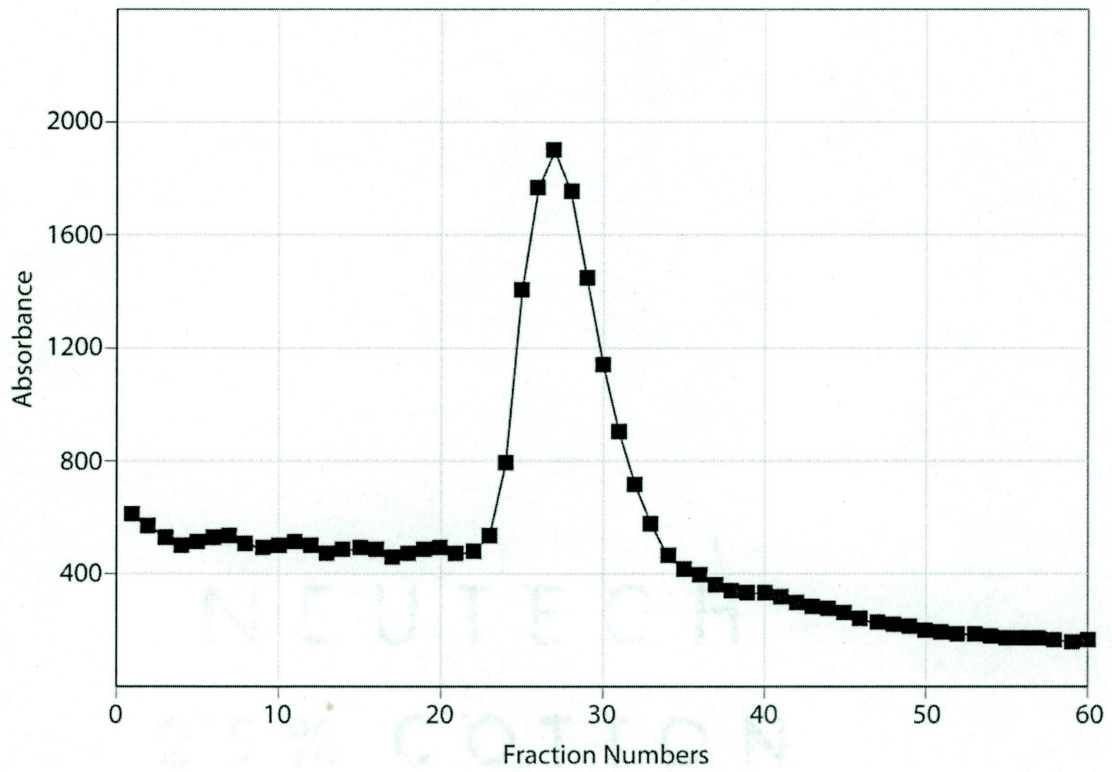
The eluants from S-200 column were analyzed on 15% SDS-PAA gels stained with SYPRO Ruby, to assess apparent purity. An increasing amount of carbonic anhydrase is also loaded on the gels to provide a reference standard to quantify the amount of MLC₂₀ present in the samples.

Figure 4: Alignment of Isoform-Specific Amino Acid Substitutions

Proteolytic fragments were resolved and identified by electrospray-injection mass spectrometry (ESI-MS) on a Waters/Micromass Q-TOF Ultima instrument.

Figures

FIGURE-1



Western Blot

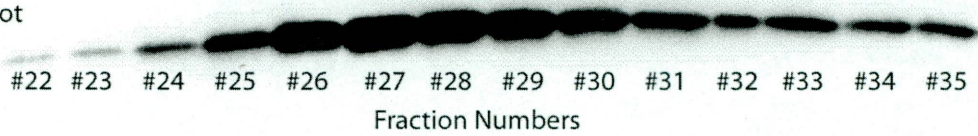
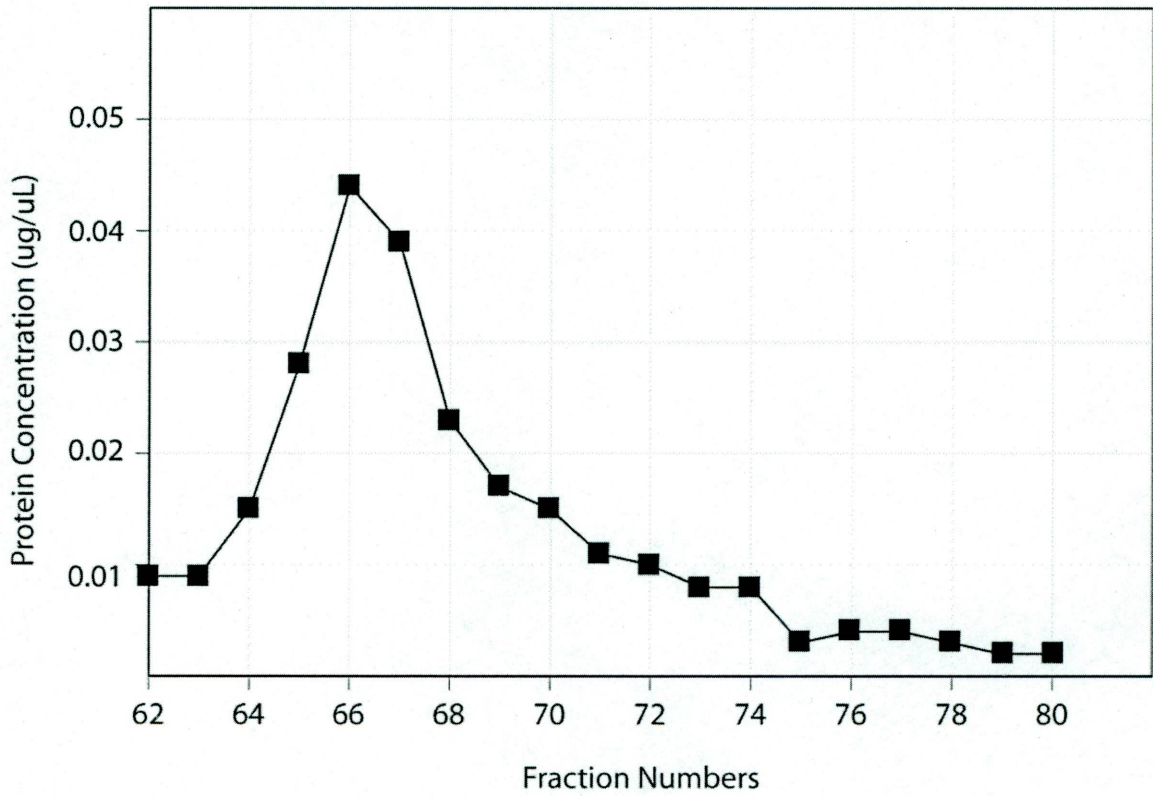


FIGURE-2



Immunoblot

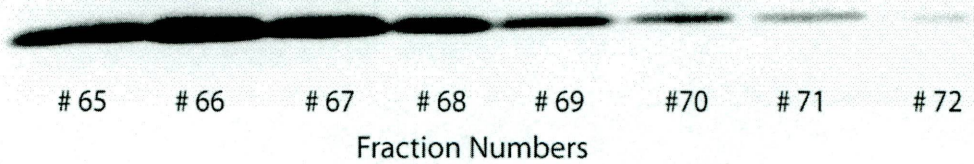


FIGURE-3

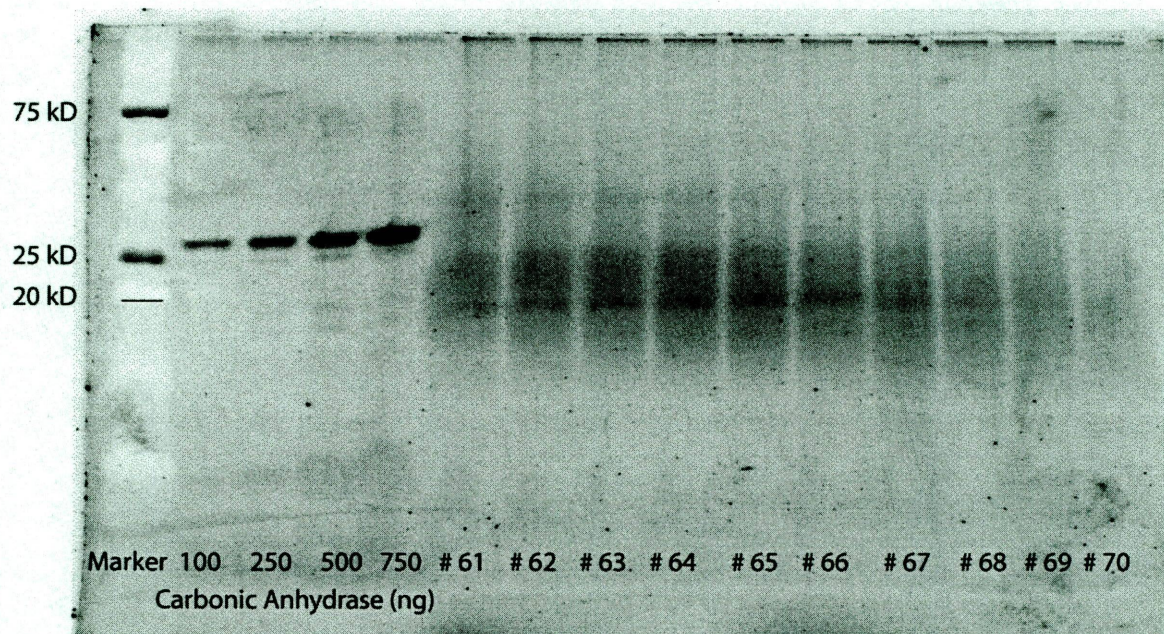


FIGURE 4

	10	20	30	40	50

Ovine isoform 1	MSSKRAKAKT	TKKRPQRATS	NVFAMFDQSQ	IQEFKEAFNM	IDQNRDGFID
Ovine isoform 2	MSSKRAKTKT	TKKRPQRATS	NVFAMFDQSQ	IQEFKEAFNM	IDQNRDGFID
	60	70	80	90	100

Ovine isoform 1	KEDLHDMLAS	MGKNPTDEYL	EGMMSEAPG-	-----PINFT	MFLTMFG--E
Ovine isoform 2	KEDIHDMLAS	MGKMPTDEYL	DAMMMEAPG-	-----PINFT	MFLTMFG--E
	110	120	130	140	150

Ovine isoform 1	KLNGTDPEDV	IRNAFACFDE	EASGFIHEDH	LRELLTTMGD	RFTDEEVDEM
Ovine isoform 2	KLNGTDPEDV	IRNAFACFDE	EAIGTIQEDY	LRELLTTMGD	RFTDEEVDEL
	160	170	180		
		
Ovine isoform 1	YREAPIDKKG	NFNYVEFTRI	LKHGAKDKDD		
Ovine isoform 2	YREAPIDKKG	NFNYIEFTRI	LKHGAKDKDD		

CHAPTER 5

CONCLUSIONS & FUTURE DIRECTIONS

The present studies investigated the hypothesis that age-related differences in myofilament calcium sensitivity involve upregulation of myosin light chain kinase activity in fetal compared to adult carotids. To test this hypothesis, as the first specific aim, MLCK and MLC abundances in fetal and adult carotid arteries were measured. The results clearly showed that MLCK abundance is about 6 fold greater in adult compared to fetal carotid arteries. However, MLC abundance remained relatively same in both fetal and adult carotid arteries. From these results it is clear that expression of myosin light chain kinase protein is regulated very differently in fetus and adult. This could be due to differences in either protein synthesis or protein degradation. Further studies can be conducted using molecular biology techniques like RT-PCR to test mRNA abundance of MLCK in both fetal and adult arteries. These studies will clarify if the differences in MLCK protein abundance are due to differences in mechanisms involved in protein synthesis. Using these techniques, the transcription rate and translation efficiency of MLCK can also be determined. Together these studies will provide a basis to explain the 6 fold greater abundance of MLCK protein in adult compared to fetal arteries. As the abundance of myosin light chain did not change significantly it is possible that the regulatory mechanisms involved in its synthesis are highly conserved. As myosin is a highly conserved protein expressed in most of the eukaryotic cells, it is possible that its expression is not influenced by age dependent changes.

In the second specific aim, MLCK *in-situ* specific activity is measured. For this purpose, the conditions required for maximal activation of MLCK were optimized and verified. These experiments also necessitated the designing of a custom-made rapid freeze apparatus that can maximally activate MLCK by electrical field stimulation and simultaneously freeze the tissue at very short intervals of time using a computer controlled solenoid valves. This apparatus enabled most accurate and reliable measurements of MLCK velocity. The results from these studies indicated that MLCK velocity (% MLC phosphorylated/sec) is significantly greater in fetal (7.39 ± 0.53) as compared to adult (6.56 ± 0.29) arteries. When these values are normalized to the total MLC present in the artery segments, the results indicated that there is no significant difference in MLCK velocity (ng MLC phosphorylated/sec) between the fetal (89.4 ± 6.4) and adult (93.2 ± 4.1) arteries. Further correction of these MLCK velocities (ng MLC phosphorylated/sec/ng MLCK) for differences in MLCK abundance did reveal that fetal MLCK velocity (1.52 ± 0.11) is significantly greater than adult (0.26 ± 0.01) values. Together, these results clearly indicate that MLCK *in-situ* specific activity is upregulated in fetal compared to adult arteries.

These results raise interesting possibilities regarding the factors that contribute to these differences in MLCK *in-situ* specific activity. The first possibility is that differences in intracellular calcium transients in response to stimuli may be a key factor in explaining the differences in MLCK *in-situ* specific activity between fetus and adult. In light of previously published results that intracellular calcium pools are significantly different in fetal and adult arteries, further studies must be conducted to measure intracellular calcium transients in response to electrical field stimulation. These

experiments will require further modification of the existing model of rapid freeze apparatus. Alternatively, this relationship between MLCK *in-situ* specific activity and intracellular calcium concentration can be measured using buffers containing graded calcium concentration. These studies will help in explaining if the differences in MLCK *in-situ* specific activity are due to differences in intracellular calcium transients. The second possibility that can explain the observed differences in MLCK *in-situ* specific activity is availability of calmodulin. As calmodulin is necessary for activation of MLCK, colocalization of calmodulin with MLCK is critical for its activation. Owing to the fact that ultra structural organization of fetal and adult arteries are dramatically different, the distribution of MLCK and calmodulin must be tested using methods like immunohistochemistry, confocal microscopy with corresponding transmural morphometry. These studies will reveal the role of co-factors like calmodulin in explaining the differences in MLCK *in-situ* specific activity. Similar studies must also be conducted to verify the spatial organization and distribution of MLCK and MLC in both fetal and adult arteries.

The results from MLCK *in-situ* specific activity measurements lead to the third specific aim where the maximal velocity (V_{\max}) and K_m of MLCK in artery homogenates was measured in both fetal and adult arteries. The results from these studies indicate that V_{\max} (ng MLC₂₀ phosphorylated/sec) is significantly greater in fetal (163 ± 11) compared to adult (130 ± 9) arteries. The K_m values in fetal ($4.80 \pm 1.20 \mu\text{M}$) were not significantly different than adult values ($3.30 \pm 0.98 \mu\text{M}$). Taking these results together with MLCK *in-situ* velocity measurements, we estimated the fractional activation of the enzyme in intact

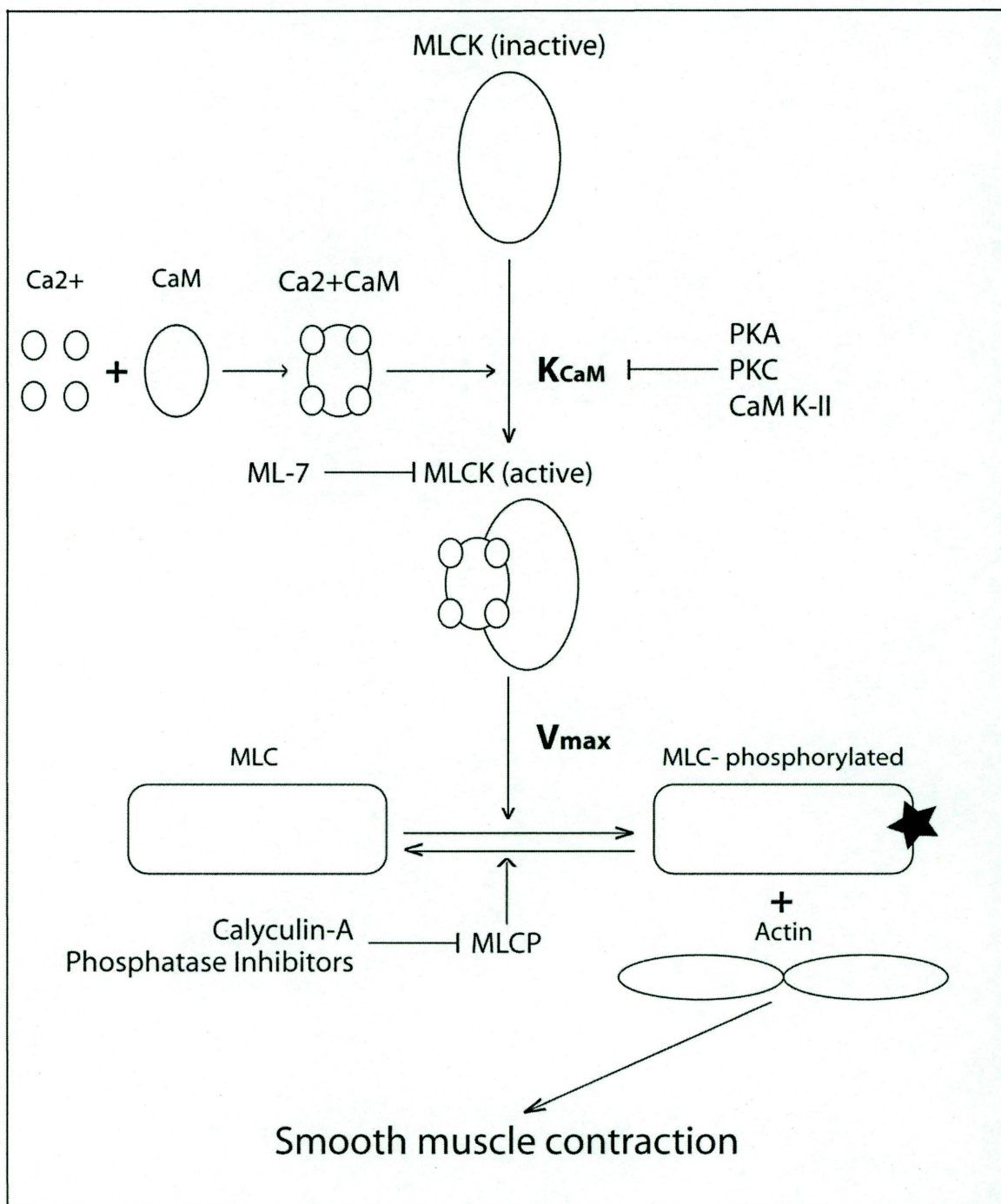
tissue. The results revealed that fractional activation of MLCK is about 5 fold greater in fetal arteries compared to adult arteries.

These results also raise interesting possibilities that can be further explored. Firstly, the significant differences in V_{\max} of MLCK observed can be due to presence of MLCK isoforms. This possibility can be investigated using both RT-PCR and Western blots. For this purpose, specific primers that can differentiate MLCK isoforms must be developed. Similarly, for Western blots specific primary antibodies for each MLCK isoform must be developed. This will eliminate the error in detecting MLCK isoforms, which are less abundant and co-migrate as a single band. Secondly, the differences in V_{\max} of MLCK can be due to presence of MLC₂₀ isoforms. The results from our mass spectrometry studies do reveal that fetal and adult arteries express different MLC₂₀ isoforms. As the present V_{\max} measurements were conducted using a common substrate (chicken gizzard MLC₂₀) further studies using purified isoforms of MLC₂₀ from both fetal and adult arteries are necessary to elucidate the role of MLC₂₀ isoforms in influencing MLCK velocity. For this purpose, MLC₂₀ must be purified from both fetal and adult arteries and MLCK & MLC₂₀ cross over studies must be conducted.

In conclusion, these studies are the first to offer a quantitative assessment of in-situ MLCK activity in fetal and adult carotid arteries and indicate the relative extents to which specific activity and fractional activation contribute to these differences. In addition, they also reveal how the expression of MLCK and MLC abundances influence the overall activity of the enzyme. Together, these studies support our core hypothesis that age related differences in myofilament calcium sensitivity involve upregulation of MLCK activity.

Future studies on the contribution of other thick and thin filament regulatory proteins in age related difference in myofilament calcium sensitivity is an interesting and intriguing area that needs to be explored. There is already enough evidence in the literature that multiple signaling pathways regulate myosin light chain phosphatase activity and that it plays a key role in thick filament reactivity. However, the effect of age-related changes on myosin light chain phosphatase activity and its impact on myofilament calcium sensitivity needs to be investigated. Similar studies on thin filament regulatory proteins like caldesmon, HSP27 & HSP20 is an other exciting area of research that needs to be explored. Together, all these studies will help in establishing the significance of myofilament calcium sensitivity in regulating the overall contractile function of vascular smooth muscle. This in turn can provide a solid basis for developing new strategies based on myofilament calcium sensitivity for pharmacological management of premature babies with cerebrovascular and cardiovascular instabilities.

FIGURE-1



REFERENCES

1. Adelstein RS, Conti MA, and Pato MD. Regulation of myosin light chain kinase by reversible phosphorylation and calcium-calmodulin. *Ann N Y Acad Sci* 356: 142-150, 1980.
2. Akopov SE, Zhang L, and Pearce WJ. Developmental changes in the calcium sensitivity of rabbit cranial arteries. *Biol Neonate* 74: 60-71, 1998.
3. Akopov SE, Zhang L, and Pearce WJ. Physiological variations in ovine cerebrovascular calcium sensitivity. *Am J Physiol* 272: H2271-2281, 1997.
4. Akopov SE, Zhang L, and Pearce WJ. Regulation of Ca²⁺ sensitization by PKC and rho proteins in ovine cerebral arteries: effects of artery size and age. *Am J Physiol* 275: H930-939, 1998 Sep.
5. Aksoy MO, Williams D, Sharkey EM, and Hartshorne DJ. A relationship between Ca²⁺ sensitivity and phosphorylation of gizzard actomyosin. *Biochem Biophys Res Commun* 69: 35-41, 1976.
6. Ammit AJ, Armour CL, and Black JL. Smooth-muscle myosin light-chain kinase content is increased in human sensitized airways. *Am J Respir Crit Care Med* 161: 257-263, 2000.
7. Belik J, Kerc E, and Pato MD. Rat pulmonary arterial smooth muscle myosin light chain kinase and phosphatase activities decrease with age. *Am J Physiol Lung Cell Mol Physiol* 290: L509-516, 2006.
8. Blue EK, Goeckeler ZM, Jin Y, Hou L, Dixon SA, Herring BP, Wysolmerski RB, and Gallagher PJ. 220- and 130-kDa MLCKs have distinct tissue distributions and intracellular localization patterns. *Am J Physiol Cell Physiol* 282: C451-460, 2002 Mar.
9. Carsten ME. Uterine smooth muscle: troponin. *Arch Biochem Biophys* 147: 353-357, 1971.

10. Chacko S, Conti MA, and Adelstein RS. Effect of phosphorylation of smooth muscle myosin on actin activation and Ca²⁺ regulation. *Proc Natl Acad Sci U S A* 74: 129-133, 1977.
11. Choudhury N, Khromov AS, Somlyo AP, and Somlyo AV. Telokin mediates Ca²⁺-desensitization through activation of myosin phosphatase in phasic and tonic smooth muscle. *J Muscle Res Cell Motil* 25: 657-665, 2004.
12. Conti MA and Adelstein RS. The relationship between calmodulin binding and phosphorylation of smooth muscle myosin kinase by the catalytic subunit of 3':5' cAMP-dependent protein kinase. *J Biol Chem* 256: 3178-3181, 1981.
13. Dakshinamurti S. Pathophysiologic mechanisms of persistent pulmonary hypertension of the newborn. *Pediatr Pulmonol* 39: 492-503, 2005.
14. Ebashi S. The Croonian lecture, 1979: Regulation of muscle contraction. *Proc R Soc Lond B Biol Sci* 207: 259-286, 1980.
15. Ebashi S and Kodama A. Interaction of troponin with F-actin in the presence of tropomyosin. *J Biochem* 59: 425-426, 1966.
16. Ebashi S and Kodama A. Native tropomyosin-like action of troponin on trypsin-treated myosin B. *J Biochem* 60: 733-734, 1966.
17. Ebashi S, Mikawa T, Kuwayama H, Suzuki M, Ikemoto H, Ishizaki Y, and Koga R. Ca²⁺ regulation in smooth muscle; dissociation of myosin light chain kinase activity from activation of actin-myosin interaction. *Prog Clin Biol Res* 245: 109-117, 1987.
18. Fisher SA and Ikebe M. Developmental and tissue distribution of expression of nonmuscle and smooth muscle isoforms of myosin light chain kinase. *Biochem Biophys Res Commun* 217: 696-703, 1995.
19. Gallagher PJ, Garcia JG, and Herring BP. Expression of a novel myosin light chain kinase in embryonic tissues and cultured cells. *J Biol Chem* 270: 29090-29095, 1995.
20. Gallagher PJ, Herring BP, and Stull JT. Myosin light chain kinases. *J Muscle Res Cell Motil* 18: 1-16, 1997 Feb.

21. Gilbert EK, Weaver BA, and Rembold CM. Depolarization decreases the $[Ca^{2+}]_i$ sensitivity of myosin light-chain kinase in arterial smooth muscle: comparison of aequorin and fura 2 $[Ca^{2+}]_i$ estimates. *FASEBJ* 5: 2593-2599, 1991.
22. Gong MC, Fuglsang A, Alessi D, Kobayashi S, Cohen P, Somlyo AV, and Somlyo AP. Arachidonic acid inhibits myosin light chain phosphatase and sensitizes smooth muscle to calcium. *J Biol Chem* 267: 21492-21498, 1992.
23. Gorecka A, Aksoy MO, and Hartshorne DJ. The effect of phosphorylation of gizzard myosin on actin activation. *Biochem Biophys Res Commun* 71: 325-331, 1976.
24. Grand RJ and Perry SV. Calmodulin-binding proteins from brain and other tissues. *Biochem J* 183: 285-295, 1979.
25. Grand RJ, Perry SV, and Weeks RA. Troponin C-like proteins (calmodulins) from mammalian smooth muscle and other tissues. *Biochem J* 177: 521-529, 1979.
26. Hartshorne DJ, Ito M, and Erdodi F. Myosin light chain phosphatase: subunit composition, interactions and regulation. *J Muscle Res Cell Motil* 19: 325-341, 1998 May.
27. Hartshorne DJ and Siemankowski RF. Regulation of smooth muscle actomyosin. *Annu Rev Physiol* 43: 519-530, 1981.
28. Hashimoto Y and Soderling TR. Phosphorylation of smooth muscle myosin light chain kinase by Ca^{2+} /calmodulin-dependent protein kinase II: comparative study of the phosphorylation sites. *Arch Biochem Biophys* 278: 41-45, 1990.
29. Head JF, Weeks RA, and Perry SV. Affinity-chromatographic isolation and some properties of troponin C from different muscle types. *Biochem J* 161: 465-471, 1977.
30. Herring BP, El-Mounayri O, Gallagher PJ, Yin F, and Zhou J. Regulation of myosin light chain kinase and telokin expression in smooth muscle tissues. *Am J Physiol Cell Physiol* 291: C817-827, 2006.
31. Herring BP, Lyons GE, Hoggatt AM, and Gallagher PJ. Telokin expression is restricted to smooth muscle tissues during mouse development. *Am J Physiol Cell Physiol* 280: C12-21, 2001 Jan.

32. Hori M and Karaki H. Regulatory mechanisms of calcium sensitization of contractile elements in smooth muscle. *Life Sci* 62: 1629-1633, 1998.
33. Horowitz A, Menice CB, Laporte R, and Morgan KG. Mechanisms of smooth muscle contraction. *Physiol Rev* 76: 967-1003, 1996.
34. Ichikawa K, Ito M, and Hartshorne DJ. Phosphorylation of the large subunit of myosin phosphatase and inhibition of phosphatase activity. *J Biol Chem* 271: 4733-4740, 1996.
35. Ikebe M, Aiba T, Onishi H, and Watanabe S. Calcium sensitivity of contractile proteins from chicken gizzard muscle. *J Biochem* 83: 1643-1655, 1978.
36. Ikebe M, Hartshorne DJ, and Elzinga M. Phosphorylation of the 20,000-dalton light chain of smooth muscle myosin by the calcium-activated, phospholipid-dependent protein kinase. Phosphorylation sites and effects of phosphorylation. *J Biol Chem* 262: 9569-9573, 1987.
37. Ito M, Dabrowska R, Guerriero V, Jr., and Hartshorne DJ. Identification in turkey gizzard of an acidic protein related to the C-terminal portion of smooth muscle myosin light chain kinase. *J Biol Chem* 264: 13971-13974, 1989.
38. Itoh T, Ikebe M, Kargacin G, Hartshorne D, Kemp B, and Fay FS. Modulators of myosin light chain kinase activity affect both $[Ca^{+2}]$ and contraction in single smooth muscle cells. *Prog Clin Biol Res* 327: 73-87, 1990.
39. Itoh T, Ikebe M, Kargacin GJ, Hartshorne DJ, Kemp BE, and Fay FS. Effects of modulators of myosin light-chain kinase activity in single smooth muscle cells. *Nature* 338: 164-167, 1989.
40. Kamm KE and Stull JT. The function of myosin and myosin light chain kinase phosphorylation in smooth muscle. *Annu Rev Pharmacol Toxicol* 25: 593-620, 1985.
41. Kimura K, Ito M, Amano M, Chihara K, Fukata Y, Nakafuku M, Yamamori B, Feng J, Nakano T, Okawa K, Iwamatsu A, and Kaibuchi K. Regulation of myosin phosphatase by Rho and Rho-associated kinase (Rho-kinase). *Science* 273: 245-248, 1996 Jul 12.

42. Koyama M, Ito M, Feng J, Seko T, Shiraki K, Takase K, Hartshorne DJ, and Nakano T. Phosphorylation of CPI-17, an inhibitory phosphoprotein of smooth muscle myosin phosphatase, by Rho-kinase. *FEBS Lett* 475: 197-200, 2000.
43. Liu G, Liu X, Rao K, Jiang H, and Stephens NL. Increased myosin light chain kinase content in sensitized canine saphenous vein. *J Appl Physiol* 80: 665-669, 1996.
44. MacDonald JA, Eto M, Borman MA, Brautigan DL, and Haystead TA. Dual Ser and Thr phosphorylation of CPI-17, an inhibitor of myosin phosphatase, by MYPT-associated kinase. *FEBS Lett* 493: 91-94, 2001.
45. Means AR, Bagchi IC, VanBerkum MF, and Kemp BE. Regulation of smooth muscle myosin light chain kinase by calmodulin. *Adv Exp Med Biol* 304: 11-24, 1991.
46. Means AR, VanBerkum MF, Bagchi I, Lu KP, and Rasmussen CD. Regulatory functions of calmodulin. *Pharmacol Ther* 50: 255-270, 1991.
47. Mikawa T, Nonomura Y, and Ebashi S. Does phosphorylation of myosin light chain have direct relation to regulation in smooth muscle? *J Biochem* 82: 1789-1791, 1977.
48. Mikawa T, Nonomura Y, Hirata M, Ebashi S, and Kakiuchi S. Involvement of an acidic protein in regulation of smooth muscle contraction by the tropomyosin-leiotonin system. *J Biochem* 84: 1633-1636, 1978.
49. Mikawa T, Toyo-oka T, Nonomura Y, and Ebashi S. Essential factor of gizzard "troponin" fraction. A new type of regulatory protein. *J Biochem* 81: 273-275, 1977.
50. Mino T, Yuasa U, Nakamura F, Naka M, and Tanaka T. Two distinct actin-binding sites of smooth muscle calponin. *Eur J Biochem* 251: 262-268, 1998.
51. Mrwa U and Hartshorne DJ. Phosphorylation of smooth muscle myosin and myosin light chains. *Fed Proc* 39: 1564-1568, 1980.
52. Mrwa U, Troschka M, Gross C, and Katzinski L. Calcium-sensitivity of pig-carotid-actomyosin ATPase in relation to phosphorylation of the regulatory light chain. *Eur J Biochem* 103: 415-419, 1980.

53. Murphy RA and Walker JS. Inhibitory mechanisms for cross-bridge cycling: the nitric oxide-cGMP signal transduction pathway in smooth muscle relaxation. *Acta Physiol Scand* 164: 373-380, 1998 Dec.
54. Nakamura F, Mino T, Yamamoto J, Naka M, and Tanaka T. Identification of the regulatory site in smooth muscle calponin that is phosphorylated by protein kinase C. *J Biol Chem* 268: 6194-6201, 1993.
55. Niiro N and Ikebe M. Zipper-interacting protein kinase induces Ca(2+)-free smooth muscle contraction via myosin light chain phosphorylation. *J Biol Chem* 276: 29567-29574, 2001.
56. Nishikawa M, de Lanerolle P, Lincoln TM, and Adelstein RS. Phosphorylation of mammalian myosin light chain kinases by the catalytic subunit of cyclic AMP-dependent protein kinase and by cyclic GMP-dependent protein kinase. *J Biol Chem* 259: 8429-8436, 1984.
57. Nishikori K, Weisbrodt NW, Sherwood OD, and Sanborn BM. Effects of relaxin on rat uterine myosin light chain kinase activity and myosin light chain phosphorylation. *J Biol Chem* 258: 2468-2474, 1983.
58. Numata T, Katoh T, and Yazawa M. Functional role of the C-terminal domain of smooth muscle myosin light chain kinase on the phosphorylation of smooth muscle myosin. *J Biochem (Tokyo)* 129: 437-444, 2001.
59. Ohlmann P, Tesse A, Loichot C, Ralay Ranaivo H, Roul G, Philippe C, Watterson DM, Haiech J, and Andriantsitohaina R. Deletion of MLCK210 induces subtle changes in vascular reactivity but does not affect cardiac function. *Am J Physiol Heart Circ Physiol* 289: H2342-2349, 2005.
60. Paul ER, Ngai PK, Walsh MP, and Groschel-Stewart U. Embryonic chicken gizzard: expression of the smooth muscle regulatory proteins caldesmon and myosin light chain kinase. *Cell Tissue Res* 279: 331-337, 1995.
61. Poperechnaya A, Varlamova O, Lin PJ, Stull JT, and Bresnick AR. Localization and activity of myosin light chain kinase isoforms during the cell cycle. *J Cell Biol* 151: 697-708, 2000.
62. Ringer S. A further Contribution regarding the influence of the different Constituents of the Blood on the Contraction of the Heart. *J Physiol* 4: 29-42 23, 1883.

63. Ringer S. A third contribution regarding the Influence of the Inorganic Constituents of the Blood on the Ventricular Contraction. *J Physiol* 4: 222-225, 1883.
64. Sandoval RJ, Injeti ER, Gerthoffer WT, and Pearce WJ. Postnatal maturation modulates relationships among cytosolic Ca²⁺, myosin light chain phosphorylation, and contractile tone in ovine cerebral arteries. *Am J Physiol Heart Circ Physiol* 293: H2183-2192, 2007.
65. Savineau JP and Marthan R. Modulation of the calcium sensitivity of the smooth muscle contractile apparatus: molecular mechanisms, pharmacological and pathophysiological implications. *Fundam Clin Pharmacol* 11: 289-299, 1997.
66. Shirinsky VP, Vorotnikov AV, Birukov KG, Nanaev AK, Collinge M, Lukas TJ, Sellers JR, and Watterson DM. A kinase-related protein stabilizes unphosphorylated smooth muscle myosin minifilaments in the presence of ATP. *J Biol Chem* 268: 16578-16583, 1993.
67. Smith L, Parizi-Robinson M, Zhu MS, Zhi G, Fukui R, Kamm KE, and Stull JT. Properties of long myosin light chain kinase binding to F-actin in vitro and in vivo. *J Biol Chem* 277: 35597-35604, 2002.
68. Smith L and Stull JT. Myosin light chain kinase binding to actin filaments. *FEBS Lett* 480: 298-300, 2000.
69. Sobieszek A. Ca-linked phosphorylation of a light chain of vertebrate smooth-muscle myosin. *Eur J Biochem* 73: 477-483, 1977.
70. Sobieszek A, Andruchov OY, and Nieznanski K. Kinase-related protein (telokin) is phosphorylated by smooth-muscle myosin light-chain kinase and modulates the kinase activity. *Biochem J* 328 (Pt 2): 425-430, 1997.
71. Sobieszek A and Small JV. Regulation of the actin-myosin interaction in vertebrate smooth muscle: activation via a myosin light-chain kinase and the effect of tropomyosin. *J Mol Biol* 112: 559-576, 1977.
72. Somlyo AP and Somlyo AV. Ca²⁺ sensitivity of smooth muscle and nonmuscle myosin II: modulated by G proteins, kinases, and myosin phosphatase. *Physiol Rev* 83: 1325-1358, 2003 Oct.

73. Somlyo AP and Somlyo AV. Signal transduction and regulation in smooth muscle [published erratum appears in *Nature* 1994 Dec 22-29;372(6508):812]. *Nature* 372: 231-236, 1994.
74. Somlyo AV, Khromov AS, Webb MR, Ferenczi MA, Trentham DR, He ZH, Sheng S, Shao Z, and Somlyo AP. Smooth muscle myosin: regulation and properties. *Philos Trans R Soc Lond B Biol Sci* 359: 1921-1930, 2004.
75. Stull JT, Tansey MG, Word RA, Kubota Y, and Kamm KE. Myosin light chain kinase phosphorylation: regulation of the Ca²⁺ sensitivity of contractile elements. *Adv Exp Med Biol* 304: 129-138, 1991.
76. Sweeney HL, Bowman BF, and Stull JT. Myosin light chain phosphorylation in vertebrate striated muscle: regulation and function. *Am J Physiol* 264: C1085-1095, 1993.
77. Tansey MG, Luby-Phelps K, Kamm KE, and Stull JT. Ca(2+)-dependent phosphorylation of myosin light chain kinase decreases the Ca²⁺ sensitivity of light chain phosphorylation within smooth muscle cells. *J Biol Chem* 269: 9912-9920, 1994.
78. Taylor EW. Mechanism of actomyosin ATPase and the problem of muscle contraction. *CRC Crit Rev Biochem* 6: 103-164, 1979.
79. Throckmorton DC, Packer CS, and Brophy CM. Protein kinase C activation during Ca²⁺-independent vascular smooth muscle contraction. *J Surg Res* 78: 48-53, 1998.
80. Toth A, Kiss E, Gergely P, Walsh MP, Hartshorne DJ, and Erdodi F. Phosphorylation of MYPT1 by protein kinase C attenuates interaction with PP1 catalytic subunit and the 20 kDa light chain of myosin. *FEBS Lett* 484: 113-117, 2000.
81. Van Riper DA, Weaver BA, Stull JT, and Rembold CM. Myosin light chain kinase phosphorylation in swine carotid artery contraction and relaxation. *Am J Physiol* 268: H2466-2475, 1995.
82. Volpe JJ. Perinatal brain injury: from pathogenesis to neuroprotection. *Ment Retard Dev Disabil Res Rev* 7: 56-64, 2001.

83. Wainwright MS, Rossi J, Schavocky J, Crawford S, Steinhorn D, Velentza AV, Zasadzki M, Shirinsky V, Jia Y, Haiech J, Van Eldik LJ, and Watterson DM. Protein kinase involved in lung injury susceptibility: evidence from enzyme isoform genetic knockout and in vivo inhibitor treatment. *Proc Natl Acad Sci U S A* 100: 6233-6238, 2003.
84. Word RA, Stull JT, Casey ML, and Kamm KE. Contractile elements and myosin light chain phosphorylation in myometrial tissue from nonpregnant and pregnant women. *J Clin Invest* 92: 29-37, 1993.
85. Word RA, Tang DC, and Kamm KE. Activation properties of myosin light chain kinase during contraction/relaxation cycles of tonic and phasic smooth muscles. *J Biol Chem* 269: 21596-21602, 1994.
86. Wu YW, Lynch JK, and Nelson KB. Perinatal arterial stroke: understanding mechanisms and outcomes. *Semin Neurol* 25: 424-434, 2005.

UNIVERSITY LIBRARIES
LOMA LINDA, CALIFORNIA